UNIVERSITY OF CALIFORNIA, SAN DIEGO

The Unfolded Protein Response: Integrating Stress Signals from the Endoplasmic Reticulum to the Nucleolus

A dissertation submitted in partial satisfaction of the requirements for the degree Doctor of Philosophy

in

Biology

by

Jenny Bratlien DuRose

Committee in charge:

Professor Maho Niwa, Chair
Professor Randolph Hampton, Co-Chair
Professor Gourisankar Ghosh
Professor James Kadonaga
Professor Suresh Subramani

2008

The Dissertation of Jenny Bratlien DuRose is approved, and it is acceptable in quality and form for publication on microfilm and electronically.

Co-Chair

Chair

University of California, San Diego

2008

DEDICATION

I dedicate this work to my loving husband Eric who was always there when I needed him, where I needed him, and how I need him.

EPIGRAPH

Veni, vidi, vici

Julius Cesar

TABLE OF CONTENTS

LIST OF ABBREVIATIONS

The abbreviations used are: ER, endoplasmic reticulum; UPR, unfolded protein response; GRP78, glucose-regulated protein of 78 kDa; GRP94, glucose-regulated protein of 94 kDa; BiP, immunoglobulin heavy chain binding protein; KAR2, karyogamy 2; IRE1, inositol- requiring enzyme 1; HAC1, protein homologous to ATF/CREB; bZIP, basic leucine zipper; RNase, ribonuclease; XBP1, X-box binding protein 1; ERAD, ER-associated degradation; ERSE, ER stress response element; ATF6, activating transcription factor 6; SREBP, sterol response element binding protein; S1P, site 1 protease; S2P, site 2 protease; SCAP, SREBP cleavage activating protein; eIF2a, eukaryotic translation initiation factor alpha; HRI, heme-regulated inhibitor of translation; PKR, double-stranded RNA dependent protein kinase; PERK, PKR-like ER protein kinase; ATF4, activating transcription factor 4; NFκB, nuclear factor kappa B; rRNA, ribosomal RNA; DTT, dithiothreitol; Tg, thapsigargin; Tm, tunicamycin; ANS, anisomycin; Rap, rapamycin; mTOR, mammalian target of rapamycin; 4E-BP, translation initiation factor 4E binding protein; pre-rRNA, 47S precursor ribosomal RNA; 5' ETS, 5' external transcribed spacer; RPA, ribonuclease protection assay; ITS-1, internal transcribed spacer 1; S6, ribosomal protein S6; S6K, S6 kinase; UBF, upstream binding factor; SL1, selectivity factor 1; RRN3, protein required for transcription of rDNA by RNA polymerase I.

LIST OF FIGURES

CHAPTER 1

LIST OF TABLES

CHAPTER 2

CHAPTER 3

ACKNOWLEDGEMENTS

I would like to thank my advisor, Professor Maho Niwa, for giving me the opportunity to work in this group, for giving me the freedom to pursue my own scientific interests, and for always pushing me to be the best I could be.

Special thanks goes to all the members of the Niwa lab past and present for all their advice, encouragement, and for making the best lab working environment for these many years.

I would like to thank Dr Lawrence Rothblum for all of his advice and assistance in developing our *in vitro* system for analyzing ribosomal RNA transcription, and for providing recombinant RRN3 and UBF proteins and plasmids.

Chapter 1, in full, is a reprint of the material as it appears in Molecular Biology of the Cell 2006. DuRose, Jenny B.; Tam, Arvin B.; Niwa, Maho, The American Society for Cell Biology, 2006. The manuscript is reproduced with the permission of all co-authors. The dissertation author, Jenny Bratlien DuRose was the primary investigator and author of this paper.

Chapter 2, in part, will be submitted for publication of the material as it may appear. The dissertation author, Jenny Bratlien DuRose was the primary investigator and will be the primary author of this paper.

VITA

1997	Associate of Arts, Santa Rosa Junior College, Santa Rosa, CA
2000	Associate of Science, Santa Rosa Junior College, Santa Rosa, CA
2002	Bachelor of Arts in Molecular, Cellular, and Developmental Biology, University of California, Santa Cruz, Santa Cruz, CA
2008	Doctor of Philosophy in Biology, University of California, San Diego, San Diego, CA

PUBLICATIONS

"Intrinsic Capacities of Molecular Sensors of the Unfolded Protein Response to Sense Alternate Forms of Endoplasmic Reticulum Stress" Molecular Biology of the Cell. vol. 17 pp 3095-3107, July 2006.

FIELDS OF STUDY

Identification of aryl hydrocarbon receptor agonists previously identified from a combinatorial library. Undergraduate internship in environmental toxicology with Professor Michael Denison, University of California, Davis.

Development of an RNase protection assay for study of aromatase enzyme expression in rodent breast cancer models. Professor Frank Talamantes, University of California, Santa Cruz.

Evaluation of stress specific activation of unfolded protein response sensors, and impact of the unfolded protein response on ribosome biogenesis. Professor Maho Niwa, University of California, San Diego.

ABSTRACT OF THE DISSERTATION

The Unfolded Protein Response: Integrating Stress Signals from the Endoplasmic Reticulum to the Nucleolus

by

Jenny Bratlien DuRose

Doctor of Philosophy in Biology

University of California, San Diego, 2008

Professor Maho Niwa, Chair
Professor Randall Hampton, Co-Chair

All living organisms must adapt to their ever-changing environment in order to maintain homeostasis and viability. The folding, processing, and assembly of secreted proteins or proteins residing within the secretory pathway begins in the endoplasmic reticulum (ER). When the equilibrium between the client protein load and the ERs capacity to process that load is off balance, the ER must quickly respond to prevent toxic accumulation of improperly folded proteins within the ER. In mammalian cells ER homeostasis

is maintained by three signaling pathways initiated by ER transmembrane proteins, IRE1, PERK, and ATF6, and are collectively referred to as the unfolded proteins response (UPR).

The work in Chapter 1 demonstrates that UPR components display distinct sensitivities towards different forms of ER stress. Disruption of ER calcium in particular revealed fundamental differences in the properties of UPR signaling branches. Depletion of ER calcium by thapsigargin, an inhibitor of the ER calcium ATPase, lead to the rapid activation of both IRE1 and PERK while the response of ATF6 was markedly delayed. This study was the first side-by-side comparison of UPR signaling branch activation revealing intrinsic properties of UPR stress sensors in response to alternate forms of ER stress.

Chapter 2 focuses on the coordinate regulation of ribosomal RNA (rRNA) transcription and translation inhibition by the PERK signaling branch during ER stress. Here we show that phosphorylation of eukaryotic translation initiation factor alpha (eIF2α) by PERK is necessary for disrupting the rRNA preinitiation complex leading inactivation of at least one rRNA transcription factor and dissociation of RNA polymerase I, thus downregulating rRNA transcription. This study is the first to link phosphorylation of eIF2α with regulation rRNA synthesis, and provides an initial framework for understanding how the UPR communicates with the nucleolus in order to maintain ER homeostasis.

INTRODUCTION

The Secretory Pathway

The secretory pathway is comprised of a network of membrane-bound compartments interconnected through vesicular traffic. Each compartment contains a set of unique proteins and lipids, allowing it to carry out specialized functions, which must be physically separated from other compartments and from the reducing cytosol. Transfer of lipids and proteins to their specific intracellular compartments, the plasma membrane, or extracellular space is critical for the overall function of the cell, and therefore must occur with high fidelity. The endoplasmic reticulum (ER) is the first step of the secretory pathway, and one of its major functions is to properly fold, process, and assemble secreted proteins and proteins that reside within the secretory pathway. The ER provides a unique oxidizing environment enriched in chaperones and modifying enzymes required for nascent proteins to achieve their appropriate three-dimensional structures. Misfolding of proteins occurs when the folding process is perturbed by environmental stress, or when the amount of proteins entering the ER exceeds its capacity to fold them. Proteins that fail to acquire their proper three-dimensional structure are retained in the ER until they are properly folded or degraded. Accumulation of unfolded

proteins within the ER results in the activation of the unfolded protein response (UPR) pathway. The UPR signaling pathway is responsible for monitoring the protein-folding environment of the ER and modulating the expression of ER chaperones and modifying enzymes in order to adjust the capacity of the ER according to cellular needs.

Defining the Unfolded Protein Response: Importance of ER Chaperones

In 1974 it was first reported that transformation of chick embryonic fibroblasts by Rous sarcoma viruses lead to increased production of two proteins with apparent molecular weights of 78 and 94 kDa (Stone et al., 1974). The induction of these two proteins were originally thought to be a consequence of transformation, but it was later shown by the lab of Ira Pastan that they were cellular proteins expressed under normal conditions and induced upon infection with the virus. The Pastan Lab found that accumulation of these proteins was not directly related to transformation but rather a secondary effect of depletion of glucose from the culture media resulting from the rapid growth of transformed cells (Shiu et al., 1977). Furthermore, it was shown that these proteins could be induced in non-transformed fibroblasts upon glucose depletion or by blocking protein glycosylation (Pouyssegur et al., 1977). Thus, it was postulated that the proteins were involved with glucose transport or metabolism and hence they were named glucose-regulated protein 78 (GRP78) and 94 (GRP94).

Clues toward the actual function of GRP78 did not come about until the mid 1980s where it was found to be a member of the 70 kDa heat shock protein chaperone family localized to the ER lumen, and identical to immunoglobulin heavy-chain binding protein (BiP) (Kozutsumi et al., 1989; Munro and Pelham, 1986). Work by a number of groups showed that GRP78/BiP displayed characteristics of a chaperone which bound to incompletely assembled nascent proteins in the ER lumen as well as mutant proteins, or proteins containing incorrect glycosylation or disulfide bonds (Bole et al., 1986; Gething et al., 1986; Haas and Wabl, 1983; Kassenbrock et al., 1988). It was also found that GRP78 was induced by number of conditions in addition to glucose starvation, including treatment with calcium ionophores to deplete ER calcium, reducing agents, glycosylation inhibitors, and low extracellular pH (Lee, 1987). The ability of GRP78/BiP to bind unfolded proteins and the number of conditions that induce its production, lead to the speculation that the common stimulus for GRP protein induction was the presence of malfolded proteins within the ER. In late 1980s two groups demonstrated that induction of GRP proteins could occur in response to misfolded or unassembled nascent proteins in the ER, while the properly assembled and folded proteins could not (Kozutsumi et al., 1988; Nakaki et al., 1989). This observation did not explain how unfolded proteins were sensed

within the ER or how the GRP proteins were induced, but it was critical for the identification of the first UPR component.

The Power of Yeast Genetics: Identification of the UPR Sensor

The cloning of the GRP78 and 94 promoters from a number of mammalian species led to the identification of promoter elements that were required for stress-induced stimulation (Chang et al., 1989; Resendez et al., 1988). It was shown that both promoters contained conserved regulatory elements, however the factors that bound them remained elusive. In 1989, the karyogamy 2 (KAR2) gene was found to be the homolog of GRP78/BiP in *Saccharomyces cerevisiae* (Normington et al., 1989; Rose et al., 1989). Not only was the amino acid sequence of the protein conserved between yeast and man, but it was also similarly induced by agents causing unfolded proteins in the ER. Shortly after the cloning of yeast KAR2, the unfolded protein response element (UPRE) inducing KAR2 expression in response to unfolded proteins was identified (Kohno et al., 1993; Mori et al., 1992). The UPRE was used in a genetic screen in yeast, which lead to the identification of the first UPR component, inositol-requiring enzyme 1 (IRE1) (Cox et al., 1993; Mori et al., 1993).

IRE1 is a very unique protein that spans the ER membrane. Its large N-terminal domain resides within the ER and is believed to sense unfolded proteins within the organelle. The cytoplasmic portion of IRE1 contains a

serine/threonine kinase domain and a c-terminal endoribonuclease (RNase) domain. Upon accumulation of unfolded proteins in the ER, IRE1 is activated by oligomerization followed by autophosphorylation (Shamu and Walter, 1996; Welihinda and Kaufman, 1996). The only known substrate for the kinase domain is IRE1, and its function is critical for activation of the IRE1 RNase domain. The IRE1 RNase catalyses the non-spliceosomal mediated cleavage of HAC1 mRNA, which is then ligated by tRNA ligase (Sidrauski et al., 1996; Sidrauski and Walter, 1997). The splicing of the UPR intron from HAC1 mRNA is essential for increasing the abundance of HAC1 protein because removal of the UPR intron is required for efficient translation (Chapman and Walter, 1997; Kawahara et al., 1997; Ruegsegger et al., 2001). HAC1 is a basic leucine zipper (bZIP) transcription factor that is required for inducing ER chaperones, including KAR2 the yeast homolog of mammalian GRP78 (Cox and Walter, 1996; Mori et al., 1996; Nikawa et al., 1996). The induction of chaperone genes is essential for regaining homeostasis within the ER, as mutation in any part of the yeast UPR pathway leads to severe sensitivity of cells to ER stress.

The power of yeast genetics made it possible to quickly identify IRE1 as the yeast UPR sensor rapidly after the identification of the UPRE in the KAR2 promoter in 1992. For the remainder of the decade following the identification of IRE1, significant advances were made in the understanding of the

mechanisms resulting in IRE1 and HAC1 activation during the UPR in yeast. In addition, it provided a starting point for the identification of UPR components in higher eukaryotes. The UPR signaling pathway in higher eukaryotes is much more complex with three ER stress sensors identified to date. IRE1 is the only UPR sensor that has been identified in yeast, and is the only component that is conserved from yeast to man.

Mammalian UPR Pathway: A Tripartite Signaling Pathway

Identification of the first UPR component in higher eukaryotes was accomplished by searching for mammalian homologs using the yeast IRE1 sequence (Tirasophon et al., 1998; Wang et al., 1998). In mammals there are two isoforms of IRE1. IRE1α is ubiquitously expressed in all cell types, and is an essential gene in mice, with homozygous knockout embryos dying after 9.5-11.5 days of gestation (Urano et al., 2000). IRE1β is not an essential gene and its expression is restricted to the gastrointestinal epithelia. IRE1β knockout mice have increased sensitivity to agents that cause inflammatory bowel disease indicating a special requirement for IRE1 activity in those highly active secretory cells (Bertolotti et al., 2001). Prior to the identification of an IRE1 substrate in mammals, it was shown that mammalian IRE1 was capable of correctly splicing HAC1 precursor mRNA (Niwa et al., 1999). This suggested that a HAC1-like transcription factor was present in mammalian cells, but no mammalian homolog has been identified to date.

In order to identify the IRE1 substrate in higher eukaryotes, two groups independently returned to the GRP promoters for assistance. The functional equivalent of HAC1 was then identified in mammals to be x-box binding protein 1 (XBP1) (Calfon et al., 2002; Yoshida et al., 2001). Unlike HAC1, XBP1 mRNA is constitutively translated, however the presence of the 26-nucleotide UPR intron leads to a smaller protein due to a premature stop codon. Removal of the UPR intron induces a frame-shift which extends the open reading frame of the XBP1 mRNA producing a c-terminal transcription activation domain resulting in a more potent XBP1 transcription factor (Calfon et al., 2002; Yoshida et al., 2001). The unspliced form of XBP1 contains the same DNA binding domain as spliced XBP1, but a stop codon in the UPR intron-containing open reading frame prevents translation of the c-terminal activation domain making it a weak transcriptional activator. While it is not fully understood why the unspliced form of XBP1 is constitutively translated, there is some evidence that suggests it functions as a negative regulator of XBP1 target genes (Yoshida et al., 2006). XBP1 is the only substrate for IRE1 that has been identified in metazoans to date and like IRE1, homozygous knock out of XBP1 is embryonic lethal. However, XBP1 knockouts die from liver hypotrophy at a later developmental stage than IRE1 knockouts suggesting that IRE1 may have additional functions or substrates in mammals (Reimold et al., 2000). The active XBP1 transcription factor is involved in

increasing transcription of ER chaperones and components of the ER-associated protein degradation (ERAD) pathway, and has recently been shown to be critical for lipid production in the liver (Lee et al., 2003; Lee et al., 2008; Yoshida et al., 2003). In addition, XBP1 is particularly required for the development of antibody secreting plasma cells from naïve B cells (Reimold et al., 2001). Like most transcription factors, XBP1 protein functions as a homodimer to affect UPR target gene expression and has more recently been shown to heterodimerize with transcription factors activated by the other UPR signaling branches (Yamamoto et al., 2007).

The second UPR transcription factor was identified in a one-hybrid screen utilizing the ER stress response element (ERSE) in the promoters of mammalian GRP78 and GRP94 (Yoshida et al., 1998). The screen identified a 90-kDa bZIP transcription factor that binds to the ERSE directing the transcription of ER chaperones upon UPR activation. When activating transcription factor 6 (ATF6) was identified as a UPR transcription factor it was observed that the ATF6 protein reduced in size upon UPR stimulation. When ATF6 mRNA was analyzed it was determined that it did not undergo a splicing reaction similar to HAC1 mRNA, but rather the ATF6 protein was subject to an ER stress regulated posttranslational modification resulting in the 50 kDa active form (Yoshida et al., 1998). At the time it was not understood how the conversion of the large form to the smaller form resulted in activation, however

when the nature of the posttranslational modification was further explored it became clear why ATF6 was regulated in this manner.

It was shown that the full-length 90 kDa ATF6 protein is in fact a type II transmembrane protein localized in the ER membrane (Haze et al., 1999). The c-terminal ER sensor domain of ATF6 resides within the ER lumen, while the n-terminal portion containing the bZIP transcription factor is localized to the cytosol. ATF6 undergoes regulated intramembrane proteolysis by the same proteases that process sterol regulatory element binding proteins (SREBPs) upon UPR induction (Ye et al., 2000). However, the site 1 and site 2 proteases (S1P and S2P respectively) that cleave SREBPs are not localized to the ER, but reside within the golgi apparatus (Rawson et al., 1997; Sakai et al., 1998b; Zelenski et al., 1999). Under conditions of sterol limitation, SREBPs are escorted from the ER to the golgi by the SREBP cleavage-activating protein (SCAP) to be sequentially cleaved by S1P and S2P (DeBose-Boyd et al., 1999; Nohturfft et al., 1999; Sakai et al., 1998a). In the case of ATF6, no SCAP-like protein has been identified (Ye et al., 2000). When ATF6 is activated by ER stress a golgi localization signal in its lumenal domain is revealed allowing ATF6 to translocate from the ER into the golgi where it is sequentially cleaved by S1P and S2P releasing the membrane bound n-terminal transcription factor domain into the cytosol (Chen et al., 2002; Shen et al., 2002). The free 50 kDa ATF6 protein is then targeted to the nucleus

where it increases transcription of UPR target genes including GRP78 and GRP94 (Haze et al., 1999). In mammals there are two isoforms of ATF6, neither of which are essential, however embryos die after 8.5 days of gestation in ATF6α and ATF6β double knockouts (Yamamoto et al., 2007). Deletion of ATF6α severely impairs induction of ER chaperones and proteins involved in ER quality control, while deletion of ATF6β results in a much less severe phenotype (Wu et al., 2007; Yamamoto et al., 2007). Transcription of ER quality control genes has previously been shown to be predominantly under the control of XBP1 (Lee et al., 2003; Yoshida et al., 2003). However, recent results suggest that ATF6α and XBP1 function as a heterodimer to upregulate ER quality control genes (Yamamoto et al., 2007). In addition, XBP1 transcription is stimulated by ATF6 during UPR, which may have a secondary effect on the transcription of XBP1 target genes (Yoshida et al., 2001).

The final UPR component was independently identified by two separate groups, however this time the strategy did not employ the use the GRP promoter elements. During the 1980s, pioneering work by Margaret and Charles Brostrom illustrated the importance of calcium in the regulation of protein synthesis. In particular they noted that depletion of ER calcium lead to a marked decrease in the rate of protein synthesis (Reviewed in Brostrom et al., 1983). In the early 1990s they showed that phosphorylation of eukaryotic translation initiation factor 2 alpha (eIF2α) was responsible for inhibition of

translation initiation during conditions that disrupted protein folding in the ER, and that synthesis of GRP78 was necessary for recovery of translation (Prostko et al., 1993; Prostko et al., 1992).

The eIF2 complex is a heterotrimer consisting of α, β, and γ subunits, which form a ternary complex with GTP and initiator tRNA (Safer et al., 1975; Schreier and Staehelin, 1973). Completion of each round of translation initiation results in hydrolysis of GTP, and release of eIF2-GDP when the 60S ribosomal subunit joins the 43S preinitiation complex to form a complete ribosome. Phosphorylation of eIF2α impairs guanine nucleotide exchange of the eIF2 complex inhibiting recycling of eIF2 for successive rounds of translation initiation (Clemens et al., 1982; Panniers and Henshaw, 1983; Siekierka et al., 1982). In the mid 1990s, only two eIF2α kinases had been identified in mammals, heme-regulated inhibitor of translation (HRI; Chen et al., 1991) and double-stranded RNA dependent protein kinase (PKR; Berry et al., 1985). Early reports suggested that PKR might be involved in regulating translation upon depletion of ER calcium, making it a good candidate for the ER stress regulator of translation (Srivastava et al., 1995). In the late 1990s, two groups independently searching for additional eIF2α kinases in mammals discovered a transmembrane ER resident eIF2α kinase homolog (Harding et al., 1999; Shi et al., 1998). It was demonstrated that PKR-like ER protein

kinase (PERK) was in fact necessary and sufficient for phosphorylating eIF2α in response to ER stress (Harding et al., 2000b; Harding et al., 1999).

PERK is not an essential gene, however 30-40% of mice carrying homozygous deletion of PERK die prenatally and only ~ 40% survive past the first few days after birth (Zhang et al., 2002). Surviving PERK -/- mice exhibit severe growth retardation and have defects in the development of the skeletal system resulting from impaired secretion and survival of osteoblasts. PERK -/- mice have defects in both exocrine and endocrine pancreatic function, and develop a very early onset diabetes mellitus resulting from complete loss of insulin secreting pancreatic β cells (Harding et al., 2001; Zhang et al., 2002). The phenotype of PERK -/- mice is very similar to that of humans suffering from Wolcott-Rallison Syndrome, a rare recessive disorder characterized by early onset diabetes and skeletal dysplasia which was mapped to the PERK gene (Delepine et al., 2000; Wolcott and Rallison, 1972). Interestingly, knockout of the other three eIF2α kinases does not result in such drastic developmental defects suggesting a special need for translational control in the survival and function secretory tissues.

Downregulation of global protein synthesis by PERK is thought to reduce the protein load on the ER, thus preventing toxic accumulation of malfolded proteins in the organelle. Phosphorylation of eIF2α paradoxically leads to increased translation of bZIP activating transcription factor 4 (ATF4;

Deng et al., 2004; Harding et al., 2000a). Downstream targets of ATF4 include genes involved in amino acid import and metabolism as well as growth arrest and DNA damage 153 (GADD153) transcription factor, which regulates genes involved with programmed cell death. In addition, the inhibition of translation during the UPR also activates nuclear factor kappa B (NFκB) during ER stress (Jiang et al., 2003; Pahl and Baeuerle, 1995). Thus pro-apoptotic signals from GADD153 and anti-apoptotic signals from NFκB combine to make cell fate decisions under the control of the PERK pathway. When PERK is absent, survival of fibroblasts is severely impaired upon exposure to ER stress inducing agents (Harding et al., 2000b).

In general, survival of cells upon ER stress requires an intact UPR. This is demonstrated by the fact that cells bearing deletion of one branch of the UPR are able to survive until they are challenged with ER stress. The transcription factors from each signaling branch coordinate the reprogramming of gene expression in the nucleus, and PERK reduces global translation in order to combat the effects of ER stress. In the last thirty years since it was first discovered that interfering with ER protein folding induces the expression of ER chaperones, significant advances have been made in defining the UPR and identifying its components. It is now becoming clear that the UPR is involved in a number of pathologies from neurodegeneration disorders to diabetes and tumor development resulting from constitutive activation of one

or more UPR branches. The UPR has become an attractive target for small molecule inhibitors with the hope of reducing off target effects because it is a stress response and is generally not required for the survival of healthy cells. One of the major challenges for the future is dissecting the individual contributions of each UPR signaling branch, and understanding how they work together to relieve ER stress and maintain ER homeostasis.

Focus of Dissertation

The aim of chapter 1 is to characterize activation of each UPR signaling branch induced by pharmacological agents that produce misfolded proteins by different mechanisms. Previous studies of UPR activation in physiological settings (e.g. B cell development) have suggested that under certain conditions not all UPR components are simultaneously activated. While the ER performs a variety of protein processing functions, the demand for specific functions may vary depending on the prevailing conditions and cell type. In this study we have compared the activation kinetics of each UPR signaling branch in response to alternate forms of ER stress induced by three different pharmacological agents. In particular, ER stress induced by depletion of ER calcium revealed differences in the activation IRE1 and PERK branches compared to ATF6. This study was the first side-by-side comparison of all three UPR signaling branches in response to alternate forms of ER stress,

revealing fundamental differences between UPR sensors in their ability to recognize alternate forms of ER stress.

The work in chapter 2 explores the impact of UPR induction on ribosome biogenesis. We found that upon UPR activation, PERK rapidly downregulates ribosomal RNA (rRNA) transcription. A literature survey of stresses that activate eIF2α kinases revealed that rRNA transcription is also affected, although no direct relationship has previously been suggested. We found the phosphorylation of eIF2α through PERK activation is necessary for rRNA regulation during the UPR. Our study is the first to link phosphorylation of eIF2α with regulation rRNA transcription. Furthermore, we identified the rRNA transcription factor involved in regulation of rRNA synthesis and have begun to unravel the mechanism of how the ER communicates with the nucleolus to maintain ER homeostasis.

References

Berry, M.J., Knutson, G.S., Lasky, S.R., Munemitsu, S.M., and Samuel, C.E. (1985). Mechanism of interferon action. Purification and substrate specificities of the double-stranded RNA-dependent protein kinase from untreated and interferon-treated mouse fibroblasts. The Journal of biological chemistry *260*, 11240-11247.

Bertolotti, A., Wang, X., Novoa, I., Jungreis, R., Schlessinger, K., Cho, J.H., West, A.B., and Ron, D. (2001). Increased sensitivity to dextran sodium sulfate colitis in IRE1beta-deficient mice. The Journal of clinical investigation *107*, 585-593.

Bole, D.G., Hendershot, L.M., and Kearney, J.F. (1986). Posttranslational association of immunoglobulin heavy chain binding protein with nascent heavy chains in nonsecreting and secreting hybridomas. The Journal of cell biology *102*, 1558-1566.

Brostrom, C.O., Bocckino, S.B., and Brostrom, M.A. (1983). Identification of a Ca2+ requirement for protein synthesis in eukaryotic cells. The Journal of biological chemistry *258*, 14390-14399.

Calfon, M., Zeng, H., Urano, F., Till, J.H., Hubbard, S.R., Harding, H.P., Clark, S.G., and Ron, D. (2002). IRE1 couples endoplasmic reticulum load to secretory capacity by processing the XBP-1 mRNA. Nature *415*, 92-96.

Chang, S.C., Erwin, A.E., and Lee, A.S. (1989). Glucose-regulated protein (GRP94 and GRP78) genes share common regulatory domains and are coordinately regulated by common trans-acting factors. Molecular and cellular biology *9*, 2153-2162.

Chapman, R.E., and Walter, P. (1997). Translational attenuation mediated by an mRNA intron. Curr Biol *7*, 850-859.

Chen, J.J., Throop, M.S., Gehrke, L., Kuo, I., Pal, J.K., Brodsky, M., and London, I.M. (1991). Cloning of the cDNA of the heme-regulated eukaryotic initiation factor 2 alpha (eIF-2 alpha) kinase of rabbit reticulocytes: homology to yeast GCN2 protein kinase and human double-stranded-RNA-dependent eIF-2 alpha kinase. Proceedings of the National Academy of Sciences of the United States of America *88*, 7729-7733.

Chen, X., Shen, J., and Prywes, R. (2002). The luminal domain of ATF6 senses endoplasmic reticulum (ER) stress and causes translocation of ATF6 from the ER to the Golgi. The Journal of biological chemistry *277*, 13045-13052.

Clemens, M.J., Pain, V.M., Wong, S.T., and Henshaw, E.C. (1982). Phosphorylation inhibits guanine nucleotide exchange on eukaryotic initiation factor 2. Nature *296*, 93-95.

Cox, J.S., Shamu, C.E., and Walter, P. (1993). Transcriptional induction of genes encoding endoplasmic reticulum resident proteins requires a transmembrane protein kinase. Cell *73*, 1197-1206.

Cox, J.S., and Walter, P. (1996). A novel mechanism for regulating activity of a transcription factor that controls the unfolded protein response. Cell *87*, 391-404.

DeBose-Boyd, R.A., Brown, M.S., Li, W.P., Nohturfft, A., Goldstein, J.L., and Espenshade, P.J. (1999). Transport-dependent proteolysis of SREBP: relocation of site-1 protease from Golgi to ER obviates the need for SREBP transport to Golgi. Cell *99*, 703-712.

Delepine, M., Nicolino, M., Barrett, T., Golamaully, M., Lathrop, G.M., and Julier, C. (2000). EIF2AK3, encoding translation initiation factor 2-alpha kinase 3, is mutated in patients with Wolcott-Rallison syndrome. Nature genetics *25*, 406-409.

Deng, J., Lu, P.D., Zhang, Y., Scheuner, D., Kaufman, R.J., Sonenberg, N., Harding, H.P., and Ron, D. (2004). Translational repression mediates activation of nuclear factor kappa B by phosphorylated translation initiation factor 2. Molecular and cellular biology *24*, 10161-10168.

Gething, M.J., McCammon, K., and Sambrook, J. (1986). Expression of wild-type and mutant forms of influenza hemagglutinin: the role of folding in intracellular transport. Cell *46*, 939-950.

Haas, I.G., and Wabl, M. (1983). Immunoglobulin heavy chain binding protein. Nature *306*, 387-389.

Harding, H.P., Novoa, I., Zhang, Y., Zeng, H., Wek, R., Schapira, M., and Ron, D. (2000a). Regulated translation initiation controls stress-induced gene expression in mammalian cells. Molecular cell *6*, 1099-1108.

Harding, H.P., Zeng, H., Zhang, Y., Jungries, R., Chung, P., Plesken, H., Sabatini, D.D., and Ron, D. (2001). Diabetes mellitus and exocrine pancreatic dysfunction in perk-/- mice reveals a role for translational control in secretory cell survival. Molecular cell *7*, 1153-1163.

Harding, H.P., Zhang, Y., Bertolotti, A., Zeng, H., and Ron, D. (2000b). Perk is essential for translational regulation and cell survival during the unfolded protein response. Molecular cell *5*, 897-904.

Harding, H.P., Zhang, Y., and Ron, D. (1999). Protein translation and folding are coupled by an endoplasmic-reticulum-resident kinase. Nature *397*, 271-274.

Haze, K., Yoshida, H., Yanagi, H., Yura, T., and Mori, K. (1999). Mammalian transcription factor ATF6 is synthesized as a transmembrane protein and activated by proteolysis in response to endoplasmic reticulum stress. Molecular biology of the cell *10*, 3787-3799.

Jiang, H.Y., Wek, S.A., McGrath, B.C., Scheuner, D., Kaufman, R.J., Cavener, D.R., and Wek, R.C. (2003). Phosphorylation of the alpha subunit of eukaryotic initiation factor 2 is required for activation of NF-kappaB in response to diverse cellular stresses. Molecular and cellular biology *23*, 5651-5663.

Kassenbrock, C.K., Garcia, P.D., Walter, P., and Kelly, R.B. (1988). Heavy-chain binding protein recognizes aberrant polypeptides translocated in vitro. Nature *333*, 90-93.

Kawahara, T., Yanagi, H., Yura, T., and Mori, K. (1997). Endoplasmic reticulum stress-induced mRNA splicing permits synthesis of transcription factor Hac1p/Ern4p that activates the unfolded protein response. Molecular biology of the cell *8*, 1845-1862.

Kohno, K., Normington, K., Sambrook, J., Gething, M.J., and Mori, K. (1993). The promoter region of the yeast KAR2 (BiP) gene contains a regulatory domain that responds to the presence of unfolded proteins in the endoplasmic reticulum. Molecular and cellular biology *13*, 877-890.

Kozutsumi, Y., Normington, K., Press, E., Slaughter, C., Sambrook, J., and Gething, M.J. (1989). Identification of immunoglobulin heavy chain binding protein as glucose-regulated protein 78 on the basis of amino acid sequence,

immunological cross-reactivity, and functional activity. Journal of cell science *11*, 115-137.

Kozutsumi, Y., Segal, M., Normington, K., Gething, M.J., and Sambrook, J. (1988). The presence of malfolded proteins in the endoplasmic reticulum signals the induction of glucose-regulated proteins. Nature *332*, 462-464.

Lee, A.H., Iwakoshi, N.N., and Glimcher, L.H. (2003). XBP-1 regulates a subset of endoplasmic reticulum resident chaperone genes in the unfolded protein response. Molecular and cellular biology *23*, 7448-7459.

Lee, A.H., Scapa, E.F., Cohen, D.E., and Glimcher, L.H. (2008). Regulation of hepatic lipogenesis by the transcription factor XBP1. Science (New York, N.Y *320*, 1492-1496.

Lee, A.S. (1987). Coordinated regulation of a set of genes by glucose and calcium ionophores in mammalian cells. Trends Biochem Sci *12*, 20-23.

Mori, K., Kawahara, T., Yoshida, H., Yanagi, H., and Yura, T. (1996). Signalling from endoplasmic reticulum to nucleus: transcription factor with a basic-leucine zipper motif is required for the unfolded protein-response pathway. Genes Cells *1*, 803-817.

Mori, K., Ma, W., Gething, M.J., and Sambrook, J. (1993). A transmembrane protein with a cdc2+/CDC28-related kinase activity is required for signaling from the ER to the nucleus. Cell *74*, 743-756.

Mori, K., Sant, A., Kohno, K., Normington, K., Gething, M.J., and Sambrook, J.F. (1992). A 22 bp cis-acting element is necessary and sufficient for the induction of the yeast KAR2 (BiP) gene by unfolded proteins. The EMBO journal *11*, 2583-2593.

Munro, S., and Pelham, H.R. (1986). An Hsp70-like protein in the ER: identity with the 78 kd glucose-regulated protein and immunoglobulin heavy chain binding protein. Cell *46*, 291-300.

Nakaki, T., Deans, R.J., and Lee, A.S. (1989). Enhanced transcription of the 78,000-dalton glucose-regulated protein (GRP78) gene and association of GRP78 with immunoglobulin light chains in a nonsecreting B-cell myeloma line (NS-1). Molecular and cellular biology *9*, 2233-2238.

Nikawa, J., Akiyoshi, M., Hirata, S., and Fukuda, T. (1996). Saccharomyces cerevisiae IRE2/HAC1 is involved in IRE1-mediated KAR2 expression. Nucleic acids research *24*, 4222-4226.

Niwa, M., Sidrauski, C., Kaufman, R.J., and Walter, P. (1999). A role for presenilin-1 in nuclear accumulation of Ire1 fragments and induction of the mammalian unfolded protein response. Cell *99*, 691-702.

Nohturfft, A., DeBose-Boyd, R.A., Scheek, S., Goldstein, J.L., and Brown, M.S. (1999). Sterols regulate cycling of SREBP cleavage-activating protein (SCAP) between endoplasmic reticulum and Golgi. Proceedings of the National Academy of Sciences of the United States of America *96*, 11235-11240.

Normington, K., Kohno, K., Kozutsumi, Y., Gething, M.J., and Sambrook, J. (1989). S. cerevisiae encodes an essential protein homologous in sequence and function to mammalian BiP. Cell *57*, 1223-1236.

Pahl, H.L., and Baeuerle, P.A. (1995). A novel signal transduction pathway from the endoplasmic reticulum to the nucleus is mediated by transcription factor NF-kappa B. The EMBO journal *14*, 2580-2588.

Panniers, R., and Henshaw, E.C. (1983). A GDP/GTP exchange factor essential for eukaryotic initiation factor 2 cycling in Ehrlich ascites tumor cells and its regulation by eukaryotic initiation factor 2 phosphorylation. The Journal of biological chemistry *258*, 7928-7934.

Pouyssegur, J., Shiu, R.P., and Pastan, I. (1977). Induction of two transformation-sensitive membrane polypeptides in normal fibroblasts by a block in glycoprotein synthesis or glucose deprivation. Cell *11*, 941-947.

Prostko, C.R., Brostrom, M.A., and Brostrom, C.O. (1993). Reversible phosphorylation of eukaryotic initiation factor 2 alpha in response to endoplasmic reticular signaling. Molecular and cellular biochemistry *127-128*, 255-265.

Prostko, C.R., Brostrom, M.A., Malara, E.M., and Brostrom, C.O. (1992). Phosphorylation of eukaryotic initiation factor (eIF) 2 alpha and inhibition of eIF-2B in GH3 pituitary cells by perturbants of early protein processing that induce GRP78. The Journal of biological chemistry *267*, 16751-16754.

Rawson, R.B., Zelenski, N.G., Nijhawan, D., Ye, J., Sakai, J., Hasan, M.T., Chang, T.Y., Brown, M.S., and Goldstein, J.L. (1997). Complementation

cloning of S2P, a gene encoding a putative metalloprotease required for intramembrane cleavage of SREBPs. Molecular cell *1*, 47-57.

Reimold, A.M., Etkin, A., Clauss, I., Perkins, A., Friend, D.S., Zhang, J., Horton, H.F., Scott, A., Orkin, S.H., Byrne, M.C*., et al.* (2000). An essential role in liver development for transcription factor XBP-1. Genes & development *14*, 152-157.

Reimold, A.M., Iwakoshi, N.N., Manis, J., Vallabhajosyula, P., Szomolanyi-Tsuda, E., Gravallese, E.M., Friend, D., Grusby, M.J., Alt, F., and Glimcher, L.H. (2001). Plasma cell differentiation requires the transcription factor XBP-1. Nature *412*, 300-307.

Resendez, E., Jr., Wooden, S.K., and Lee, A.S. (1988). Identification of highly conserved regulatory domains and protein-binding sites in the promoters of the rat and human genes encoding the stress-inducible 78-kilodalton glucose-regulated protein. Molecular and cellular biology *8*, 4579-4584.

Rose, M.D., Misra, L.M., and Vogel, J.P. (1989). KAR2, a karyogamy gene, is the yeast homolog of the mammalian BiP/GRP78 gene. Cell *57*, 1211-1221.

Ruegsegger, U., Leber, J.H., and Walter, P. (2001). Block of HAC1 mRNA translation by long-range base pairing is released by cytoplasmic splicing upon induction of the unfolded protein response. Cell *107*, 103-114.

Safer, B., Adams, S.L., Anderson, W.F., and Merrick, W.C. (1975). Binding of MET-TRNAf and GTP to homogeneous initiation factor MP. The Journal of biological chemistry *250*, 9076-9082.

Sakai, J., Nohturfft, A., Goldstein, J.L., and Brown, M.S. (1998a). Cleavage of sterol regulatory element-binding proteins (SREBPs) at site-1 requires interaction with SREBP cleavage-activating protein. Evidence from in vivo competition studies. The Journal of biological chemistry *273*, 5785-5793.

Sakai, J., Rawson, R.B., Espenshade, P.J., Cheng, D., Seegmiller, A.C., Goldstein, J.L., and Brown, M.S. (1998b). Molecular identification of the sterol-regulated luminal protease that cleaves SREBPs and controls lipid composition of animal cells. Molecular cell *2*, 505-514.

Schreier, M.H., and Staehelin, T. (1973). Initiation of eukaryotic protein synthesis: (Met-tRNA f -40S ribosome) initiation complex catalysed by purified initiation factors in the absence of mRNA. Nature: New biology *242*, 35-38.

Shamu, C.E., and Walter, P. (1996). Oligomerization and phosphorylation of the Ire1p kinase during intracellular signaling from the endoplasmic reticulum to the nucleus. The EMBO journal *15*, 3028-3039.

Shen, J., Chen, X., Hendershot, L., and Prywes, R. (2002). ER stress regulation of ATF6 localization by dissociation of BiP/GRP78 binding and unmasking of Golgi localization signals. Developmental cell *3*, 99-111.

Shi, Y., An, J., Liang, J., Hayes, S.E., Sandusky, G.E., Stramm, L.E., and Yang, N.N. (1998). Characterization of a mutant pancreatic eIF-2alpha kinase, PEK, and co-localization with somatostatin in islet delta cells. The Journal of biological chemistry *274*, 5723-5730.

Shiu, R.P., Pouyssegur, J., and Pastan, I. (1977). Glucose depletion accounts for the induction of two transformation-sensitive membrane proteinsin Rous sarcoma virus-transformed chick embryo fibroblasts. Proceedings of the National Academy of Sciences of the United States of America *74*, 3840-3844.

Sidrauski, C., Cox, J.S., and Walter, P. (1996). tRNA ligase is required for regulated mRNA splicing in the unfolded protein response. Cell *87*, 405-413.

Sidrauski, C., and Walter, P. (1997). The transmembrane kinase Ire1p is a site-specific endonuclease that initiates mRNA splicing in the unfolded protein response. Cell *90*, 1031-1039.

Siekierka, J., Mauser, L., and Ochoa, S. (1982). Mechanism of polypeptide chain initiation in eukaryotes and its control by phosphorylation of the alpha subunit of initiation factor 2. Proceedings of the National Academy of Sciences of the United States of America *79*, 2537-2540.

Srivastava, S.P., Davies, M.V., and Kaufman, R.J. (1995). Calcium depletion from the endoplasmic reticulum activates the double-stranded RNA-dependent protein kinase (PKR) to inhibit protein synthesis. The Journal of biological chemistry *270*, 16619-16624.

Stone, K.R., Smith, R.E., and Joklik, W.K. (1974). Changes in membrane polypeptides that occur when chick embryo fibroblasts and NRK cells are transformed with avian sarcoma viruses. Virology *58*, 86-100.

Tirasophon, W., Welihinda, A.A., and Kaufman, R.J. (1998). A stress response pathway from the endoplasmic reticulum to the nucleus requires a novel

bifunctional protein kinase/endoribonuclease (Ire1p) in mammalian cells. Genes & development *12*, 1812-1824.

Urano, F., Wang, X., Bertolotti, A., Zhang, Y., Chung, P., Harding, H.P., and Ron, D. (2000). Coupling of stress in the ER to activation of JNK protein kinases by transmembrane protein kinase IRE1. Science (New York, N.Y *287*, 664-666.

Wang, X.Z., Harding, H.P., Zhang, Y., Jolicoeur, E.M., Kuroda, M., and Ron, D. (1998). Cloning of mammalian Ire1 reveals diversity in the ER stress responses. The EMBO journal *17*, 5708-5717.

Welihinda, A.A., and Kaufman, R.J. (1996). The unfolded protein response pathway in Saccharomyces cerevisiae. Oligomerization and trans-phosphorylation of Ire1p (Ern1p) are required for kinase activation. The Journal of biological chemistry *271*, 18181-18187.

Wolcott, C.D., and Rallison, M.L. (1972). Infancy-onset diabetes mellitus and multiple epiphyseal dysplasia. The Journal of pediatrics *80*, 292-297.

Wu, J., Rutkowski, D.T., Dubois, M., Swathirajan, J., Saunders, T., Wang, J., Song, B., Yau, G.D., and Kaufman, R.J. (2007). ATF6alpha optimizes long-term endoplasmic reticulum function to protect cells from chronic stress. Developmental cell *13*, 351-364.

Yamamoto, K., Sato, T., Matsui, T., Sato, M., Okada, T., Yoshida, H., Harada, A., and Mori, K. (2007). Transcriptional induction of mammalian ER quality control proteins is mediated by single or combined action of ATF6alpha and XBP1. Developmental cell *13*, 365-376.

Ye, J., Rawson, R.B., Komuro, R., Chen, X., Dave, U.P., Prywes, R., Brown, M.S., and Goldstein, J.L. (2000). ER stress induces cleavage of membrane-bound ATF6 by the same proteases that process SREBPs. Molecular cell *6*, 1355-1364.

Yoshida, H., Haze, K., Yanagi, H., Yura, T., and Mori, K. (1998). Identification of the cis-acting endoplasmic reticulum stress response element responsible for transcriptional induction of mammalian glucose-regulated proteins. Involvement of basic leucine zipper transcription factors. The Journal of biological chemistry *273*, 33741-33749.

Yoshida, H., Matsui, T., Hosokawa, N., Kaufman, R.J., Nagata, K., and Mori, K. (2003). A time-dependent phase shift in the mammalian unfolded protein response. Developmental cell *4*, 265-271.

Yoshida, H., Matsui, T., Yamamoto, A., Okada, T., and Mori, K. (2001). XBP1 mRNA is induced by ATF6 and spliced by IRE1 in response to ER stress to produce a highly active transcription factor. Cell *107*, 881-891.

Yoshida, H., Oku, M., Suzuki, M., and Mori, K. (2006). pXBP1(U) encoded in XBP1 pre-mRNA negatively regulates unfolded protein response activator pXBP1(S) in mammalian ER stress response. The Journal of cell biology *172*, 565-575.

Zelenski, N.G., Rawson, R.B., Brown, M.S., and Goldstein, J.L. (1999). Membrane topology of S2P, a protein required for intramembranous cleavage of sterol regulatory element-binding proteins. The Journal of biological chemistry *274*, 21973-21980.

Zhang, P., McGrath, B., Li, S., Frank, A., Zambito, F., Reinert, J., Gannon, M., Ma, K., McNaughton, K., and Cavener, D.R. (2002). The PERK eukaryotic initiation factor 2 alpha kinase is required for the development of the skeletal system, postnatal growth, and the function and viability of the pancreas. Molecular and cellular biology *22*, 3864-3874.

CHAPTER 1

Intrinsic Capacities of Molecular Sensor of the Unfolded Protein Response to Sense Alternate forms of Endoplasmic Reticulum Stress

Molecular Biology of the Cell
Vol. 17, 3095–3107, July 2006

Intrinsic Capacities of Molecular Sensors of the Unfolded Protein Response to Sense Alternate Forms of Endoplasmic Reticulum Stress[D]

Jenny B. DuRose, Arvin B. Tam, and Maho Niwa

Division of Biological Sciences, Section of Molecular Biology, University of California, San Diego, La Jolla, CA, 92093-0377

Submitted January 24, 2006; Revised March 27, 2006; Accepted April 26, 2006
Monitoring Editor: Benjamin Glick

The unfolded protein response (UPR) regulates the protein-folding capacity of the endoplasmic reticulum (ER) according to cellular demand. In mammalian cells, three ER transmembrane components, IRE1, PERK, and ATF6, initiate distinct UPR signaling branches. We show that these UPR components display distinct sensitivities toward different forms of ER stress. ER stress induced by ER Ca^{2+} release in particular revealed fundamental differences in the properties of UPR signaling branches. Compared with the rapid response of both IRE1 and PERK to ER stress induced by thapsigargin, an ER Ca^{2+} ATPase inhibitor, the response of ATF6 was markedly delayed. These studies are the first side-by-side comparisons of UPR signaling branch activation and reveal intrinsic features of UPR stress sensor activation in response to alternate forms of ER stress. As such, they provide initial groundwork toward understanding how ER stress sensors can confer different responses and how optimal UPR responses are achieved in physiological settings.

INTRODUCTION

The endoplasmic reticulum (ER) is an initial checkpoint for the folding and modification of proteins that reside within the secretory pathway, because only properly folded and modified proteins can exit the ER (Gilmore, 1993; Walter and Johnson, 1994; Voeltz *et al.*, 2002). Depending upon environmental changes or developmental stages, the capacity of the ER to perform protein folding must adjust according to cellular needs. The unfolded protein response (UPR) signaling pathway plays a major role in this regulation by sensing the ER lumen environment and transmitting this information to the nucleus to up-regulate transcription of genes that increase both ER protein folding and secretory capacities (Kaufman, 1999; Mori, 2000; Patil and Walter, 2001; Harding *et al.*, 2002).

The yeast *S. cerevisiae* senses unfolded proteins with a single sensor, IRE1 (Cox, 1993; Mori, 1993). In mammalian cells, the UPR response is induced by three initiator/sensor molecules on the ER membrane, IRE1, PERK, and ATF6. Each sensor undergoes activation in response to elevated levels of unfolded proteins. IRE1 is an ER transmembrane receptor with kinase and endoribonuclease domains in its cytoplasmic C-terminal portion. IRE1 senses the protein folding needs of the ER through its N-terminal lumenal domain (Cox *et al.*, 1993; Mori *et al.*, 1993; Tirasophon *et al.*, 1998; Wang *et al.*, 1998). Once sensed, this signal is transmitted across the ER membrane to the IRE1 cytosolic domain, causing IRE1 oligomerization and autophosphorylation (Shamu and Walter, 1996; Papa *et al.*, 2003). A unique feature of IRE1 is its function as an endoribonuclease (RNase) which, after activation by unfolded proteins, mediates the cleavage step in the nonconventional splicing of XBP1 mRNA encoding a bZiP transcription factor (Sidrauski and Walter, 1997; Shen *et al.*, 2001; Yoshida *et al.*, 2001; Calfon *et al.*, 2002). Removal of the UPR intron in XBP1 causes a frame-shift, producing an XBP1 protein that is a more potent transcription factor and is an obligate step in the UPR pathway (Yoshida *et al.*, 2001).

A second initiator, PERK, is a type-I ER-transmembrane kinase that phosphorylates the α subunit of eukaryotic translation initiation factor 2 (eIF2α; Shi *et al.*, 1998; Harding *et al.*, 1999). Phosphorylated eIF2α interferes with the formation of the 43S translation initiation complex, leading to overall translational repression in UPR-induced cells; presumably to alleviate ER stress by reducing the influx of the newly synthesized proteins into the ER (Harding *et al.*, 2000a). Moreover, when eIF2α is phosphorylated, a second transcription factor, ATF4, is produced preferentially (Harding *et al.*, 2000b; Scheuner *et al.*, 2001a). In addition to XBP1, ATF4 also participates in transcription of some UPR target genes.

A third component transmitting UPR activating signals from the ER in mammalian cells is ATF6, a 90-kDa type-II ER-membrane transcription factor also required for activating many UPR target genes (Li *et al.*, 2000; Ye *et al.*, 2000; Yoshida *et al.*, 2000). On UPR induction, ATF6 is released from the membrane by sequential cleavage by Site 1 (S1P) and Site 2 Proteases (S2P; Ye *et al.*, 2000), producing a 50-kDa cytosolic fragment that moves to the nucleus to activate genes that ameliorate ER stress. S1P and S2P also mediate cleavage of the ER membrane transcription factor sterol response element binding protein (SREBP), involved in reg-

This article was published online ahead of print in *MBC in Press* (http://www.molbiolcell.org/cgi/doi/10.1091/mbc.E06–01–0055) on May 3, 2006.

[D] The online version of this article contains supplemental material at *MBC Online* (http://www.molbiolcell.org).

Address correspondence to: Maho Niwa (niwa@ucsd.edu).

Abbreviations used: DTT, dithiothreitol; ER, endoplasmic reticulum; Tg, thapsigargin; Tm, tunicamycin; UPR, unfolded protein response.

ulating cholesterol biosynthesis (Wang *et al.*, 1994; Sakai *et al.*, 1996).

In most studies of UPR function, elevated levels of ER unfolded proteins are typically induced by treating cells with pharmacological agents including dithiothreitol (DTT), which disrupts or prevents protein disulfide bonding; thapsigargin (Tg), an inhibitor of the ER Ca^{2+}-dependent ATPase; or tunicamycin (Tm), an inhibitor of protein glycosylation. Although UPR induction by pharmacological agents has proven extremely valuable for characterizing UPR pathway signaling components, functional roles for the UPR in physiological settings are not well defined. A well-studied example among the few known settings where the UPR is active is during the terminal differentiation of mature B lymphocytes (B-cells) into antibody secreting plasma cells (Calfon *et al.*, 2002; Gass *et al.*, 2002; Gunn and Brewer, 2003; Iwakoshi *et al.*, 2003; van Anken *et al.*, 2003; Zhang *et al.*, 2005). It is reported that during this process IRE1 and ATF6, but not PERK, are activated, and further that activation of ATF6 is preceded by activation of IRE1 (Gass *et al.*, 2002; Rutkowski and Kaufman, 2004). These observations indicate that activation of the tripartite UPR signaling branches is not a concerted process in vivo and suggest differences in the abilities of individual UPR initiators to recognize or respond to various forms of ER stress. In turn, individual branches may be specialized to respond to particular conditions.

As the ER performs a variety of protein maturation functions, the actual demand for specific protein folding functions may differ depending on prevailing conditions. An ability to selectively modulate individual UPR signaling branches might allow UPR responses to be customized to provide the most appropriate response. The contribution of each signaling branch to a custom response could be determined by the sensitivity of a UPR initiator to a given stress type alone or with the help of additional "discriminator" components.

Previous studies have focused on the individual signaling events mediated by each of the UPR components to understand their roles in the UPR. Very little is known about the relationships between the signaling branches initiated by IRE1, PERK, and ATF6. The activation behavior of UPR sensors in B-cell differentiation, however, highlights the importance of such studies in order to provide better understanding of UPR functions in physiological settings. Direct comparisons of the kinetic responses of UPR signaling branch activation, particularly during the experimentally well-defined ER stress caused by pharmacological agents, will provide a first step toward uncovering intrinsic differences in the behavior of, and relationships between signaling branches mediated by IRE1, PERK, and ATF6.

Here, we have compared the activation kinetics of IRE1, PERK, and ATF6 signaling branches in response to altered forms of ER stress induced by three pharmacological agents. ER stress induced by ER calcium release in particular revealed fundamental differences between UPR sensors; during Tg-induced UPR, both IRE1 and PERK were activated quickly, whereas ATF6 responded with significantly delayed kinetics. Furthermore, we observed that phosphorylation of the PERK kinase substrate, eIF2α, was modulated independent of PERK activation in Chinese hamster ovary (CHO) cells, suggesting the presence of an additional regulatory mechanism mediating events downstream of PERK kinase. Curiously, PERK-independent eIF2α phosphorylation may be specific to certain cell types because it was observed only in CHO cell. Further experiments also suggested that the observed kinetics were unlikely to be caused by disruption of the UPR sensor structure. Thus, our studies directly compare UPR signaling branch activation and reveal similarities, but importantly, fundamental differences between UPR sensors in their recognition of alternate forms of ER stress.

MATERIALS AND METHODS

Cell Culture and Induction of ER Stress

CHO cells were maintained in DMEM/F12 media (Cellgro, Herndon, VA) supplemented with 5% fetal calf serum (FCS; Invitrogen, Carlsbad, CA), 100 U/ml penicillin, and 100 μg/ml streptomycin (Cellgro). Cells were maintained at 37°C in a 5% CO_2 incubator. To induce ER stress, cells were seeded onto 10-cm plates at a density of 2–2.5 $\times$ 10^6. Twenty-four hours after seeding, cells were incubated for 2–3 h in fresh media without antibiotics before treating with 2 mM DTT (Invitrogen), or 200 nM Tg (Calbiochem, La Jolla, CA), or 10 μg/ml tunicamycin (Calbiochem). Although cells used in experiment shown in Figures 1B and 2 were treated with 20 μM MG-132 (Calbiochem) for 1 h before addition of 2 mM dithiothreitol, cells for all the rest of time-course experiments were not treated with this proteasome inhibitor. NIH3T3, mouse embryonic fibroblasts (MEFs), and HeLa cells were cultured in DMEM (Cellgro) supplemented with 10% FCS (Invitrogen), 100 U/ml penicillin, and 100 μg/ml streptomycin (Cellgro).

XBP1 Splicing Assay

Total RNA was prepared using RNeasy mini kit (Qiagen, Chatsworth, CA) and treated twice with RQ1 DNase (Promega, Madison, WI). DNase was removed by phenol chloroform extraction before ethanol precipitation. RNA was reverse-transcribed with ThermoScript reverse transcriptase (Invitrogen), and PCR was performed with iTaq polymerase (Bio-Rad, Hercules, CA). XBP1 mRNA was amplified using (CACCTGAGCCCCGAGGAG) and (TTAGTTCATTAATGGCTTCCAGC). PCR products were run on 1.5% agarose gels.

Western Blotting

For Western blotting anti-ATF6 (Imgenex, San Diego, CA), anti-β-actin (Sigma, St. Louis, MO), anti-BiP (StressGen, Victoria, British Columbia, Canada), anti-phospho-eIF2α (Cell Signaling, Beverly, MA), anti-total eIF2α and anti-ATF4 (both from Santa Cruz Biotechnology, Santa Cruz, CA) were purchased commercially. Antibodies against mouse PERK and mouse IRE1α were directed against the C-terminal residues of PERK (residues 1079–1100) and a protein fragment containing both kinase and endoribonuclease domains, respectively. Whole cell extracts were resolved by SDS-PAGE and transferred to nitrocellulose. Membranes were developed with ECL Plus Western blotting detection reagent (Amersham Biosciences, Piscataway, NJ).

Immunoprecipitation

Immunoprecipitation of PERK and IRE1α were carried out based on the protocols described in Bertolotti *et al.* (2000). Briefly, treated CHO cells (see above) were washed twice in ice-cold phosphate-buffered saline (PBS) and lysed in 200 μl 1% Triton buffer on ice. All following steps were performed at 4°C unless otherwise stated. Extracts were rotated end-over-end for 15 min, clarified by centrifugation at 16,000 $\times$ *g* for 10 min, and preincubated for 1 h with 10 μl protein G-agarose (Upstate Biotechnology, Lake Placid, NY). PERK and IRE1 were incubated overnight with anti-PERK (Santa Cruz Biotechnology) or anti-IRE1α and then incubated for 3 h with 10 μl protein G-agarose. Beads were washed three times in 1% Triton buffer and once in ice-cold PBS with 100 mM NaF. Proteins were boiled 10 min in 2$\times$ Laemmli buffer with 100 mM DTT and resolved by SDS-PAGE. Proteins were transferred to nitrocellulose and probed with antibodies.

Detection and Quantification

Chemifluorescence of Western blots and ethidium staining of agarose gels were visualized using a Typhoon 9400 imager (Amersham Biosciences). Bands were quantified using ImageQuant 5.2 software (Amersham Biosciences).

RESULTS

To uncover potential differences or similarities in their responses to UPR-activating agents, we first monitored the activation kinetics of UPR initiators (ATF6, IRE1, PERK) in CHO cells after ER-stress induction with pharmacological agents that induce unfolded proteins by different mechanisms. We used DTT to disrupt disulfide bond formation, Tg to inhibit ER Ca^{2+}-dependent ATPase, and Tm to inhibit glycosylation of newly synthesized proteins in the ER. We

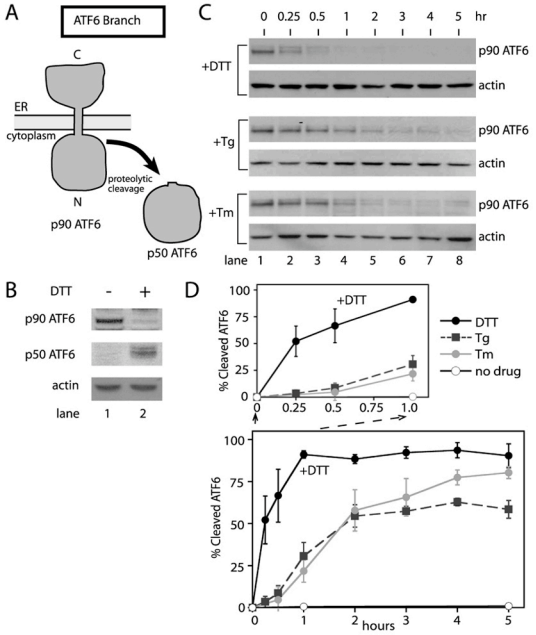

Figure 1. The ATF6 branch of the UPR is most responsive to the accumulation of unfolded proteins disrupted by disulfide bond formation in the ER. (A) ATF6 processing during the UPR induction. ATF6 (p90ATF6) is proteolytically cleaved during UPR induction. The transcriptional transactivation domain (p50ATF6) is released in the cytoplasm and subsequently migrates into the nucleus. (B) Conversion of p90ATF6 to p50ATF6 upon DTT treatment of CHO cells. Total cell lysate prepared from CHO cells pretreated with proteasome inhibitor was incubated with (lane 2; 2 mM for 1 h) or without DTT (lane 1) and analyzed by immunoblotting using anti-ATF6 antiserum raised against the N-terminal portion of ATF6 (Imgenex) and β-actin as a control. (C) Immunoblots of ATF6 from lysates of CHO cells treated with 2 mM DTT, 200 nM thapsigargin (Tg), and 10 μg/ml tunicamycin (Tm) for the indicated amount of time. At each time point, treated cells were collected and divided into two samples (for protein and RNA analysis) before quick freezing in liquid nitrogen. β-Actin immunoblotting of the same lysate, from each time course was carried out by reprobing blots with anti-β-actin antibody. (D) Quantitation of p90ATF6 cleavage over the time courses shown in C. p90ATF6 cleavage was quantitated with a Typhoon 9400 phosphorimager (Amersham Biosciences) and normalized with levels of β-actin from corresponding treatments. Percent cleaved ATF6 was calculated by subtracting the p90ATF6 at each time point from the level of p90ATF6 at time zero. The graph shown represents three independent time-course experiments carried out with each drug. Differences in the initial phases of the responses were shown with the close-up of the first hour of treatment; DTT (black solid line), Tg (black dashed line), and Tm (gray solid line). Untreated is represented as a solid black line with open circles.

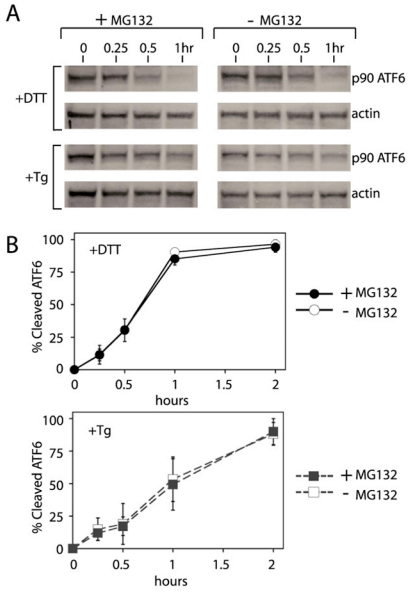

Figure 2. Rate of p90 ATF6 disappearance during the UPR is similar with or without proteasome inhibitor, MG132. (A) Immunoblots of ATF6 from HeLa cell lysates treated with 2 mM DTT, or 200 nM thapsigargin (Tg) in the presence of proteasome inhibitor, MG132, (lanes 1–4) or without MG132 (lane 5–8). β-Actin immunoblotting of the same lysates was used to normalize p90ATF6 quantitation. (B) Quantitation of p90ATF6 shown in A. Levels of p90ATF6 were quantitated using a Typhoon phosphorimager and normalized with levels of β-actin. Percent cleaved ATF6 was calculated as described in Figure 1 and were shown during DTT treatment with (●) or without (○) MG132 or during Tg treatment with (■) or without (□) MG132.

then compared the activation status IRE1, PERK, and ATF6 over time.

ATF6 Responds Most Quickly to DTT-induced UPR

ATF6 activation was measured by following its proteolytic cleavage over time by Western blotting with a monoclonal antibody raised against an N-terminal region of ATF6. This antibody was previously used and characterized by others and allowed observation of both p90 full-length and p50 cleaved ATF6 (Thuerauf *et al.*, 2002, 2004; Hong *et al.*, 2004). Thus, using this antibody, we detected a 90-kDa protein (p90 ATF6) in untreated CHO cells (Figure 1B, lane 1). Using the same antibody, UPR activation causes the disappearance of p90 ATF6 and the concomitant appearance of a 50-kDa fragment (p50 ATF6; Figure 1B, lane 2). Robust detection of p50 ATF6 required the presence of a proteasome inhibitor, indicating that the cleaved fragment is relatively unstable as previously reported (Haze *et al.*, 1999). Thus, ATF6 activation was quantitated by calculating the disappearance of full-length ATF6 over time. We found ~50% of p90 was cleaved at 15 min after DTT treatment (Figure 1C, lane 2, +DTT). Beyond 1 h essentially all full-length ATF6 had disappeared, indicating ATF6 activation is sustained throughout the time course (Figure 1, C and D).

During UPR induction by either Tm or Tg, ATF6 activation was comparatively slow. Almost no ATF6 was cleaved 15 min after Tm or Tg exposure and only ~50% was cleaved after 2 h (Figure 1, C and D, +Tg and +Tm). Beyond 2 h a more gradual increase in ATF6 cleavage was observed. Taken together, these results demonstrated that ATF6 responded to DTT- induced ER stress more quickly and more efficiently than to stress induced by Tg or Tm.

Activation of the UPR also induces ER-associated degradation (ERAD) to clear permanently misfolded proteins from the ER (Kaufman, 1999; Mori, 2000; Patil and Walter,

2001; Harding *et al.*, 2002; Meusser *et al.*, 2005; Sayeed and Ng, 2005). Thus, if a portion of p90ATF6 was degraded by ERAD instead of conversion to p50ATF6, quantitation of p90ATF6 might have overestimated the ATF6 activation rate. This could become a problem particularly if ERAD degradation of p90ATF6 differed depending on the agents used to induce ER stress. Thus, we measured p90ATF6 disappearance during DTT and Tg treatment in the presence of a well-characterized proteasome inhibitor, MG132, to inhibit ERAD (Figure 2). During both DTT- and Tg-induced UPR, slightly higher levels of p90ATF6 were detected in the presence of MG132. Furthermore, with DTT or Tg, quantitation of p90ATF6 showed similar rate of activation (p90ATF6 disappearance) between cells treated with or without MG132. Thus, ERAD mediated degradation of ATF6 is unlikely to account for differences in the rate of ATF6 activation during DTT- and Tg-induced UPR.

We also measured p90ATF6 disappearance in mouse embryonic fibroblasts derived from *Perk* knockout embryo (*Perk*−/− MEFs) in order to test if UPR-induced translation repression contributed to the disappearance of p90ATF6 (Supplementary Figure 1). During UPR induction by either DTT or Tg in *Perk*−/− MEFs, phosphorylation of the eIF2α translational initiator did not take place to repress translation (see below and Supplementary Figure 2). In *Perk*−/− MEFs, we found that the differences in the rates of P90ATF6 activation between DTT- and Tg-induced ER stress were similar to those of wild-type mouse 3T3 fibroblast (Supplementary Figure 1, and unpublished data). Together, these experiments provided further support for the use of p90ATF6 disappearance as a measure of p90ATF6 activation, and thus, that ATF6 responds more efficiently to DTT-induced ER stress than to Tg.

The PERK Signaling Branch Responds Efficiently to ER Stress Induced by Tg and by DTT

To allow direct comparisons, we analyzed the activation kinetics of both IRE1 and PERK signaling branches in the same lysates used for the ATF6 time-course experiments. UPR induction by DTT, Tm and Tg has been shown to induce PERK autophosphorylation that can be monitored by the appearance of a slower migrating band on SDS-PAGE (Shi *et al.*, 1998; Harding *et al.*, 1999; Bertolotti *et al.*, 2000). Thus, we examined PERK autophosphorylation to probe PERK activation after UPR induction. By immunoprecipitating with an antibody against the PERK N-terminal region followed by immunoblotting with an antibody raised against the C-terminal kinase domain, we could detect PERK efficiently in untreated or UPR-activated CHO cells (Figure 3). A slower migrating form of PERK was detected within 15 min of incubation (Figure 3B, indicated as p-PERK) with DTT and Tg treatment of CHO cells. Furthermore, this form continued to increase over a 1-h incubation. Phosphatase treatment of immunoprecipitated PERK changed its mobility on SDS-PAGE, consistent with the previous reports that phosphorylation was responsible for the slow mobility form of PERK (unpublished data). Together, kinetic appearance of autophosphorylated PERK (p-PERK) during DTT-induced UPR was almost identical to that during Tg-induced UPR (Figure 3, B and C).

Treatment of CHO cells with Tm also produced autophosphorylated PERK, but with significantly slower kinetics; autophosphorylated PERK was not detected until 1 h after Tm treatment. Together, these results suggested that PERK could sense UPR induced by either DTT or Tg equally well, whereas ATF6 response to Tg was much slower than that to DTT (compare Figures 1 and 3). Thus, ER stress caused by Tg revealed differences in intrinsic abilities of ATF6 and PERK to sense lumenal conditions.

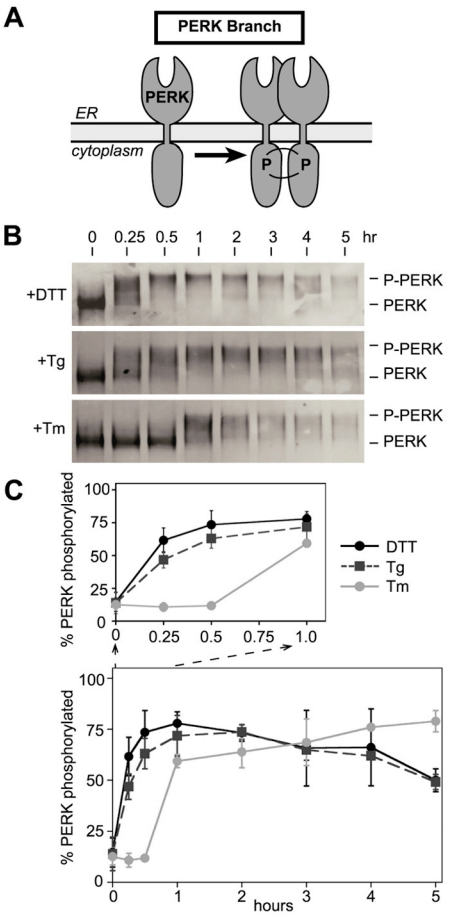

Figure 3. PERK activation measured by autophosphorylation is responsive to ER stress caused by both ER calcium release and disruption of disulfide bonds. (A) PERK autophosphorylates during the UPR response. (B) Immunoblots, after immunoprecipitation of PERK from CHO cells treated with thapsigargin (Tg; 200 nM), tunicamycin (Tm; 10 μg/ml), and DTT (2 mM) for indicated amounts of time. Immunoprecipitated PERK using anti-PERK antibody from total cell lysate of time points from each treatment were Western blotted with anti-PERK antiserum. The slower mobility PERK formed during ER stress caused by DTT, Tg, and Tm treatment is indicated as p-PERK. (C) Quantitation of p-PERK appearance shown in B. DTT (black solid line), Tg (black dashed line), and Tm (gray solid line).

Phosphorylation of the PERK Kinase Substrate, eIF2α, Occurs with Kinetics Different from Activation of PERK Itself

To further confirm the above observation, we followed the kinetics of PERK activation by quantitating its ability to phosphorylate eIF2α (p-eIF2α) by Western blotting using an antibody capable of specifically recognizing p-eIF2α in total cell lysates (Figure 4). A basal level of p-eIF2α was observed

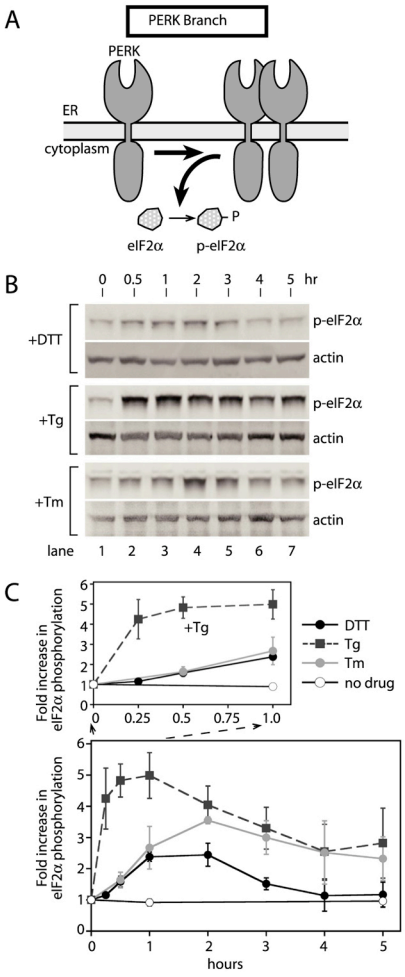

Figure 4. Phosphorylation of eIF2α, a PERK kinase substrate, is most responsive to ER stress caused by ER calcium release. (A) PERK phosphorylates eIF2α during UPR induction. (B) Immunoblots of phosphorylated eIF2α (p-eIF2α) and β-actin from lysates of CHO cells treated with DTT, thapsigargin (Tg), and tunicamycin (Tm) for the indicated amounts of time. For direct comparisons with ATF6- and IRE1-signaling branch activation, the same cell lysates used for Figure 1 were examined for phosphorylation of eIF2α. (C) Quantitation of the increase in phosphorylated eIF2α (p-eIF2α) levels over the time course shown in B. The levels of p-eIF2α were quantitated with a Typhoon 9400 phosphorimager and normalized to levels of β-actin. Fold induction was calculated by taking the ratio between the levels of normalized p-eIF2α at time zero and each time point. A close-up of the first hour is shown for comparison in the initial phases of the responses. The graph represents three independent time course experiments carried out with DTT (black solid line), Tg (black dashed line), and Tm (gray solid line). Untreated is represented as a solid black line with open circles.

in uninduced CHO cells (Figure 4B, lane 1). We also observed differences in the amount of basal p-eIF2α in other uninduced cell lines (see Figure 4 and Supplementary Figure 2). Tg treatment produced the most rapid and extensive response, within 15 min of incubation p-eIF2α was detected, increasing to fivefold within 30 min and reaching maximum induction by 1 h (Figure 4, B and C, +Tg). The rapid phosphorylation of eIF2α was consistent with the rapid autophosphorylation of PERK induced by Tg (Figure 3). Furthermore, this form continued to increase over a 1-h incubation, again correlating well with the time course of PERK autophosphorylation (compare Figure 3 with Figure 4).

The appearance of p-eIF2α after DTT and Tm treatment was both slower and less extensive (Figure 4, B and C). The increase in eIF2α phosphorylation produced by Tm was significant, but smaller and delayed compared with Tg. To our surprise, DTT treatment induced only a minimal increase in eIF2α phosphorylation throughout the time course (Figure 4, B and C). This was unexpected because autophosphorylation of PERK was much more efficient during DTT-induced UPR (Figure 3). With each inducing agent, eIF2α phosphorylation reached a maximum and then declined slowly. This decline is presumably caused by the accumulation of GADD34, a p-eIF2α specific phosphatase, as reported previously (Novoa *et al.*, 2001). In all three cases, using antibody that detects total eIF2α protein, we found that eIF2α protein levels remains unchanged after UPR induction (Supplementary Figure 3), consistent with a previous report (Harding *et al.*, 2000a). From these results, we conclude that activation of the PERK-induced UPR signaling branch or phosphorylation of a PERK kinase target at least is most responsive to ER stress caused by Tg, less responsive to that by Tm, and least responsive to DTT. Thus, PERK appeared to respond equally well to ER stress induced by DTT and Tg, based on the kinetic appearance of p-PERK, whereas PERK activation was significantly delayed with DTT when phosphorylation of eIF2α was used to determine the order of PERK activation.

BiP Dissociation from PERK Lumenal Domain Correlates with Autophosphorylation of PERK

To further investigate the discrepancy between the kinetics of PERK autophosphorylation and PERK phosphorylation of eIF2α, we examined the kinetics of BiP dissociation from PERK lumenal domain. BiP, is a major ER chaperone, that has been identified as PERK-interacting protein coimmunoprecipitating with PERK (Bertolotti *et al.*, 2000; Ma *et al.*, 2002). In addition, BiP dissociation from PERK lumenal domains has been shown to induce PERK autophosphorylation and oligomerization (Bertolotti *et al.*, 2000; Ma *et al.*, 2002). Thus, we tested if the kinetics of BiP dissociation from PERK reflected the appearance of either phosphorylated PERK or phosphorylated eIF2α in response to ER stress agents. We examined BiP association with PERK by blotting PERK immunoprecipitates with anti-BiP antibody (Figure 5, B and C), as previously established (Bertolotti *et al.*, 2000). We found that levels of coimmunoprecipitated BiP in uninduced cells (Figure 5A, lane 2; and 5B, lanes 1, 5, and 9) were comparable with these previous reports and was reduced upon UPR induction with treatment of cells with Tg (Figure 5A, lanes 2 vs. 3, or 5B, lanes 5 vs. 8). Furthermore, BiP coimmunoprecipitation was specific to anti-PERK antibody, because we detected no significant levels of BiP coimmunoprecipitated with anti-myc antibody (Figure 5A, lanes 1 vs. 2). Normalizing the levels of coimmunoprecipitated BiP to immunoprecipitated PERK revealed a significant reduction in PERK-associated BiP at 30 min after exposure of CHO cells to Tg (Figure 5C). We detected a similar reduction in BiP-associated PERK during the DTT-induced ER stress. In contrast, Tm treatment did not cause changes in the levels of BiP associated with PERK. Thus, kinetic changes in BiP levels

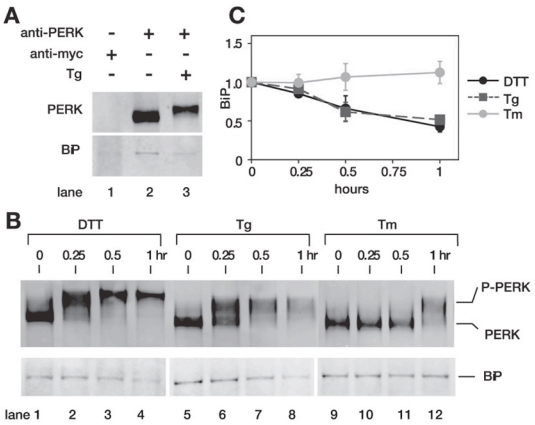

Figure 5. PERK activation measured by dissociation of BiP correlates with PERK activation measured by PERK autophosphorylation. (A) Immunoprecipitation of BiP was specific to uninduced PERK. BiP was specifically immunoprecipitated with anti-PERK antibody from uninduced lysate (lane 2), but not with anti-myc antibody (lane 1). Furthermore, UPR induction upon Tg treatment diminished levels of BiP-associated PERK (lane 3). (B) BiP associated with PERK during treatment with DTT (lanes 1–4), Tg (lanes 5–8), and Tm (lanes 9–12) is shown. Levels of BiP associated with PERK in each immunoprecipitated fraction were detected by blotting the same membranes using anti-BiP antibody. (C) Quantitation of BiP associated with PERK. Levels of BiP associated with PERK were quantitated with a phosphorimager and normalized against immunoprecipitated PERK from CHO cells treated with DTT (black solid line), Tg (black dashed line), and Tm (gray solid line). Error bars and values of each time point were averaged over three independent experiments.

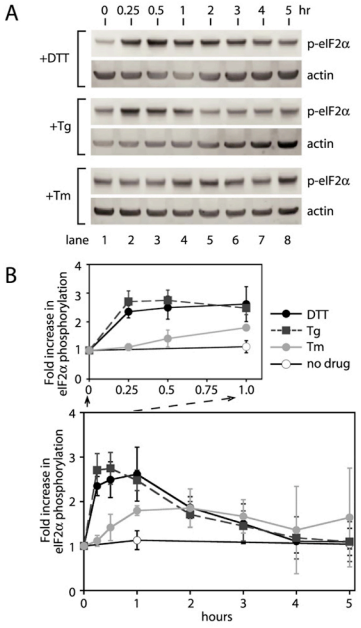

Figure 6. eIF2α phosphorylation during UPR induction in NIH3T3 cells. (A) Immunoblots of phosphorylated eIF2α (p-eIF2α) and β-actin from lysates prepared from NIH3T3 cells treated with DTT, thapsigargin (Tg), or tunicamycin (Tm) for the indicated amounts of time. (B) Quantitation of the fold increase in p-eIF2α levels over the time course shown in A. The levels of p-eIF2α were quantitated as described in Figure 2 and fold induction was calculated by taking the ratio between the levels of normalized p-eIF2α at time zero and each time point. A close-up of the first hour is shown for comparisons in the initial phase of the responses. The graph represents three independent time course experiments carried out with DTT (black solid line), Tg (black dashed line), and Tm (gray solid line). Untreated is represented as a solid black line with open circles.

were in general agreement with the appearance of phosphorylated PERK.

In addition to BiP dissociation, we also examined the kinetics of ATF4 appearance. Translation of ATF4 is regulated by small open reading frames (ORFs) present within the 5′ untranslated region (UTR) of ATF4 mRNA. When eIF2α is not phosphorylated, ATF4 translation is prevented by stop codons within the small ORFs causing translation initiation complexes to fall off the template (Vattem and Wek, 2004). In response to ER stress, phosphorylation of eIF2α suppresses initiation complex release from ATF4 mRNA, allowing ATF4 translation (Harding *et al.*, 2000b). Thus, we examined the appearance of ATF4 by Western blot in the same extract used above to analyze eIF2α phosphorylation (Supplementary Figure 4). Appreciable levels of ATF4 were detected after 3 h of incubation with DTT, whereas ATF4 started to accumulate after 1–2 h during the Tg treatment of cells. Because phosphorylation of eIF2α occurred more rapidly and efficiently with Tg than with DTT, the production of ATF4 further correlates with kinetics of eIF2α phosphorylation. Together, PERK appeared to respond equally well to ER stress induced by DTT and Tg, and thus, an additional regulatory step might exist to account for the altered kinetics of events downstream of PERK activation, including eIF2α phosphorylation and ATF4 production.

PERK Activation Kinetics in Mouse Fibroblast NIH3T3 Cells

Because differences in the kinetics of PERK activation measured by autophosphorylation and by eIF2α phosphorylation have not been reported previously, we examined eIF2α phosphorylation kinetics during UPR activation in cell lines other than CHO cells. On treatment of mouse NIH3T3 cells with DTT, Tg, or Tm, lysates were probed for phosphorylated forms of eIF2α with the same antibody used to detect p-eIF2α in CHO cells. Similar to CHO cells, we observed a robust increase in p-eIF2α levels that reached a maximum within 1 h of Tg treatment (Figure 6, A and B). NIH3T3 cells also produced a robust increase in p-eIF2α during DTT-induced ER stress. Thus, in 3T3 cells, the kinetics and the extent of increase in p-eIF2α was similar for both DTT- and Tg-induced ER stress. Therefore, a potential regulatory step conferring differences between the kinetics PERK kinase activation and of eIF2α phosphorylation might be specific to CHO cells.

IRE1 Discriminates between ER Stress Types

To monitor activation of IRE1, we examined IRE1 autophosphorylation after UPR induction by DTT, Tg, and Tm. IRE1 autophosphorylation can be monitored by mobility shift on SDS-polyacrylamide gels (SDS-PAGE; Tirasophon *et al.*, 1998; Bertolotti *et al.*, 2000; Lee *et al.*, 2002; Harding *et al.*, 2003) and has been used previously to analyze IRE1 activation. Endogenous IRE1 was detected by immunoprecipitation

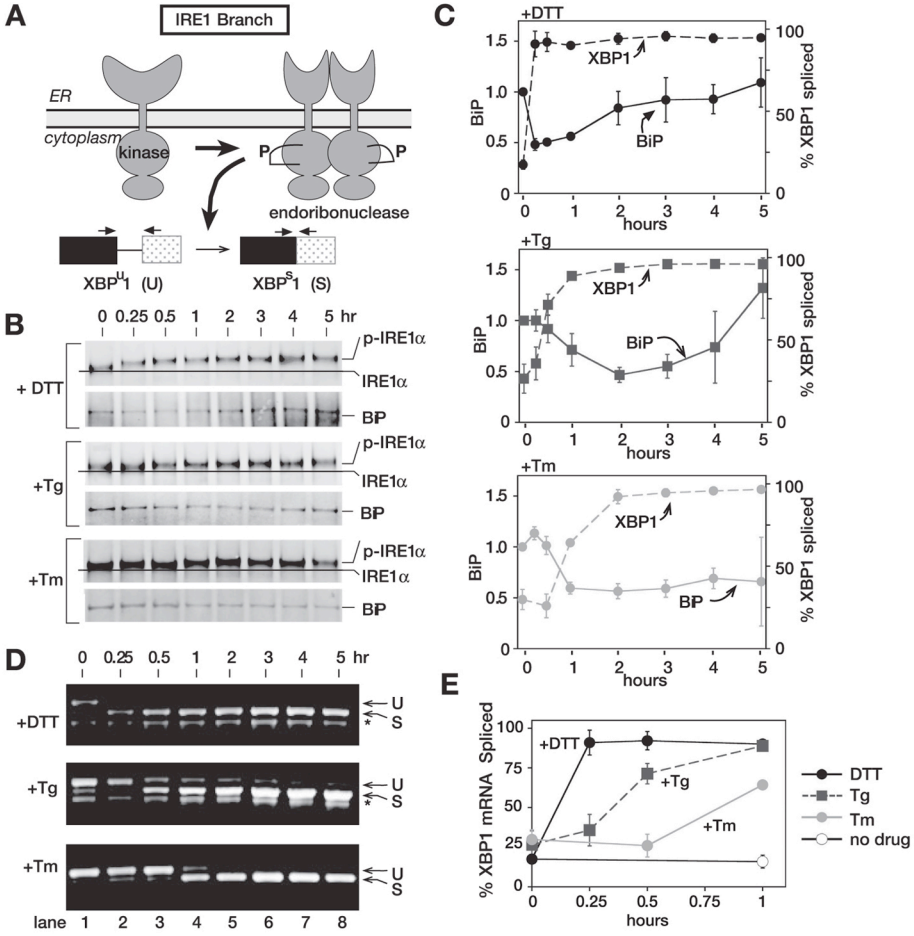

Figure 7. The IRE1 signaling branch of the UPR can respond efficiently to all types of ER stress, but is most sensitive to the accumulation of unfolded proteins due to disrupted disulfide bonds in the ER. (A) IRE1 autophosphorylates upon UPR induction. On activation, IRE1 becomes oligomerized and is an active endoribonuclease in the splicing of XBP1 mRNA. Schematic representation of both the unspliced (U) and spliced (S) forms of XBP1 mRNA and the PCR primers used. (B) Immunoblots, after immunoprecipitation, of IRE1α from CHO cells treated with DTT (2 mM), thapsigargin (Tg; 200 nM), and tunicamycin (Tm; 10 μg/ml) for indicated amounts of time using anti-IRE1α antiserum raised against the C-terminal portion of IRE1α. The slower mobility IRE1α formed during ER stress caused by DTT, Tg, and Tm treatment is indicated as p-IRE1α. BiP associated with IRE1α was detected by blotting the same membrane using anti-BiP antibody. During the analyses, we consistently observed that the extent of IRE1α mobility shift was much more pronounced during DTT-induced ER stress than during other treatments. Currently, the molecular bases for these differences are not clear, although they may represent differential phosphorylation in response to the altered forms of ER stress. (C) Quantitation of immunoprecipitated BiP. Levels of BiP associated with IRE1α were quantitated with a phosphorimager and normalized against immunoprecipitated IRE1α (shown as a solid line). Error bars and values of each time point were averaged over three independent experiments. IRE1α RNase activity indicated as % spliced XBP1 is shown as dashed line. (see E for detail). (D) RT-PCR of RNA isolated from CHO cells treated with 2 mM DTT, 200 nM thapsigargin (Tg), and 10 μg/ml tunicamycin (Tm). Total RNA was isolated from samples collected for Figures 1 and 3. cDNA was prepared using oligodT primers. PCR with primers flanking the 26-nt UPR intron of hamster XBP1 RNA. PCR products were analyzed on 1.5% agarose gels and stained with ethidium bromide. DNA fragments derived from unspliced (U) and spliced (S) are indicated. Bands marked as (*) are nonspecific PCR fragments. (E) Quantitation of the spliced XBP1 shown in D. Both unspliced and spliced forms of XBP1 were quantitated with a phosphorimager. Percent spliced at each time point was calculated by $S/(S + U) \times 100$. The graph represents three independent time-course experiments carried out with DTT (black solid line), thapsigargin (black dashed line), and tunicamycin (gray solid line). Untreated is represented as a solid black line with open circles. Quantitation of the spliced XBP1 for the entire 5-h time course was shown in C as dashed lines, whereas that for the first hour is shown in E.

with a polyclonal antibody against the C-terminal portion of IRE1 followed by immunoblotting with same antibody (Figure 7), allowing efficient detection of IRE1 in lysates from untreated and UPR-induced CHO cells. In response to DTT, we observed a decrease in IRE1 mobility starting after 15 min, consistent with the time frame we observed for XBP1 mRNA

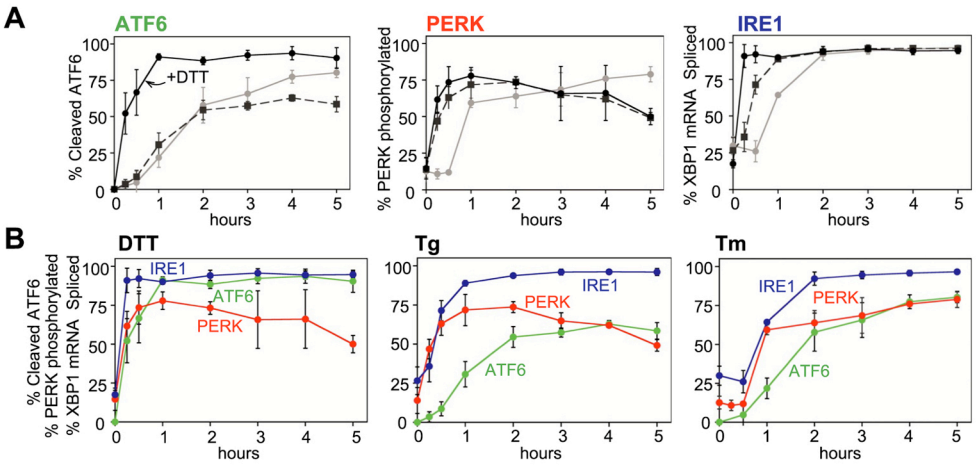

Figure 8. Preferential activation of UPR signaling branches by alternate types of ER stress. (A) ATF6 is activated quickly to disruption of disulfide bonds of ER proteins caused by DTT (black solid line), whereas both IRE1 and PERK are activated rapidly and extensively in response to ER stress caused by thapsigargin (black dashed line), an ER Ca^{2+} release agent. For all ER stress tested, IRE1 reacts relatively fast and efficiently, resulting in splicing of XBP1 mRNA. (B) Because all activation profiles for ATF6, PERK, and IRE1α described in Figures 1, 2, and 6 were performed with the same extract samples, the kinetic induction of the three UPR initiators was reanalyzed by the type of ER stress imposed. ER stress caused by DTT activated both IRE1α (blue) and ATF6 (green) rapidly and efficiently. UPR induced by thapsigargin was detected by both PERK (red) and IRE1 (blue), whereas all three UPR sensors respond to ER stress activated by tunicamycin with relatively similar kinetics.

splicing (Figure 7, B and C, and see below). The small mobility shifts upon IRE1 autophosphorylation has been reported previously, and we have found it to be consistent over multiple experiments (Tirasophon *et al.*, 1998; Bertolotti *et al.*, 2000; Lee *et al.*, 2002; Harding *et al.*, 2003). Phosphorylated IRE1 appeared at 30 min in Tg-treated CHO cells and at 1 h in Tm-treated cells.

BiP Dissociation from IRE1 Confers Specificity for Different ER Stress

In addition to autophosphorylation of IRE1, we examined the kinetics of BiP dissociation from IRE1 lumenal domains. BiP is a major ER chaperone, identified as an IRE1-interacting protein coimmunoprecipitating with IRE1 (Bertolotti *et al.*, 2000; Okamura *et al.*, 2000; Kimata *et al.*, 2004). In addition, BiP dissociation from IRE1α lumenal domains was shown to induce IRE1 autophosphorylation and oligomerization (Bertolotti *et al.*, 2000; Okamura *et al.*, 2000; Kimata *et al.*, 2004). Thus, we expected the kinetics of BiP dissociation to reflect the appearance of phosphorylated IRE1α in response to ER stress agents. We examined BiP association with IRE1α by blotting IRE1α immunoprecipitates with anti-BiP antibody (Figure 7B), as previously established (Bertolotti *et al.*, 2000). We found that levels of coimmunoprecipitated BiP were compatible with previous reports. Normalization of coimmunoprecipitated BiP levels to immunoprecipitated IRE1 revealed a significant reduction in IRE1-associated BiP 15 min after exposure of CHO cells to DTT (Figure 7, B and C), in agreement with the appearance of both phosphorylated IRE1α and spliced XBP1 mRNA (see below). Curiously however, levels of IRE1-asscociated BiP returned to unstimulated levels by 2 h after DTT treatment, contrasting with the sustained presence of phosphorylated IRE1α and spliced XBP1 over the 5-h time course. These results suggest that BiP reassociation precedes inactivation of IRE1α. Similarly, in direct agreement with the delayed appearance of phosphorylated IRE1α and spliced XBP1 mRNA after Tg treatment compared with DTT, we observed a significant decrease in IRE1-associated BiP at 1 h after treatment with Tg. This was followed by BiP reassociation starting at the 3-h time point (Figure 7, B and C). Thus, taken together, these results suggest that affinity of BiP for IRE1α differ depending upon the types of ER stress imposed.

The IRE1 Signaling Branch Responds Rapidly to Different Forms of Stress

To further monitor IRE1 activation, we assayed splicing of the 26-nucleotide UPR-specific intron (UPR intron) from XBP1 mRNA; an event dependent on activation of the IRE1 endoribonuclease domain. Splicing was quantitated by reverse transcription followed by PCR (RT-PCR) of cellular RNA isolated from cells at each time point (Figure 7, C–E). In untreated CHO cells, PCR amplification of cDNA using primers flanking the UPR intron produced the 599-base pair fragment predicted for unspliced XBP1 mRNA (U; Figure 7, A and D) and the 573-base pair fragment corresponding to spliced XBP1 RNA after UPR induction (S; Figure 7, A and D). Quantitation of the PCR fragments produced in untreated cells shows that ~20% of cellular XBP1 mRNA is present in the spliced form (Figure 7D, lane 1). This finding suggested that IRE1 was constitutively activated at a low level in normal cells, consistent with the low level of p-eIF2α also observed in these cells before UPR induction (Figures 4B and 7D).

IRE1 was maximally and nearly completely activated (~90% spliced) by DTT within 15 min of DTT treatment (Figure 7, C–E) and remained fully activated throughout the time course. As reported previously (Yoshida *et al.*, 2001), we also noted an increase in XBP1 mRNA at later time points (Figure 7D), consistent with the idea that XBP1 is a UPR target gene induced by ATF6. Because the splicing efficiency of XBP1 mRNA remained high throughout the time course, these results suggest that IRE1 endoribonuclease activity

remains active and capable of splicing all newly synthesized XPB1 mRNA.

In contrast to DTT, Tg treatment produced only a minimal increase in XBP1 splicing at 15 min after treatment (30% spliced), taking about 1 h to reach maximal levels, which were sustained throughout the time course (Figure 7, C–E). Tm-induced splicing did not occur until 1 h after incubation but did reach maximal levels by 2 h, which were also sustained through the time course (Figure 7, C–E). Thus, the timing of IRE1 autophosphorylation in response to UPR induction by DTT, Tg, and Tm correlated with the activation of IRE1-dependent splicing of XBP1 mRNA (compare Figure 7, B and D). Together these results showed that in contrast to the ATF6 and PERK signaling branches, which responded maximally to distinct ER stressors, the IRE1 signaling branch responded to each stressor in comparatively short time periods.

Differential Activation of UPR Signaling Branches Reflects Intrinsic Properties of UPR Sensors

A direct comparison of our findings, which were essentially all obtained from a single cell extract for each inducing agent, is shown in Figure 8A. In summary, the ATF6 branch responds rapidly to disulfide bond disruption and slowly to other forms of ER stress. The PERK signaling branch responds most rapidly to changes in ER Ca^{2+} release, whereas the IRE1 branch responds efficiently and relatively rapidly to each ER stress agent, although some discrimination was seen at early time points. When data from Figures 1, 3, and 7 were replotted by individual UPR-inducing agent (Figure 8B), it was clearly seen that activation of IRE1 and ATF6 by DTT was rapid and robust. Furthermore, although eIF2α phosphorylation was significantly delayed and inefficient in CHO cells, activation of PERK itself judged by its autophosphorylation occurred rapidly. Presumably, disruption of disulfide bonds by DTT results in accumulation of unfolded proteins quickly. On the other hand, ER stress due to Tg treatment revealed different properties of the initiators; a quick response to PERK and IRE1, but a significantly slower response to ATF6.

A trivial explanation for the differential responses we observed is structural damage to UPR sensors caused by the UPR-inducing agent. The lumenal domains of IRE1, PERK, and ATF6 each contain conserved cysteines as well as glycosylation sites. Thus, for example, the delayed activation of PERK by Tm could be due to structural disruption of its sensor domain. To test this possibility, we asked if Tm affected the rapid activation of PERK by DTT. Accordingly, we treated CHO cells simultaneously with DTT (2 mM) and Tm (10 μg/ml) and followed the activation of PERK, IRE1, and ATF6 activation by measuring PERK autophosphorylation, XBP1 mRNA splicing, and the disappearance of p90ATF6, respectively. If slow activation of PERK were caused by structural damage to PERK during Tm treatment, we would expect that its presence during DTT-induced ER stress should delay the rapid activation of PERK observed during DTT alone. As shown in Figure 9, we found that the addition of Tm did not change PERK, IRE1, or ATF6 activation kinetics compared with DTT treatment alone (compare DTT only, lanes 2–4, with DTT+Tm, lanes 5–7). Similar results were obtained when CHO cells were pretreated with Tm for 1 h before DTT addition (unpublished data). Thus, together, these results suggest that differences we observed in UPR sensor activation are likely to reflect differences intrinsic to the manner in which each sensor recognizes different stress types.

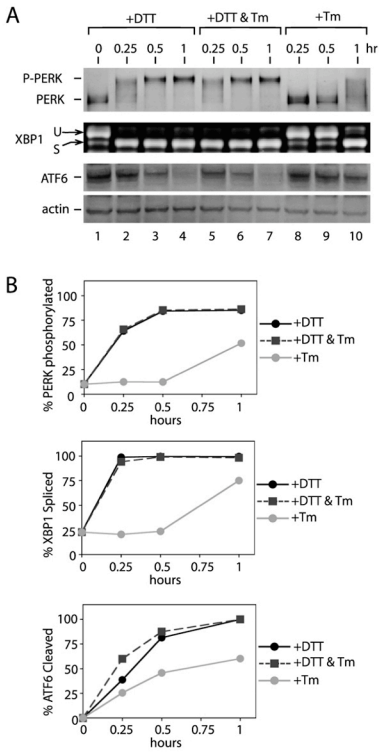

Figure 9. Differential activation of three UPR sensors is likely to reflect their intrinsic properties. (A) Activation kinetics of PERK, IRE1, and ATF6 signaling branches during DTT (2 mM) or tunicamycin (Tm; 10 μg/ml) treatment, or during treatment with both DTT (2 mM) and tunicamycin (Tm; 10 μg/ml) together for indicated amounts of time. Immunoblots, after immunoprecipitation, of PERK using anti-PERK antiserum, and of ATF6 using anti-ATF6 antibody and RT-PCR of XBP1 mRNA from total RNA isolated, are shown. (B) Quantitation of PERK autophosphorylation, ATF6 p90 fragment disappearance, and XBP1 mRNA splicing, shown in A during ER stress caused by DTT only (black solid line), both DTT and tunicamycin (black dashed line), and tunicamycin only (gray solid line).

DISCUSSION

The ER performs a variety of protein maturation steps including chaperone-assisted folding, modification, and complex assembly, for secreted proteins and proteins residing in the secretory pathway. Cellular demand for such functions fluctuates according to environmental or other specific growth conditions. In mammalian cells, at least three ER-proximal molecules (IRE1, PERK, and ATF6) sense ER protein-folding needs and initiate cellular responses to meet increased demand, collectively referred to as the UPR. Activation of each sensor results in the activation of specific transcription factors: XBP1 for IRE1, ATF4 for PERK, and activated ATF6 for ATF6—and thus, a major consequence of UPR activation is transcriptional induction of UPR target genes (Harding *et al.*, 2000a, 2003; Scheuner *et al.*, 2001b; Okada *et al.*, 2002; Lee *et al.*, 2003; Shen *et al.*, 2005). XPB1, ATF4, and ATF6 share some targets, but also activate unique sets of genes. Thus, selective activation and/or kinetic differences in the activation of specific transcription factors

may allow the ER to mount a "best-fit" response to prevailing ER conditions. Future experiments will be required to delineate how the observed differences in activation of the UPR sensors dictate overall transcription outputs, depending on types of ER stress.

Alternate transcriptional profiles of UPR target genes in response to different forms of ER stress could be achieved by regulation at several levels. Here we show that such regulation begins at the ER lumen. We show that although IRE1 and PERK display similar sensitivities to alternate stress types, ATF6 behaves differently. IRE1 and PERK were activated with nearly equal efficiency during UPR induction by DTT (disulfide bond inhibition) and also similarly to Tg (ER calcium efflux). However ATF6 was significantly less sensitive than IRE1 or PERK to Tg-induced ER stress. Because IRE1, PERK, and ATF6 each respond with approximately equal efficiencies to DTT, the inefficient response of ATF6 to Tg may reflect intrinsic differences in how ATF6 senses ER stress. In physiological settings, UPR activation could be caused by multiple forms of ER stress, possibly obscuring an objective analysis of UPR initiator properties. Thus, our use of pharmacological agents to induce defined types of stress in tissue culture cells was key to observing differences in the properties of UPR initiators. Because these similarities and differences between the properties of UPR initiators have never been examined side-by-side, our findings have paved a road for further studies to determine detail molecular mechanisms underlying these differences.

How can the kinetic responses we observed for each ER sensor be explained? A trivial explanation could postulate that pharmacological agents used to induce the UPR produce direct structural "damage" to UPR sensors. For example, the PERK lumenal (sensor) domain contains at least one conserved glycosylation site. If Tm disrupted proper PERK folding, PERK function could be diminished and cause delayed activation kinetics. However, based on our two drug experiments, this would seem unlikely because Tm did not prevent the rapid appearance of phosphorylated PERK caused by DTT (Figure 9). Thus, kinetic differences between sensor activation seem more likely to reflect intrinsic differences in stress-type recognition by the sensors themselves.

Topologically, IRE1 and PERK are similar; both are transmembrane receptor kinases with N-terminal domains that sense conditions within the ER lumen (Liu *et al.*, 2000, 2002). The recently published crystal structure of the yeast IRE1 (yIre1p) lumenal domain provides exciting insights into how UPR sensors may recognize ER lumenal conditions (Credle *et al.*, 2005). yIre1p contains a structural element similar to the peptide-binding groove of major histocompatibility complexes (MHC). Modeling experiments followed by mutagenesis predicted that a 10-residue poly-valine peptide can fit in the yIre1p MHC-like peptide-binding groove without steric-hindrance. Interestingly, a conserved stretch of hydrophobic and hydrophilic residues facing the groove floor appear important for IRE1 function because mutations within this conserved stretch diminish IRE1 function (Credle *et al.*, 2005). Thus, the model allows that unfolded polypeptides or partially folded protein could bind directly to the IRE1 groove to affect Ire1 activation. Critical determinants for peptide binding to the IRE1 groove might therefore reside with specific amino acids or with steric features of "unfolded" or "partially unfolded" polypeptides. Amino acid sequence conservation between IRE1 and PERK infers a similarly sized peptide-binding groove in the PERK lumenal domain. Thus, regardless of specific requirements for binding, the mechanism of polypeptide recognition by PERK seems likely to be similar to IRE1. The similarity we observed between IRE1 and PERK activation kinetics is therefore consistent with this structure-based model. It would be interesting to determine if "unfolded" polypeptides produced by different forms of ER stress have similar binding properties for the IRE1 (or PERK) polypeptide-binding groove.

Based on the amino acid alignments, however, two specific loops (between β10 and β11 and between β17 and β18, based on the yIre1 lumenal structure) differ significantly in length when compared between IRE1 and PERK (Credle *et al.*, 2005). For yIre1, these loops appear to be exposed to the surface of the peptide-binding groove. Thus, differences in sizes of these loops could provide subtle alterations in peptide binding. On close inspection, our data suggest that IRE1 responds slightly faster to DTT than Tg, whereas PERK responds almost identically to each drug. In addition to differences in loop size, one of the PERK loops contains two cysteines that are conserved between species. Although mutational studies have not assigned significant structural importance to these residues, they may be involved in discriminating between different types of ER stress (Ma *et al.*, 2002; Narasimhan *et al.*, 2004).

Finally, structural differences between MHC class I (MHC I) and class II (MHC II) molecules may also provide interesting mechanistic insights into the specificity of polypeptide binding between IRE1 and PERK. Although the overall structures of the MHC I and MHC II peptide-binding grooves are similar, amino acids at the ends of the two α-helices comprising the MHC I groove are in closer proximity to each other and are involved in peptide binding (Bjorkman, 1997). This structural feature seems to place constraints on the size and sequence of polypeptides available for binding. In addition to size, most peptides bound by MHC I contain hydrophobic or basic residues at their C-termini. In contrast, the MHC II groove is more open, allowing longer peptides to bind. Furthermore, residues within the MHC I groove are directly involved in peptide binding. These structural variations contribute the differences in polypeptide bindings between MHC I and II such that MHC I binds smaller peptides, whereas MHC II can accommodate larger polypeptides (Bjorkman, 1997). Thus, structural differences between IRE1 and PERK determined by residues at the end of the groove, or differences in the types of amino acid residues surrounding the groove surface could play a role in their differential activation kinetics with specific types of ER stress.

In contrast to IRE1 and PERK, less structure-function information is available for the lumenal portion of ATF6. On activation, ATF6 might create polypeptide-binding pockets different from IRE1 or PERK. ATF6 is a type II transmembrane protein, with its C-terminus in the ER lumen and a cytoplasmic N-terminus. Although an MHC-like peptide binding pocket is not predicted by the ATF6 amino acid sequence, two stretches of homologous sequence approximately 40 residues each in the ATF6 lumenal domain appear to be conserved across species (Shen *et al.*, 2002, 2005) and may thus be involved in binding unfolded polypeptides when dimerized/oligomerized. Alternatively, they might provide a binding site for potential UPR-associated regulatory factors. In addition, these ATF6 also contains conserved cysteines and conserved sites of potential glycosylation. In contrast to IRE1, mutations in conserved ATF6 glycosylation sites caused either constitutive activation or increased rate of ATF6 responses (Hong *et al.*, 2004). Thus, these conserved glycosylation sites, as well as the conserved cysteines might be located on the surface of a polypeptide-binding pocket and play a role in regulating the kinetic response of ATF6 to

different stress types. Further structural analysis of the ATF6 lumenal domain will help to answer such mechanistic questions.

Before the IRE1 crystal structure, the most widely discussed model of UPR sensor activation proposed a single mechanism for activating all three sensors. This model proposes that under nonstressed conditions, sensor activation is repressed by binding of the major ER chaperone BiP to sensor lumenal domains, whereas under stressed conditions, high levels of unfolded proteins cause BiP dissociation from UPR sensors, allowing activation to proceed (Bertolotti *et al.*, 2000; Ma *et al.*, 2002; Shen *et al.*, 2002).

Based on the BiP dissociation model then, the kinetic behaviors of UPR sensor activation could be governed by the affinity of BiP for unfolded proteins or the dissociation constants of BiP from each UPR sensor. Our observations, however, suggest a more complicated scenario. On one hand, rapid dissociation of BiP from both IRE1 and PERK during Tg-induced UPR might suggest a high-affinity of BiP for unfolded protein induced by Tg (Figures 5 and 7). On the other hand, the slower activation of ATF6 by Tg suggests the opposite. In contrast, if the affinity of BiP for UPR sensors plays a major role, the kinetic order of IRE1, PERK, and ATF6 should be the same for any type of ER stress. However, this was not what we observed because ATF6 activation was rapid in response to DTT but slow in response to Tg (Figures 1 and 8). In addition, although the antibody we used to detect ATF6 by Western blot was unable to immunoprecipitate ATF6 (and thus subsequent examination of BiP association was not possible), the behavior of BiP with both IRE1 and PERK provide further support for the presence of an additional control(s). We observed that robust PERK autophosphorylation within 15 min of DTT or Tg treatment, but did not observe significant BiP dissociation until at least 30 min (Figure 5). We have also observed BiP reassociation at time points when IRE1 was still active (Figure 7). Thus, although BiP dissociation clearly occurs during UPR activation, the kinetic behavior of all three UPR sensors suggests the presence of additional regulatory mechanisms or components. Presumably, such additional control mechanism(s) would allow UPR sensors to fine tune both the speed and extent of activation, depending on specific types and magnitude of ER stress. Together, our observation is consistent with both recent x-ray crystal structural study and deletion analysis where the putative BiP-binding domain within yIre1 lumenal domain can be deleted without significant changes in Ire1 activity (Kimata *et al.*, 2004).

Events downstream of sensor activation may also be regulated by additional components. During DTT-induced ER stress in CHO cells, PERK phosphorylation of eIF2α was inefficient although PERK activation, measured by either autophosphorylation or by BiP dissociation, occurred efficiently (Figures 3–5). Although several kinases are reported to phosphorylate eIF2α, we and others have shown that eIF2α phosphorylation does not occur in PERK knockout MEFs treated with UPR-inducing agents, indicating that PERK is the only kinase that phosphorylates eIF2α during the UPR (Supplementary Figure 2; Harding *et al.*, 2000a, 2002b). Thus, additional components or regulatory mechanisms must also exist to explain the kinetics of eIF2α phosphorylation we observed. Curiously, because this alteration occurred only in CHO cells but not in mouse 3T3 cells, this regulatory machinery may be specific to certain cell types or species. Perhaps, the kinetics of UPR sensor activation can be further modulated this machinery, again to meet specific demands, as seen by kinetic production of ATF4 transcription factor followed the eIF2α phosphorylation kinetics (Supplementary Figure 4). Such localized modulation could also influence final outcomes of the UPR without drastically changing the signaling pathway.

Time-dependent expression of mammalian genes has been described previously (Yoshida *et al.*, 2003). Transcription of certain genes regulated specifically by XBP1, including EDEM (involved in degrading glycosylated proteins), are up-regulated at much later times than some ATF6-regulated genes, including ER chaperones. This is due to the time required to produce UPR-specific transcription factors. The time required to produce active ATF6 transcription factor is considerably shorter than that to produce XBP1 because ATF6 requires only proteolytic cleavage of a preexisting ATF6 protein, whereas XBP1 production requires mRNA splicing (by activated IRE1) and translation. The differential kinetics of UPR signaling branch activation could therefore alter the time and/or the magnitude of the downstream events they control while maintaining the overall order of ATF6 and XBP1 activation. For example, the time to produce functional XBP1 protein after ATF6 activation varies with the UPR-inducing agent. Depending on type of ER stress, this could be caused by modulating either the absolute amount of activated transcription factor produced or by controlling the extent of translational repression, with either one resulting in a best-fit UPR response.

Finally, our work also provides important insights to further understand the behavior of UPR sensors in physiological settings. During terminal differentiation of mature B-cells to plasma cells, IRE1 and ATF6, but not PERK, were found to be activated (Gass *et al.*, 2002; Rutkowski *et al.*, 2004). Our results here show that IRE1 and PERK respond similarly to different type of ER stress (disruption of glycosylation, disruption of disulfide bonds, ER calcium release). Thus, the lack of PERK activation during B-cell differentiation suggests an additional level of regulatory control in physiological settings. For example, a specific inhibitor might prevent PERK activation during B-cell differentiation. Future studies will be needed to uncover such additional regulatory mechanisms.

ACKNOWLEDGMENTS

We thank Dr. Doug Cavener for providing *Perk*$-/-$ and $+/+$ MEFs and Dr. Douglass Forbes for discussion and critical comments on the manuscript. We also thank Drs. Douglass Forbes, Randy Hampton, and Vivek Malhotra for critical reading of the manuscript and Alicia Bicknell, Aditi Chawla, and Ryan Brunsing for valuable discussion and their helpful comments throughout this work. This work was supported by a National Institutes of Health predoctoral training grant to J.B.D. and by the Searle Scholar Program to M.N. via the University of California, Cancer Research Committee and American Cancer Society Grant RSG-05-059-01-GMC to M.N.

REFERENCES

Bertolotti, A., Zhang, Y., Hendershot, L. M., Harding, H. P., and Ron, D. (2000). Dynamic interaction of BiP and ER stress transducers in the unfolded-protein response. Nat. Cell Biol. *2*, 326–332.

Bjorkman, P. J. (1997). MHC restriction in three dimensions: a view of T cell receptor/ligand interactions. Cell *89*, 167–170.

Calfon, M., Zeng, H. Q., Urano, F., Till, J. H., Hubbard, S. R., Harding, H. P., Clark, S. G., and Ron, D. (2002). IRE1 couples endoplasmic reticulum load to secretory capacity by processing the XBP-1 mRNA. Nature *415*, 92–96.

Cox, J. S., Shamu, C. E., and Walter, P. (1993). Transcriptional induction of genes encoding endoplasmic-reticulum resident proteins requires a transmembrane protein- kinase. Cell *73*, 1197–1206.

Credle, J. J., Finer-Moore, J. S., Papa, F. R., Stroud, R. M., and Walter, P. (2005). On the mechanism of sensing unfolded protein in the endoplasmic reticulum. Proc. Natl. Acad. Sci. USA *102*, 18773–18784.

Gass, J. N., Gifford, N. M., and Brewer, J. W. (2002). Activation of an unfolded protein response during differentiation of antibody-secreting B cells. J. Biol. Chem. *277*, 49047–49054.

Gilmore, R. (1993). Protein translocation across the endoplasmic-reticulum—a tunnel with toll booths at entry and exit. Cell *75*, 589–592.

Gunn, K. E., and Brewer, J. W. (2003). The unfolded protein response in marginal zone and follicular zone B cells. FASEB J. *17*, C209–C209.

Harding, H. P., Calfon, M., Urano, F., Novoa, I., and Ron, D. (2002). Transcriptional and translational control in the mammalian unfolded protein response. Annu. Rev. Cell Dev. Biol. *18*, 575–599.

Harding, H. P., Novoa, I., Zhang, Y. H., Zeng, H. Q., Wek, R., Schapira, M., and Ron, D. (2000a). Regulated translation initiation controls stress-induced gene expression in mammalian cells. Mol. Cell *6*, 1099–1108.

Harding, H. P., Zhang, Y., and Ron, D. (1999). Protein translation and folding are coupled by an endoplasmic-reticulum-resident kinase. Nature *397*, 271–274.

Harding, H. P., Zhang, Y. H., Bertolotti, A., Zeng, H. Q., and Ron, D. (2000b). Perk is essential for translational regulation and cell survival during the unfolded protein response. Mol. Cell *5*, 897–904.

Harding, H. P. *et al.* (2003). An integrated stress response regulates amino acid metabolism and resistance to oxidative stress. Mol. Cell *11*, 619–633.

Haze, K., Yoshida, H., Yanagi, H., Yura, T., and Mori, K. (1999). Mammalian transcription factor ATF6 is synthesized as a transmembrane protein and activated by proteolysis in response to endoplasmic reticulum stress. Mol. Biol. Cell *10*, 3787–3799.

Hong, M., Luo, S. Z., Baumeister, P., Huang, J. M., Gogia, R. K., Li, M. Q., and Lee, A. S. (2004). Underglycosylation of ATF6 as a novel sensing mechanism for activation of the unfolded protein response. J. Biol. Chem. *279*, 11354–11363.

Iwakoshi, N. N., Lee, A. H., Vallabhajosyula, P., Otipoby, K. L., Rajewsky, K., and Glimcher, L. H. (2003). Plasma cell differentiation and the unfolded protein response intersect at the transcription factor XBP-1. Nat. Immunol. *4*, 321–329.

Kaufman, R. J. (1999). Stress signaling from the lumen of the endoplasmic reticulum: coordination of gene transcriptional and translational controls. Genes Dev. *13*, 1211–1233.

Kimata, Y., Oikawa, D., Shimizu, Y., Ishiwata-Kimata, Y., and Kohno, K. (2004). A role for BiP as an adjustor for the endoplasmic reticulum stress-sensing protein Ire 1. J. Cell Biol. *167*, 445–456.

Lee, A. H., Iwakoshi, N. N., and Glimcher, L. H. (2003). XBP-1 regulates a subset of endoplasmic reticulum resident chaperone genes in the unfolded protein response. Mol. Cell. Biol. *23*, 7448–7459.

Lee, K., Tirasophon, W., Shen, X. H., Michalak, M., Prywes, R., Okada, T., Yoshida, H., Mori, K., and Kaufman, R. J. (2002). IREI-mediated unconventional mRNA splicing and S2P-mediated ATF6 cleavage merge to regulate XBP1 in signaling the unfolded protein response. Genes Dev. *16*, 452–466.

Li, M. Q., Baumeister, P., Roy, B., Phan, T., Foti, D., Luo, S. Z., and Lee, A. S. (2000). ATF6 as a transcription activator of the endoplasmic reticulum stress element: thapsigargin stress-induced changes and synergistic interactions with NF-Y and YY1. Mol. Cell. Biol. *20*, 5096–5106.

Liu, C. Y., Schroder, M., and Kaufman, R. J. (2000). Ligand-independent dimerization activates the stress response kinases IRE1 and PERK in the lumen of the endoplasmic reticulum. J. Biol. Chem. *275*, 24881–24885.

Liu, C. Y., Wong, H. N., Schauerte, J. A., and Kaufman, R. J. (2002). The protein kinase/endoribonuclease IRE1alpha that signals the unfolded protein response has a luminal N-terminal ligand-independent dimerization domain. J. Biol. Chem. *277*, 18346–18356.

Ma, K., Vattem, K. M., and Wek, R. C. (2002). Dimerization and release of molecular chaperone inhibition facilitate activation of eukaryotic initiation factor-2 kinase in response to endoplasmic reticulum stress. J. Biol. Chem. *277*, 18728–18735.

Meusser, B., Hirsch, C., Jarosch, E., and Sommer, T. (2005). ERAD: the long road to destruction. Nat. Cell Biol. *7*, 766–772.

Mori, K. (2000). Tripartite management of unfolded proteins in the endoplasmic reticulum. Cell *101*, 451–454.

Mori, K., Ma, W. Z., Gething, M. J., and Sambrook, J. (1993). A transmembrane protein with a Cdc2+/Cdc28-related kinase-activity is required for signaling from the ER to the nucleus. Cell *74*, 743–756.

Narasimhan, J., Staschke, K. A., and Wek, R. C. (2004). Dimerization is required for activation of eIF2 kinase Gcn2 in response to diverse environmental stress conditions. J. Biol. Chem. *279*, 22820–22832.

Novoa, I., Zeng, H. Q., Harding, H. P., and Ron, D. (2001). Feedback inhibition of the unfolded protein response by GADD34-mediated dephosphorylation of eIF2 alpha. J. Cell Biol. *153*, 1011–1021.

Okada, T., Yoshida, H., Akazawa, R., Negishi, M., and Mori, K. (2002). Distinct roles of activating transcription factor 6 (ATF6) and double-stranded RNA-activated protein kinase-like endoplasmic reticulum kinase (PERK) in transcription during the mammalian unfolded protein response. Biochem. J. *366*, 585–594.

Okamura, K., Kimata, Y., Higashio, H., Tsuru, A., and Kohno, K. (2000). Dissociation of Kar2p/BiP from an ER sensory molecule, Ire1p, triggers the unfolded protein response in yeast. Biochem. Biophys. Res. Commun. *279*, 445–450.

Papa, F. R., Zhang, C., Shokat, K., and Walter, P. (2003). Bypassing a kinase activity with an ATP-competitive drug. Science *302*, 1533–1537.

Patil, C., and Walter, P. (2001). Intracellular signaling from the endoplasmic reticulum to the nucleus: the unfolded protein response in yeast and mammals. Curr. Opin. Cell Biol. *13*, 349–355.

Rutkowski, D. T., and Kaufman, R. J. (2004). A trip to the ER: coping with stress. Trends Cell Biol. *14*, 20–28.

Sakai, J., Duncan, E. A., Rawson, R. B., Hua, X. X., Brown, R. S., and Goldstein, J. L. (1996). Sterol-regulated release of SREBP-2 from cell membranes requires two sequential cleavages, one within a transmembrane segment. Cell *85*, 1037–1046.

Sayeed, A., and Ng, D.T.W. (2005). Search and destroy: ER quality control and ER-associated protein degradation. Crit. Rev. Biochem. Mol. Biol. *40*, 75–91.

Scheuner, D., Song, B., McEwen, E., Liu, C., Laybutt, R., Gillespie, P., Saunders, T., Bonner-Weir, S., and Kaufman, R. J. (2001a). Translational control is required for the unfolded protein response and in vivo glucose homeostasis. Mol. Cell *7*, 1165–1176.

Scheuner, D., Song, B. B., McEwen, E., Liu, C., Laybutt, R., Gillespie, P., Saunders, T., Bonner-Weir, S., and Kaufman, R. J. (2001b). Translational control is required for the unfolded protein response and in vivo glucose homeostasis. Mol. Cell *7*, 1165–1176.

Shamu, C. E., and Walter, P. (1996). Oligomerization and phosphorylation of the Ire1p kinase during intracellular signaling from the endoplasmic reticulum to the nucleus. EMBO J. *15*, 3028–3039.

Shen, J. S., Chen, X., Hendershot, L., and Prywes, R. (2002). ER stress regulation of ATF6 localization by dissociation of BiP/GRP78 binding and unmasking of golgi localization signals. Dev. Cell *3*, 99–111.

Shen, X. *et al.* (2001). Complementary signaling pathways regulate the unfolded protein response and are required for *C. elegans* development. Cell *107*, 893–903.

Shen, X. H., Ellis, R. E., Sakaki, K., and Kaufman, R. J. (2005). Genetic interactions due to constitutive and inducible gene regulation mediated by the unfolded protein response in *C-elegans.* PLoS Genet. *1*, 355–368.

Shi, Y. G., Vattem, K. M., Sood, R., An, J., Liang, J. D., Stramm, L., and Wek, R. C. (1998). Identification and characterization of pancreatic eukaryotic initiation factor 2 alpha-subunit kinase, PEK, involved in translational control. Mol. Cell. Biol. *18*, 7499–7509.

Sidrauski, C., and Walter, P. (1997). The transmembrane kinase Ire1p is a site-specific endonuclease that initiates mRNA splicing in the unfolded protein response. Cell *90*, 1031–1039.

Thuerauf, D. J., Morrison, L., and Glembotski, C. C. (2004). Opposing roles for ATF6 alpha and ATF6 beta in endoplasmic reticulum stress response gene induction. J. Biol. Chem. *279*, 21078–21084.

Thuerauf, D. J., Morrison, L. E., Hoover, H., and Glembotski, C. C. (2002). Coordination of ATF6-mediated transcription and ATF6 degradation by a domain that is shared with the viral transcription factor, VP16. J. Biol. Chem. *277*, 20734–20739.

Tirasophon, W., Welihinda, A. A., and Kaufman, R. J. (1998). A stress response pathway from the endoplasmic reticulum to the nucleus requires a novel bifunctional protein kinase/endoribonuclease (Ire1p) in mammalian cells. Genes Dev. *12*, 1812–1824.

van Anken, E., Romijn, E. P., Maggioni, C., Mezghrani, A., Sitia, R., Braakman, I., and Heck, A.J.R. (2003). Sequential waves of functionally related proteins are expressed when B cells prepare for antibody secretion. Immunity *18*, 243–253.

Vattem, K. M., and Wek, R. C. (2004). Reinitiation involving upstream ORFs regulates ATF4 mRNA translation in mammalian cells. Proc. Natl. Acad. Sci. USA *101*, 11269–11274.

Voeltz, G. K., Rolls, M. M., and Rapoport, T. A. (2002). Structural organization of the endoplasmic reticulum. EMBO Rep. *3*, 944–950.

Walter, P., and Johnson, A. E. (1994). Signal sequence recognition and protein targeting to the endoplasmic-reticulum membrane. Annu. Rev. Cell Biol. *10*, 87–119.

Wang, X. D., Sato, R., Brown, M. S., Hua, X. X., and Goldstein, J. L. (1994). Srebp-1, a membrane-bound transcription factor released by sterol-regulated proteolysis. Cell *77*, 53–62.

Wang, X. Z., Harding, H. P., Zhang, Y., Jolicoeur, E. M., Kuroda, M., and Ron, D. (1998). Cloning of mammalian Ire1 reveals diversity in the ER stress responses. EMBO J. *17*, 5708–5717.

Ye, J., Rawson, R. B., Komuro, R., Chen, X., Dave, U. P., Prywes, R., Brown, M. S., and Goldstein, J. L. (2000). ER stress induces cleavage of membrane-bound ATF6 by the same proteases that process SREBPs. Mol. Cell *6*, 1355–1364.

Yoshida, H., Matsui, T., Hosokawa, N., Kaufman, R. J., Nagata, K., and Mori, K. (2003). A time-dependent phase shift in the Mammalian unfolded protein response. Dev. Cell *4*, 265–271.

Yoshida, H., Matsui, T., Yamamoto, A., Okada, T., and Mori, K. (2001). XBP1 mRNA is induced by ATF6 and spliced by IRE1 in response to ER stress to produce a highly active transcription factor. Cell *107*, 881–891.

Yoshida, H., Okada, T., Haze, K., Yanagi, H., Yura, T., Negishi, M., and Mori, K. (2000). ATF6 activated by proteolysis binds in the presence of NF-Y (CBF) directly to the cis-acting element responsible for the mammalian unfolded protein response. Mol. Cell. Biol. *20*, 6755–6767.

Zhang, K., Wong, H. N., Song, B., Miller, C. N., Scheuner, D., and Kaufman, R. J. (2005). The unfolded protein response sensor IRE1alpha is required at 2 distinct steps in B cell lymphopoiesis. J. Clin. Invest. *115*, 268–281.

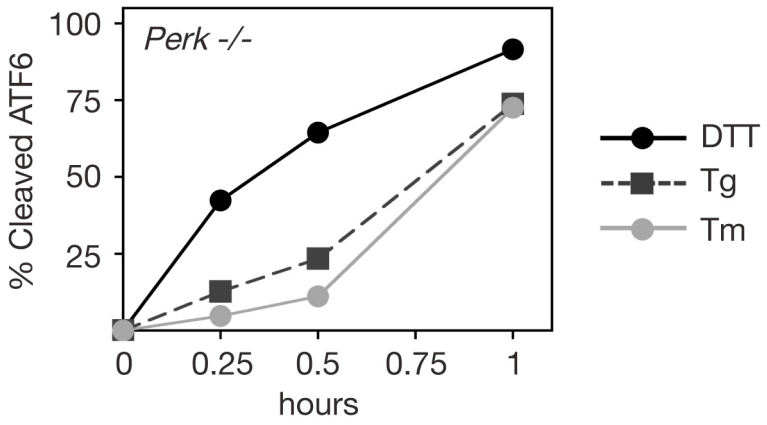

Supplementary Figure 1. Rate of disappearance of p90 ATF6 in the *Perk-/-* cells.
Percent cleaved p90 ATF6 in mouse embryonic fibroblasts (MEFs) derived from PERK knockout mouse (*PERK-/-*) treated with DTT (black solid line), thapsigargin (black dashed line), and tunicamycin (gray solid line).

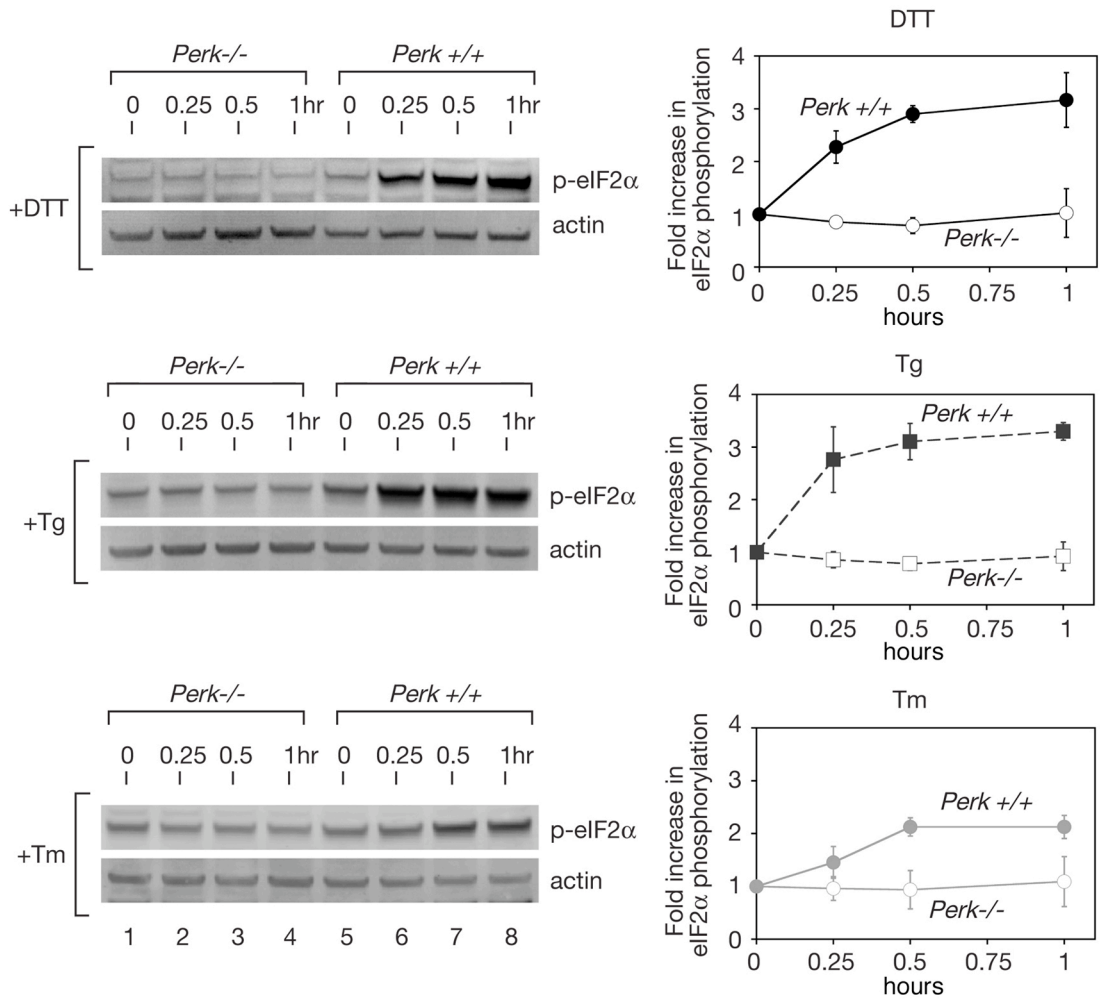

Supplementary Figure 2. PERK is the only kinase responsible for eIF2α phosphorylation during the UPR.

(A) Immunoblots of phosphorylated eIF2α (p-eIF2α) and β-Actin from lysates of mouse embryonic fibroblasts (MEFs) derived from either the wild type (*Perk+/+*) or PERK knockout mouse (*Perk-/-*) (Zhang *et al.*, 2002). Either wild type or PERK knockout cells were treated with DTT, thapsigargin (Tg), and tunicamycin (Tm) for the indicated amounts of time.

(B) Quantitation of the increase in p-eIF2α levels over the time course as shown in (A). The levels of p-eIF2α were quantitated and normalized to levels of β-Actin. Fold induction of p-eIF2α in *PERK+/+* (solid) or *PERK-/-* (open) MEFs was calculated by taking the ratio between the levels of normalized p-eIF2α at time zero and each time point. The graphs represent three independent time course experiments carried out with DTT (black solid line) Tg (black dashed line), Tm (gray solid line).

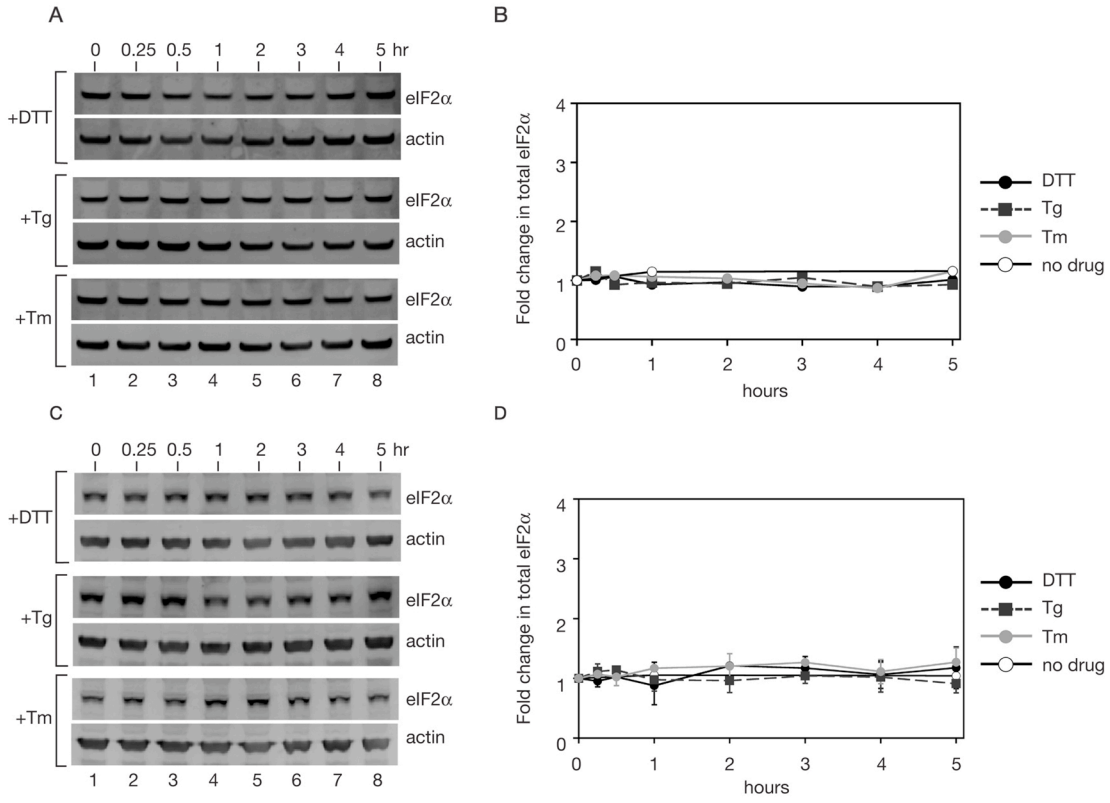

Supplementary Figure 3. Total level of eIF2α does not change during the UPR time courses.
(A) Immunoblots of total eIF2α and β-Actin from lysates of CHO cells treated with DTT, thapsigargin (Tg), and tunicamycin (Tm) for the indicated amounts of time.
(B) Quantitation of total eIF2α levels over the time course as shown in (A). The levels of eIF2α were quantitated with a Typhoon 9400 phosphorimager and normalized with levels of β-Actin. Fold induction was calculated by taking the ratio between the levels of normalized eIF2α at time zero and each time point. The graph represents three independent time course experiments carried out with DTT (black solid line), thapsigargin (black dashed line), and tunicamycin (gray solid line). Untreated (NT) is represented as a solid black line with open circles.
(C) Immunoblots of total eIF2α and β-Actin from lysates of NIH3T3 cells treated with DTT, thapsigargin (Tg), and tunicamycin (Tm) for the indicated amounts of time.
(D) Quantitation of total eIF2α levels over the time course shown in (C) was carried out and plotted as described in (B).

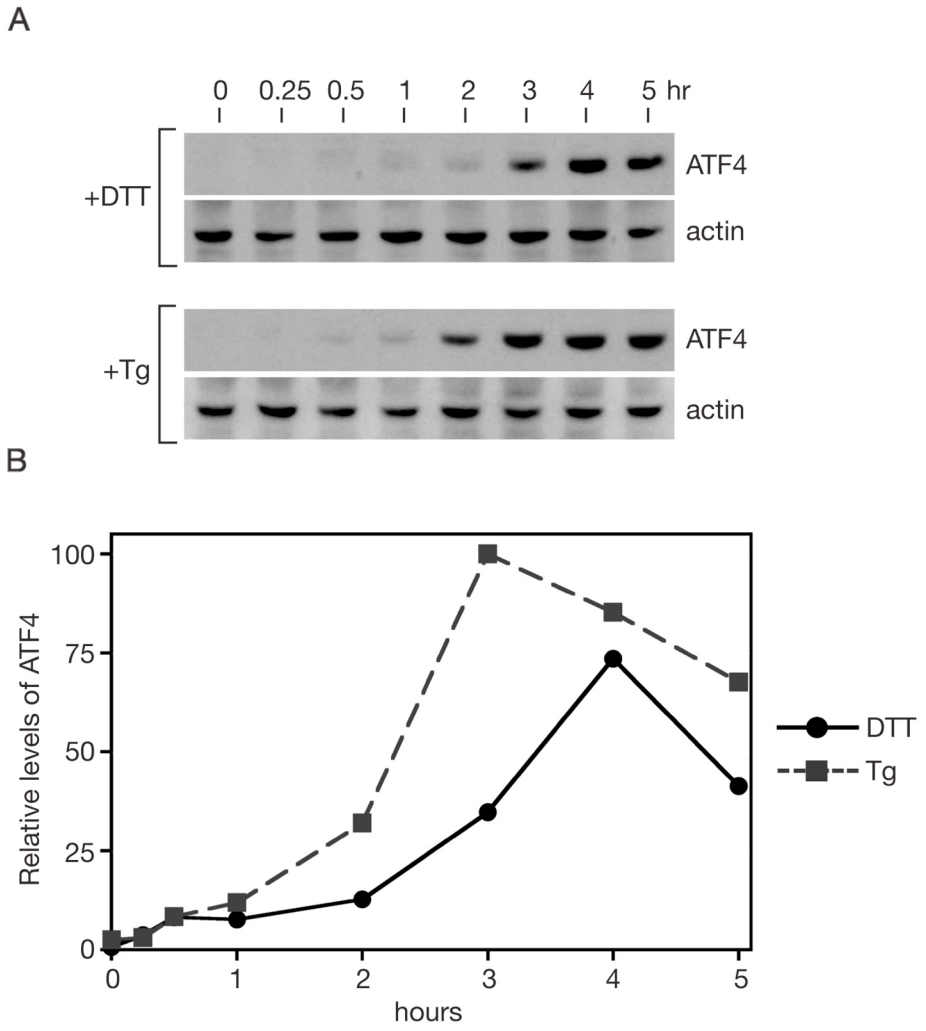

Supplementary Figure 4. Production of ATF4 protein during ER stress correlates with phosphorylation of eIF2α in CHO cells.
(A) Immunoblots of ATF4 from lysates of CHO cells treated with dithiothreiltol (DTT) and thapsigargin (Tg) for the indicated amount of time.
(B) Quantitation of ATF4 levels over the time course shown in (A). DTT is represented as a black solid line, and Tg as a black dashed line.

Acknowledgements

Chapter 1, in full, is a reprint of the material as it appears in Molecular Biology of the Cell 2006. DuRose, Jenny B.; Tam, Arvin B.; Niwa, Maho, The American Society for Cell Biology, 2006. The manuscript is reproduced with the permission of all co-authors. The dissertation author, Jenny Bratlien DuRose was the primary investigator and author of this paper.

Supplementary References

Zhang, P., McGrath, B., Li, S., Frand, A., Zambito, F., Reinert, J., Gannon, M., Ma, K., McNaughton, K., and Cavener, D.R. (2002). The PERK eukaryotic initiation factor 2 alpha kinase is required for the development of the skeletal system, postnatal growth, and the function and viability of the pancreas. Mol Cell Biol. *11*, 3864-3874.

CHAPTER 2

Regulation of Ribosomal RNA Transcription by the Unfolded Protein Response During Endoplasmic Reticulum Stress

Summary

All living organisms must adapt to their ever-changing environment in order to maintain homeostasis and viability. The folding, processing, and assembly of secreted proteins or proteins residing within the secretory pathway begins in the endoplasmic reticulum (ER). When the equilibrium between the client protein load and the ERs capacity to process that load is off balance, the ER must quickly respond to prevent toxic accumulation of improperly folded proteins within the organelle. Conditions interfering with ER protein-folding activate the unfolded protein response (UPR) signaling pathway to restore ER homeostasis by modulating gene expression and downregulating global protein synthesis. Here we report that the UPR modulates the expression of the most abundant RNA species, rRNA. Coordination of ribosome biogenesis and protein synthesis is important for balancing cell growth with nutrient availability, which is predominantly controlled by the target of rapamycin (TOR). Here we show that phosphorylation of eIF2α by PERK is necessary for disrupting the rRNA preinitiation complex downregulating rRNA transcription independent of the TOR pathway. Our study is the first to link phosphorylation of eIF2α with regulation rRNA synthesis, and provides an initial framework for understanding how the UPR coordinately regulates translation and rRNA transcription in order to maintain ER homeostasis.

Introduction

In their lifetime, all living organisms are subject to fluctuations in their environment. Evolution of systems to sense and respond to stressful conditions allows the organism to quickly counter the action of the stress minimizing potential damage or possible death. A common strategy among stress responses is modulation of gene expression programs at all stages including protein synthesis to facilitate the return to homeostasis. Currently, two major mechanisms have been described for regulation of protein production rates: one via regulation of the target of rapamycin (TOR) pathway and the other by phosphorylation of eukaryotic translation initiation factor 2 alpha (eIF2α).

The TOR pathway is responsible for coordinately regulating global translation initiation and ribosome biogenesis in response to cues promoting cell growth (e.g. growth factors) and nutrient availability. The TOR pathway adjusts cellular translation by phosphorylation of translation initiation factor 4E binding protein (Beretta et al., 1996; Brunn et al., 1997) and modulates ribosome biogenesis by increasing both translation of ribosomal proteins (Brown et al., 1995; Chung et al., 1992; Price et al., 1992) and ribosomal RNA (rRNA) transcription by RNA Polymerase I (Pol I; Hannan et al., 2003; James and Zomerdijk, 2004; Mayer et al., 2004). Building new ribosomes consumes an enormous amount of energy and represents a significant investment in the

protein biosynthetic capacity of the cell. The TOR pathway can be thought of as a dial that can tune the efficiency of translation initiation and rRNA transcription up or down in order to balance the demand for resources to sustain cell functions with the need for cell growth. While the TOR pathway balances growth signals with nutrient availability, cells must also adjust the rate of protein synthesis in response to other challenges and stressful conditions.

The other major pathway for regulating translation is through phosphorylation of eIF2α and can be thought of as an emergency brake rather than a dial for modulating protein synthesis. The importance of this pathway is demonstrated by the evolution of at least four distinct eIF2α kinases in mammalian cells, each responding to a different set of stress conditions (Berlanga et al., 1999; Chen et al., 1991; Harding et al., 1999; Meurs et al., 1990; Shi et al., 1998; Sood et al., 2000). Under normal conditions eIF2α kinases are inactive and upon stress stimulation phosphorylate eIF2α preventing recycling of the eIF2 complex, thus inhibiting formation of the 43S translation initiation complex (Cherbas and London, 1976; Clemens et al., 1982; Farrell et al., 1977; Siekierka et al., 1982). This allows cells to rapidly downregulate protein synthesis during stress even under conditions where growth signaling and nutrient availability are not immediately limiting, for example during the unfolded protein response (UPR).

The UPR signaling pathway monitors the protein folding of the endoplasmic reticulum (ER). The synthesis, folding, and modification of proteins targeted to membranes or the secretory pathway takes place within the ER. When protein folding in the ER is perturbed by environmental insult or when protein-folding demands exceeds its capacity to fold them, unfolded proteins accumulate within the ER resulting in activation of the UPR pathway. In mammals, there are three sensor molecules spanning the ER membrane that are responsible for initiating the UPR pathway: ATF6, IRE1, and PERK (Harding et al., 1999; Shi et al., 1998; Tirasophon et al., 1998; Wang et al., 1998; Yoshida et al., 1998). Although each protein is very unique, the unifying feature of the UPR initiators is that they detect ER stress through their luminal domains and transduce the signal across the ER membrane to their cytosolic effector domains. While activation of all three UPR branches increases production of ER chaperones and facilitates clearance of unfolded proteins from the organelle, the UPR specific kinase PERK phosphorylates eIF2α resulting in translation repression (Harding et al., 2000; Harding et al., 1999; Shi et al., 1998). In contrast to the TOR pathway, stress responses utilizing eIF2α phosphorylation have not been reported to regulate ribosome biogenesis. We postulate that the continued investment in ribosome synthesis during ER stress would impose an unnecessary drain on cellular resources. We hypothesize that like the TOR pathway, the UPR pathway coordinately

regulates translation and ribosome biogenesis in order to maintain homeostasis during ER stress.

In this report, we examined the impact of UPR induction on ribosome biogenesis and found that in fact, the UPR rapidly downregulates rRNA transcription. We have identified that downregulation of rRNA transcription is achieved by dissociation of Pol I and a major Pol I transcription factor from the rRNA promoter. Furthermore, we have shown that phosphorylation of eIF2α by PERK is necessary for regulation of rRNA transcription, and have begun to unravel the mechanism of how the ER communicates with the nucleolus during ER stress.

Results

Activation of UPR Inhibits Pol I Transcription

In order to examine whether rRNA is downregulated during the UPR, we measured their levels in RNA isolated from nuclei of NIH3T3 cells upon UPR induction. We reasoned this would allow us to enrich for nascent rRNA while eliminating the majority of stable steady-state rRNA in the cytoplasm. We isolated nuclear RNA from an equal number of cells upon treatment without (NT) or with thapsigargin (Tg), an inhibitor of the ER calcium ATPase that perturbs ER protein folding and induces UPR. We found a striking decrease in the level of 18S and 28S rRNA in Tg treated nuclei compared to NT nuclei on northern gels stained with ethidium (Figure 1A). The 18S and

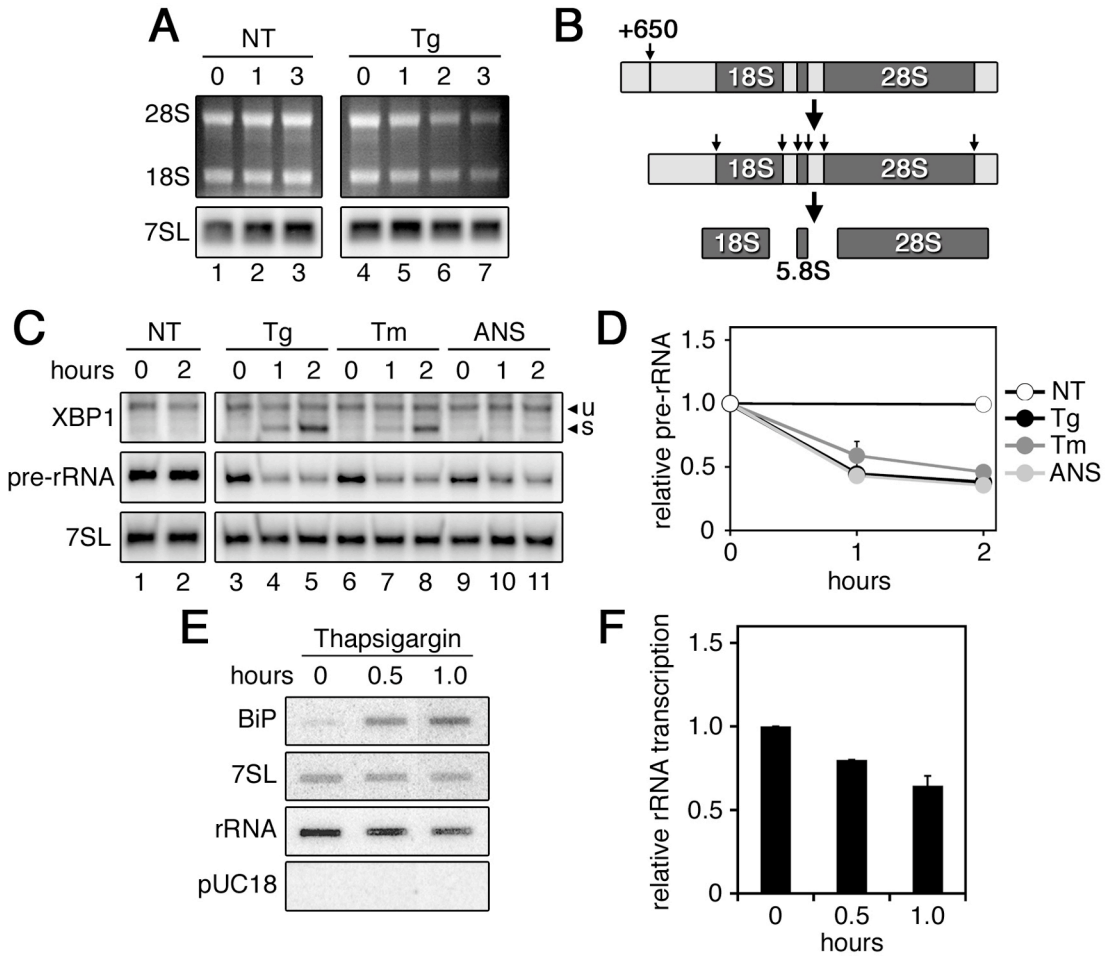

Figure 1. rRNA Transcription is Downregulated Upon UPR Activation.
(A) Northern Blot of nuclear RNA from an equal number of NIH 3T3 cells. Ethidium staining of mature 28S and 18S rRNAs (top panel). Autoradiograph of 7SL RNA (bottom panel).
(B) 47S primary rRNA transcript (not to scale). Small arrows represent endonucleolytic cleavages that occur producing mature 18S, 5.8S, and 18S rRNAs (dark gray).
(C) UPR-induced downregulation of pre-rRNA. Cellular RNA isolated from MEFs were untreated (NT) or treated with Tg (200 nM), Tm (10 μg/mL), or ANS (10 μM). At indicated time points, total RNA was analyzed by RNase protection probing for XBP1, pre-rRNA, and 7SL. Unspliced and spliced XBP1 protected fragments are indicated by U and S respectively.
(D) Quantitation of pre-rRNA relative to 7SL in NT cells (-○-) and during Tg (-●-), Tm (-●-) and ANS (-●-) treatment as shown in (C). Each point represents the mean ± standard deviation (SD) of a minimum of three independent experiments.
(E) Autoradiograph of labeled transcripts elongated *in vitro* from nuclei isolated from NIH3T3 cells treated with Tg (200 nM) and hybridized to DNA fragments corresponding to BiP mRNA, 7SL RNA, rRNA, and pUC18.
(F) Measurement of labeled rRNA transcripts relative to 7SL as shown in (E). Each bar represents the mean and SD of two independent experiments.

28S rRNA decreases within the first hour of Tg treatment, and is barely visible after 3 hr (Figure 1A, lanes 5-7). When we probed northern blots from the same gel for 7SL, an RNA polymerase III transcript that is unchanged during UPR, we found that its level remained constant suggesting that not all transcripts are decreased in nuclear RNA extracts. In addition, quantitative PCR analysis of BiP mRNA revealed that the level of this UPR target gene was increased as expected in nuclear RNA from Tg treated cells compared to NT cells, while the level of β-actin mRNA did not significantly change during either treatment (Data not shown). Together these results indicate that activation of UPR specifically decreases the level of rRNA in the nucleus, which is likely occurring by either decreasing its synthesis, or promoting its degradation.

To determine whether the UPR pathway regulates rRNA synthesis, we measured the level of newly synthesized rRNA in total RNA isolated from murine embryonic fibroblasts (MEFs) during a UPR time course. Here we chose to follow the disappearance of the rRNA primary transcript (pre-rRNA) to further substantiate our findings. Pre-rRNA is synthesized as a long 47S RNA which undergoes multiple cleavages and modifications before assembly into ribosomes (Figure 1B). The nascent rRNA undergoes processing which begins with an endonucleolytic cleavage in the 5' external transcribed spacer (5' ETS) at the +650 nt position (Miller and Sollner-Webb, 1981). Processing

of the 5'ETS occurs so rapidly that the vast majority of precursor rRNA in the nucleolus has already been cleaved, thus level of uncleaved pre-rRNA closely approximates the most newly synthesized rRNA (Miller and Sollner-Webb, 1981). We designed a probe for an RNase protection assay (RPA) that encompasses this initial cleavage site such that the uncleaved pre-rRNA generates a protected fragment that is 232 nt, whereas post-cleavage protected fragments are half the size and migrate much faster during gel electrophoresis (Figure 2A). We found that the nascent pre-rRNA decreases rapidly within the first hour of Tg treatment and decreases by nearly three folds after 2 hr Tg treatment relative to 7SL RNA (Figure 1C, lanes 3-5; and 1D). The result of this RPA was confirmed by northern blotting for full-length pre-rRNA (Figure 3) and is linear over a four-fold range of input RNA (Figure 2B). The extent of UPR induction was measured by an RPA probe detecting both spliced and unspliced forms of XBP1 mRNA (Figure 2A).

The unconventional splicing of the transcription factor XBP1 is mediated by the ER resident transmembrane UPR component IRE1 (Cox et al., 1993; Mori et al., 1993; Sidrauski and Walter, 1997; Tirasophon et al., 1998; Yoshida et al., 2001). Splicing of the UPR intron results in a frame shift that is crucial for the formation of a fully active XBP1 transcription factor and upregulation of UPR target genes (Calfon et al., 2002; Yoshida et al., 2001). XBP1 splicing is a hallmark of UPR activation, and is rapidly induced by Tg

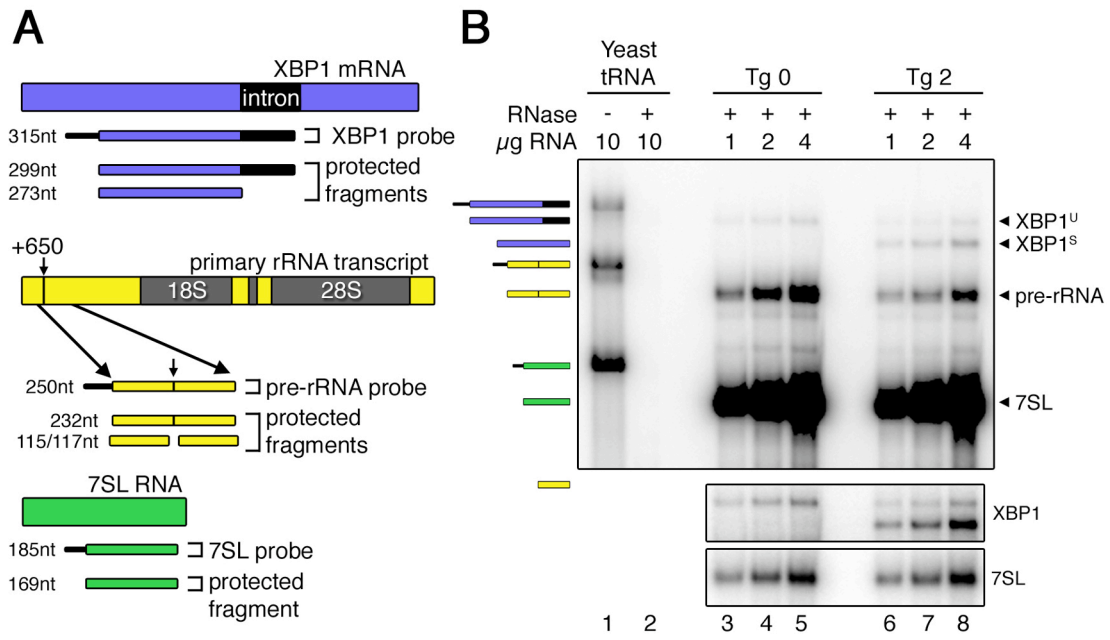

Figure 2. RNAse Protection Assay.
(A) Probe design for RNase protection assay (RPA) against murine XBP1 mRNA, pre-rRNA, and 7SL (not to scale). The XBP1 probe contains sequences complimentary to nucleotides 207-505 of the XBP1 coding region. The XBP1 probe yields two distinct protected fragments corresponding to unspliced and spliced forms XBP1. The pre-rRNA probe is complimentary to nucleotides 537-767 of the of the rRNA primary transcript yielding a protected fragment of 232 nt. If cleavage at site +650 has occurred, potential protected fragments are half the size and migrate much faster on the polyacrylamide gel. 7SL probe is complimentary to nucleotides 59-227 of 7SL RNA. All probes contain 16-18 nt of non-complementary sequence at the 5' end of the probe (black lines) in order to distinguish full length probe from full length protected fragments.
(B) Autoradiograph of a representative RPA showing a single exposure of all three probes on the top panel, and lower panels show optimal exposures of XBP1 and 7SL. Lanes 1 and 2 are control RNase protection reactions using yeast tRNA without (lane 1) or with (lane 2) addition of RNase. Lanes 3-8 are RNase protection reactions from the indicated concentration of wild type MEF RNA isolated from cells without (lanes 3-5) or with (lanes 6-7) treatment of 200 nM Tg for 2 hr. RNA was hybridized to all three probes overnight and the entire reaction was loaded onto a 6% denaturing acrylamide gel except 1/25th of the reaction was loaded in lane 1 to show undigested probes. Note the lack of protected fragments in lane 2 indicating probes do not to hybridize to one another, and in lanes 3-8 small protected fragments resulting from pre-rRNA cleaved products are not shown.

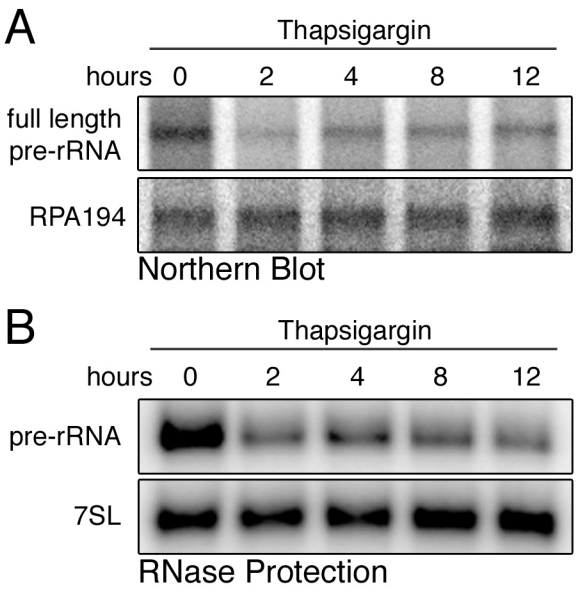

Figure 3. Comparison of pre-rRNA analyzed by Northern or RPA.
(A) Northern blot from wild type MEFs treated with Tg (200 nM) over a 12 hr time course. 10 μg of total RNA was analyzed on 1% formaldehyde northern gel, transferred to zeta-probe membrane, and probed for full length pre-rRNA and RPA194 mRNA as loading control.
(B) RPA probing for pre-rRNA and 7SL using 2.5μg of the same RNA samples as in (A).

treatment (Figure 1C, lanes 3-5). The decrease of pre-rRNA occurred with similar kinetics to the appearance of the spliced form of XBP1 mRNA suggesting that downregulation of rRNA occurs at an early point upon UPR induction (Figure 1C, lanes 3-5).

The observed decrease of pre-rRNA also occurs when MEFs are treated with agents that induce UPR by a different mechanism such as tunicamycin (Tm) which perturbs ER protein folding by inhibiting glycosylation rather than releasing ER calcium (Figure 1C, lanes 6-8; and 1D). The extent of rRNA downregulation during UPR was significant as it is comparable to treatment of MEFs with anisomycin (ANS), a ribotoxic drug that is a well-characterized inhibitor of rRNA transcription (Mayer et al., 2005). ANS treatment does not induce UPR as indicated by the lack of XBP1 splicing compared to NT cells (Figure 1C, compare lanes 1-2 with 9-11). This data suggests that the loss of 28S and 18S processed forms of rRNA in Figure 1A is likely the result of a decrease in pre-rRNA available for processing in the nucleus. Furthermore, after examining the levels of the most nascent rRNA, we reason that the decrease in pre-rRNA observed in Figure 1C is likely caused by a reduction of transcription.

In order to further investigate the effect of UPR on rRNA transcription we performed a nuclear run-on assay, or nascent chain analysis to measure the transcriptional activity of the rRNA genes. In this assay, engaged RNA

polymerases continue transcription of nascent RNAs in nuclei isolated from UPR induced cells in the presence of radiolabeled UTP. The level of labeled RNA was measured upon hybridization to DNA fragments complementary to rRNA, UPR target gene BiP, and 7SL RNA corresponding to the extent of RNA polymerases engaged in transcription (Figure 1E). Nuclei isolated from untreated cells generated significant levels of rRNA suggesting that transcriptional activity of Pol I is initially very high. In contrast, the level of radiolabeled rRNA generated from nuclei isolated from cells treated with Tg for 1 hr was significantly reduced correlating with the reduction of pre-rRNA detected by RPA (Figure 1D and 1F). The decrease in rRNA transcription is accompanied by an increase in BiP transcription indicating that canonical UPR target genes are being upregulated by UPR transcription factors as expected. It should be noted that by examining steady state levels of BiP by northern analysis, the increase in transcription does not begin to become detectable until after 2 hr of Tg treatment (Data not shown). Thus the ability to detect an increase in BiP mRNA and a decrease in pre-rRNA within 30 min of Tg treatment demonstrates the sensitivity of our assay. Taken together, these results suggest that activation of the UPR pathway leads to a decrease in rRNA transcription. Since most transcriptional changes associated with UPR reported to date have been those which increase, our observation that rRNA transcription decreases would be one of the few exceptions. Furthermore, the

abundance of rRNA relative to all other transcripts (80-90%) suggests that a reduction in rRNA transcription leading to a nearly 3-fold decrease in pre-rRNA may have a significant impact on the production of ribosomes and hence protein synthetic capacity of the cell.

The PERK Signaling Branch Regulates rRNA Transcription During UPR

To investigate the mechanism of how the ER transduces the signal to downregulate rRNA transcription in the nucleolus we analyzed the level of pre-rRNA in IRE1 and PERK knockout MEFs upon UPR treatment. First we followed the level of pre-rRNA in IRE1 +/+ and -/- MEFs upon Tg or Tm treatment and we found that rRNA is downregulated equally well in both wild type and knockout MEFs (Figure 4A and 4B). IRE1 -/- MEFs are not capable of splicing XBP1 mRNA, however in this case the extent of UPR activation can still be monitored by the increase in unspliced XBP1 mRNA presumably due to activation of the ATF6 branch of the UPR pathway. This indicates that UPR induced rRNA downregulation does not require the IRE1 signaling pathway.

We then tested the involvement of the PERK pathway in regulating rRNA transcription. In cells treated with vehicle (NT) we found that the level of pre-rRNA remains constant over a period of 12 hr (Figure 5A, lanes 1-3 and 9-11). In wild type MEFs, the level of pre-rRNA decreases by nearly three-fold within 2 hr and does not begin to recover even after 12 hr of Tg treatment (Figure 5A, lanes 4-8; and 5B). In contrast, PERK -/- MEFs are incapable of

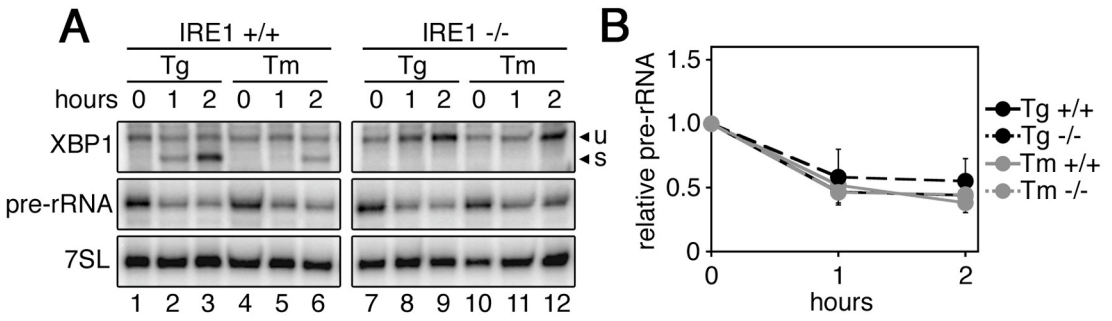

Figure 4. IRE1 Does Not Regulate rRNA During UPR.
(A) IRE1 is not involved in rRNA regulation. RPA probing for pre-rRNA, XBP1 mRNA, and 7SL in total RNA isolated from IRE1 +/+ and -/- MEFs treated with Tg (200 nM) or Tm (10 μg/mL). Unspliced and spliced XBP1 protected fragments are indicated by U and S respectively.
(B) Level of pre-rRNA relative to 7SL RNA in IRE1 +/+ MEFs (solid lines) and IRE1 -/- MEFs (dashed lines). Cells were treated with Tg (200 nM, black lines) and Tm (10 μg/mL, gray lines) as shown in (A). Each point represents the mean ± SD of a minimum of three independent experiments.

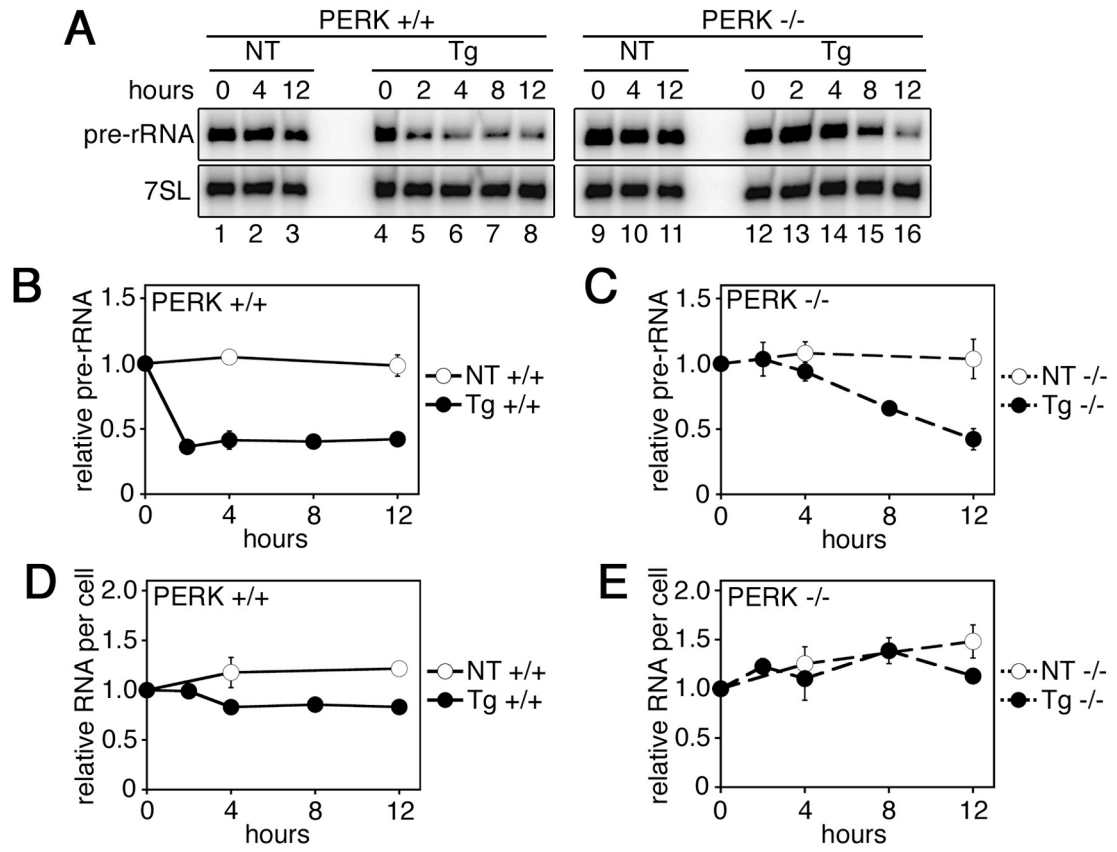

Figure 5. PERK Downregulates rRNA During UPR.
(A) RPA probing for pre-rRNA, XBP1, and 7SL in total RNA isolated from PERK +/+ and -/- MEFs treated with Tg (200 nM) or DMSO (NT, 0.1%) over a 12 hr time course.
(B) and (C) Quantitation of pre-rRNA relative to 7SL in PERK +/+ (B) and PERK -/- (C) MEFs. Cells were treated with Tg (200 nM, ●) or vehicle (0.1% DMSO, ○) as shown in (A). Each point represents the mean ± SD of a minimum of three independent experiments.
(D) and (E) Quantitation of the relative amount of RNA per cell with or without treatment of Tg (200nM) in PERK +/+ (D) and PERK -/- MEFs (E). Cells were treated with Tg (200 nM, ·●·) or vehicle (0.1% DMSO, ·○·) as shown in (A). At the indicated time points, cells were trypsinized and an aliquot was counted in the presence of trypan blue to determine total cell number. The number of dead cells per time point remained unchanged at < 5% for the entire time course. Total RNA was isolated from the remaining cells. The relative RNA per cell was calculated by dividing the total μg RNA from each time point by the number of viable cells.

downregulating rRNA until after 8 hr of Tg treatment (Figure 5A, lane 15; and 5C). Although there is a PERK-independent decrease in pre-rRNA at after 8 hr, these results suggest that PERK signaling is the major regulator of rRNA transcription during the first 8 hr of UPR activation.

To better understand the consequences of downregulating rRNA transcription during UPR we monitored cell viability and RNA content of PERK +/+ and -/- MEFs with or without Tg treatment. We analyzed cells by trypan blue staining and found that >95% of all cells excluded the dye over the entire 12 hr time course indicating that there was no change in cell viability during 12 hr of Tg treatment. When we isolated RNA from PERK +/+ MEFs we found that there was nearly a 20% decrease in the amount of RNA per cell upon 4 hr Tg treatment when compared to the initial level of RNA per cell at 0 hr (Figure 5D). This decrease in cellular RNA was sustained over the remaining 8 hr of the time course correlating with the sustained decrease in pre-rRNA over the same time (Figure 5B). In contrast, NT MEFs actually increased their RNA content so that after 12 hr the amount of RNA per cell was one third greater than that of Tg-treated MEFs (Figure 5D). The observed decrease in RNA per cell was PERK-dependent as the amount of RNA per cell in PERK -/- MEFs treated with Tg increased to the same extent as NT MEFs during the first 8 hr of the time course (Figure 5E). A decrease of RNA per cell in PERK -/- MEFs after 12 hr of Tg treatment correlated with the PERK-independent decrease in

pre-rRNA observed after 8 hr Tg treatment in PERK -/- MEFs (Compare Figures 5C and 5E). Given that rRNA makes up such a large percentage of total RNA these results suggest that PERK-regulated rRNA transcription inhibition results in an overall decrease in the amount of rRNA per cell during UPR. This decrease in total RNA per cell occurred in a relatively short period of time (4 hr) suggesting that the PERK-dependent decrease in rRNA transcription may impact the translational capacity of the cell during later stages of UPR induction.

Downregulation of Transcription and Translation Occurs Simultaneously

The hallmark of PERK activation is translation inhibition through phosphorylation of eIF2α, so we wanted to determine if rRNA downregulation occurred downstream of translation inhibition. We therefore measured the level of pre-rRNA and translation inhibition upon treatment with UPR inducers Tg and Tm. We briefly pulsed cells with [^{35}S] methionine and cysteine in order to label nascent proteins at the indicated time points. In this assay, the level of ^{35}S incorporation is used as a measure of global protein synthesis with decreasing labeling correlating with a decrease in the overall rate of protein synthesis. Based on our previous kinetic studies of UPR activation we know that PERK is activated within 15 min of Tg treatment and 60 min of Tm treatment (DuRose et al., 2006). We found that the decrease in the level of pre-rRNA is an extremely rapid event upon UPR induction occurring within 15

min of Tg treatment and 60 min of Tm treatment, which correlates exactly with and 6C, lane 4). In fact, the kinetics of pre-rRNA downregulation and translation inhibition are very similar (Figure 6B and 6D) suggesting that activation of PERK and subsequent inhibition of global protein synthesis and rRNA transcription occurs simultaneously. The major pathway known to simultaneously regulate rRNA transcription and translation initiation is the mTOR signaling pathway. Inhibition of mTOR activity by rapamycin (Rap) downregulates protein synthesis by inhibiting phosphorylation on ribosomal protein S6 kinase (S6K) (Brown et al., 1995; Chung et al., 1992; Price et al., 1992) and eukaryotic translation initiation factor 4E binding protein (4E-BP) (Beretta et al., 1996; Brunn et al., 1997). The mTOR signaling pathway also affects rRNA transcription initiation by a mechanism involving S6K (Hannan et al., 2003; Mayer et al., 2004). To date, there have been no reports indicating that the activity of mTOR or its downstream effectors are altered during UPR. To test possible involvement of the mTOR pathway in rRNA downregulation during UPR we followed the phosphorylation of ribosomal protein S6 (S6) by S6K (Figure 7A). We found that phosphorylation of S6 was unchanged upon Tg and Tm treatment, but dramatically decreased during Rap treatment as expected. It is worth noting that the steady-state level of S6 remained unchanged during Tg and Tm treatment suggesting there is no major shortage of ribosomal protein during the first 2 hr of UPR treatment while rRNA

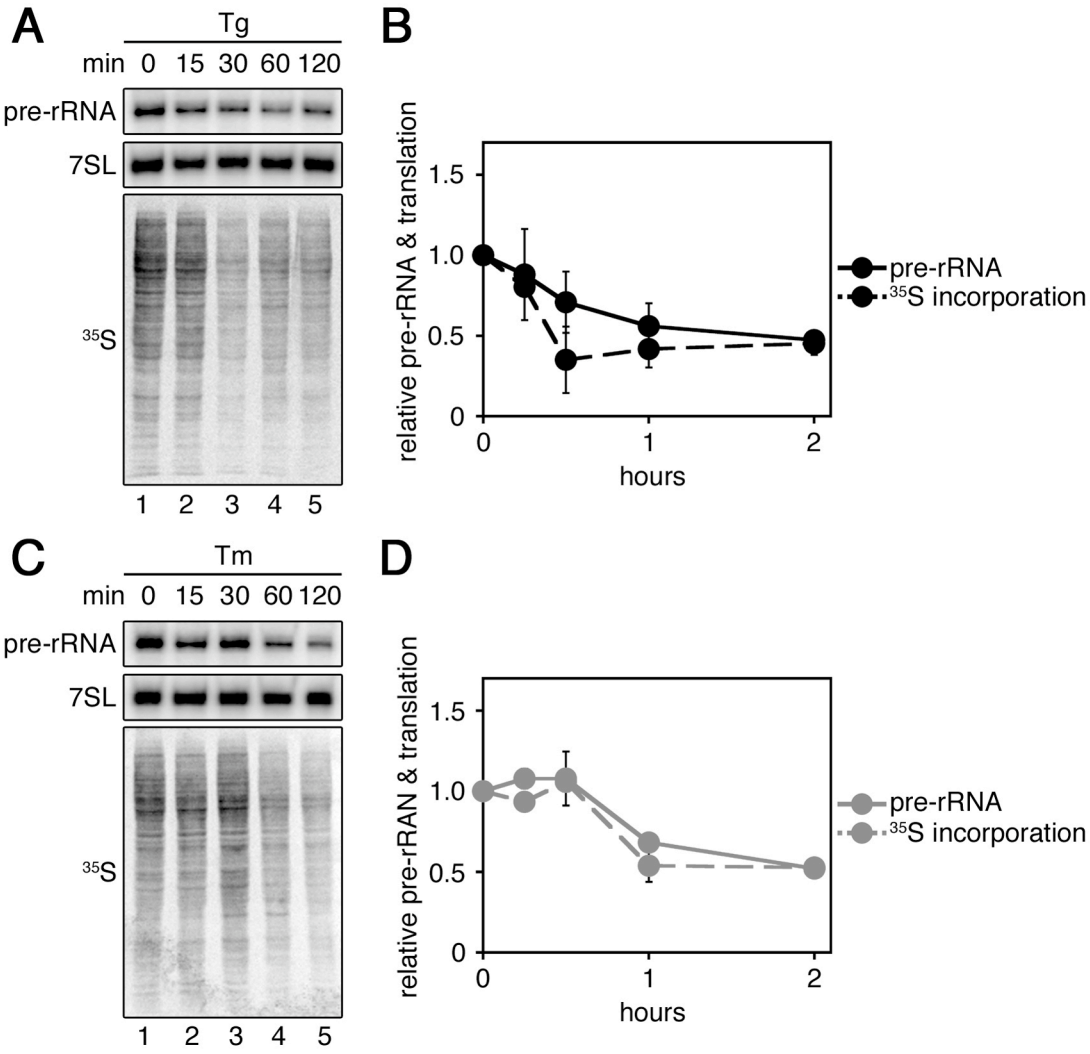

Figure 6. Comparison of rRNA Downregulation and Translation Inhibition Kinetics.
(A) Wild type MEFs were treated with Tg (200 nM) over a 2 hr time course. Total RNA was analyzed by RPA against pre-rRNA, and 7SL (top panels); and translation inhibition was analyzed by autoradiograph of ^{35}S pulse-labeled whole cell extracts subject to SDS-PAGE (bottom panel).
(B) Graphic representation of pre-rRNA relative to 7SL (—●—) compared to relative ^{35}S incorporation (···●···) as shown in (A). Each point represents the mean ± SD of a minimum of three independent experiments.
(C) Same as in (A) except wild type MEFs were treated with Tm (10μg/mL).
(D) Graphic representation of pre-rRNA relative to 7SL (—●—) compared to relative ^{35}S incorporation (···●···) as shown in (C). Each point represents the mean ± SD of a minimum of three independent experiments.

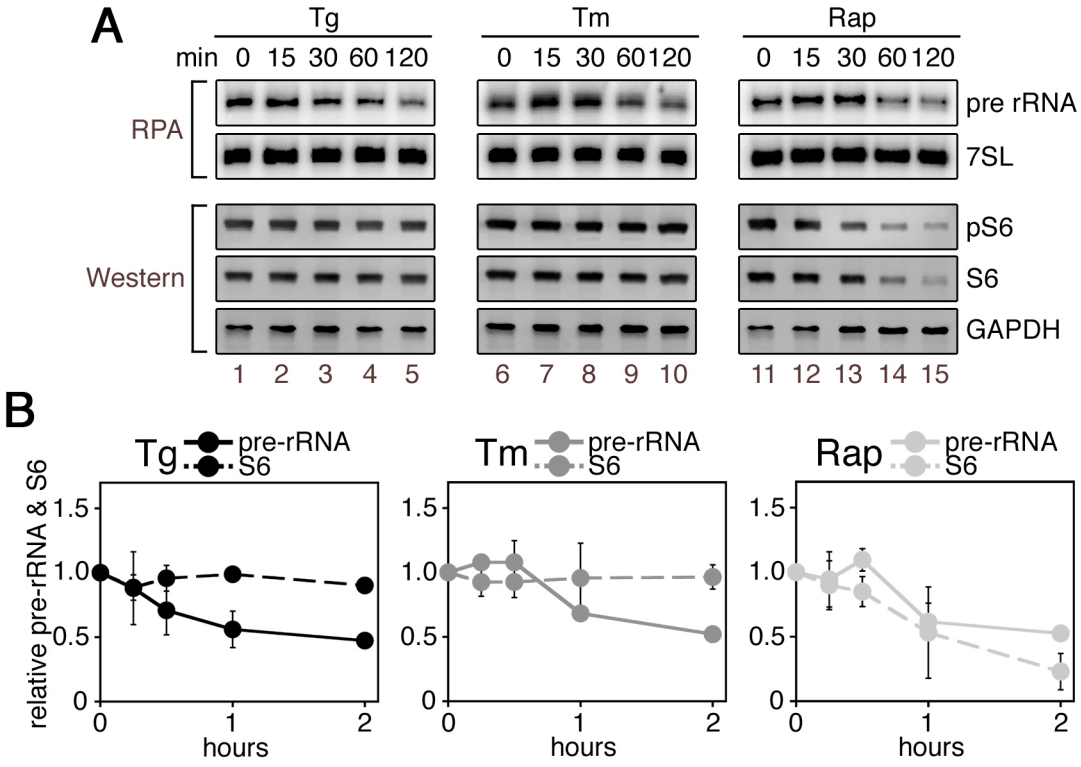

Figure 7. Phosphorylation and Steady State Levels of S6 are Unchanged During UPR.
(A) Wild type MEFs were treated with Tg (200 nM), Tm (10 μg/mL), or Rap (20 nM) for the indicated time points. Total cellular RNA was analyzed by RPA probing for pre-rRNA and 7SL (top panels). Whole cell extracts were analyzed by western blotting probing for phospho-RPS6 (pS6), total RPS6 (S6), and GAPDH (bottom panels).
(B) Graphical representation of the level of pre-rRNA relative to 7SL (solid lines), and the level of S6 protein relative to GAPDH (dashed lines) during Tg, Tm, and Rap treatment as shown in (A). Each point represents the mean ± SD of a minimum of three independent experiments. The pre-rRNA data shown in Figure 3 is replotted here to allow comparison with S6 protein levels.

transcription is being inhibited (Figure 7B). These results suggest that mTOR and S6K are not involved in regulating rRNA transcription during UPR. Furthermore, the simultaneous downregulation of translation with rRNA transcription combined the onset of translation inhibition (Figure 6A, lane 2; with no change in S6 protein levels suggest that it is unlikely that rRNA downregulation is initiated by limiting the translation of a highly unstable protein critical for rRNA synthesis.

Phosphorylation of eIF2α is Necessary for rRNA Downregulation

The most well characterized substrate of the PERK kinase is eIF2α whose only known function is as a regulatory subunit of the eIF2 complex. The eIF2 complex is required for association of the initiator tRNA with mRNA and the small ribosomal subunit (Reviewed in Sonenberg et al., 2000). In order to address whether eIF2α phosphorylation is involved in rRNA regulation during UPR, we measured pre-rRNA levels in MEFs carrying a homozygous serine to alanine mutation at the conserved eIF2α phosphorylation site (eIF2α A/A). Upon UPR induction, PERK is activated in eIF2α A/A cells, however translation attenuation does not occur (Scheuner et al., 2001). We found that both wild type (eIF2α S/S) and eIF2α A/A MEFs induce a UPR response as indicated by XBP1 splicing during Tg or Tm treatment (Figure 8A). In eIF2α S/S MEFs Tg or Tm treatment results in a rapid downregulation of pre-rRNA in coordination with translation inhibition (Figure 8A, lanes 1-3 and 7-9; and 8B).

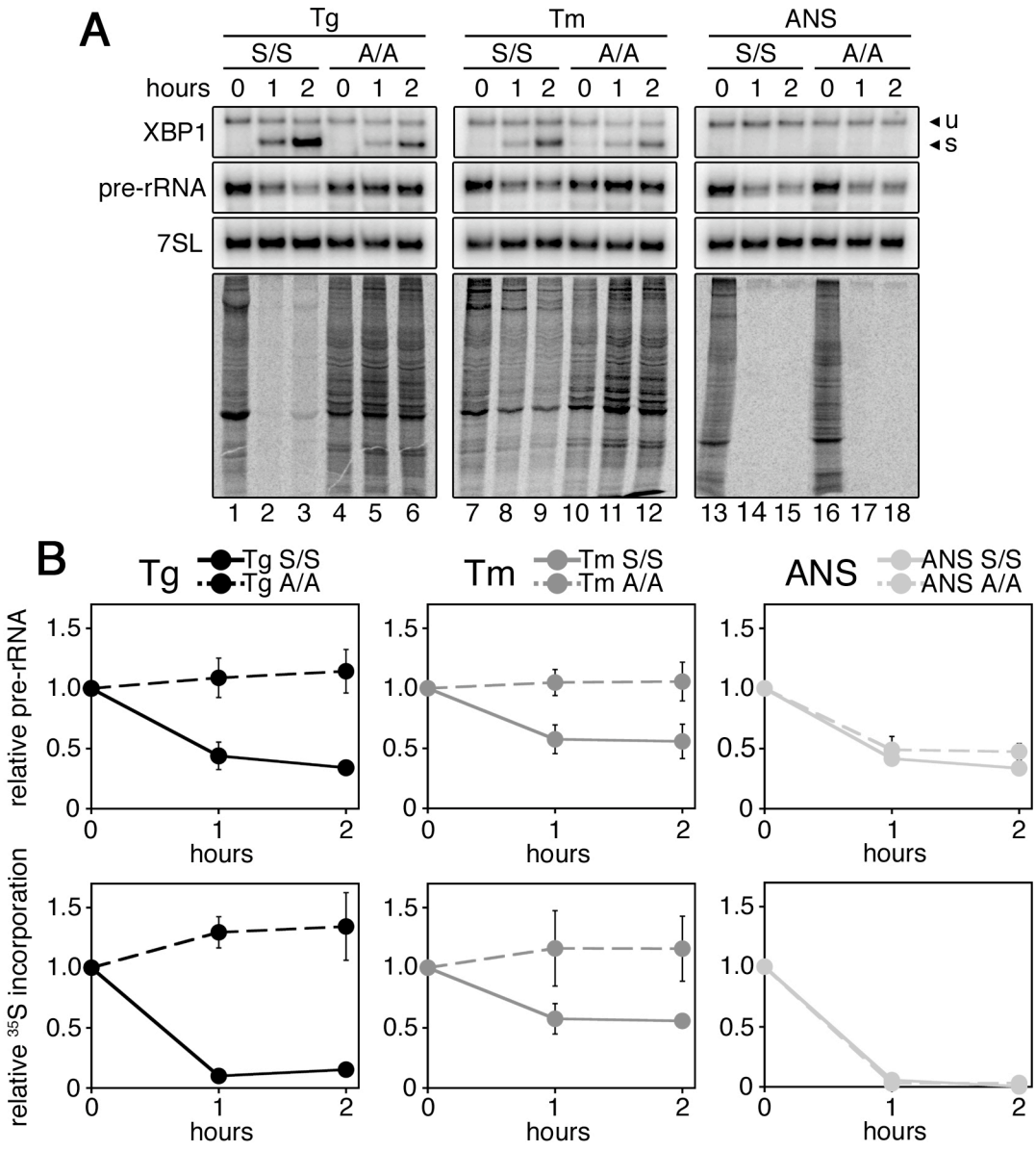

Figure 8. eIF2α phosphorylation is necessary for rRNA downregulation.
(A) Time course of eIF2α S/S and A/A MEFs treated with Tg (200 nM), Tm (10 μg/mL), or ANS (10 μM). Total cellular RNA and protein was isolated at the indicated times. The top three panels are RPAs probing for XBP1, pre-rRNA, and 7SL. Unspliced and spliced XBP1 transcripts are indicated by U and S respectively. Bottom panels are autoradiographs of [^{35}S]-labeled whole cell extracts analyzed by SDS-PAGE.
(B) Quantitation of pre-rRNA, and ^{35}S incorporation in eIF2α S/S (solid lines) and eIF2α A/A (dashed lines) MEFs as shown in (A). Top panels are graphs of pre-rRNA levels relative to 7SL, and bottom panels are graphs of relative ^{35}S incorporation. Each point represents the mean ± SD of a minimum of three independent experiments.

In contrast, we found that eIF2α A/A MEFs display impaired translation attenuation as expected, and also fail to downregulate pre-rRNA (Figure 8A, lanes 4-6 and 10-12; and 8B). Upon treatment with the rRNA transcription inhibitor ANS, the level of pre-rRNA decreases regardless of eIF2α phosphorylation indicating that the lack of rRNA regulation in eIF2α A/A MEFs during Tg and Tm treatment is UPR specific (Figure 8A, lanes 13-18; and 8B). These results suggest that phosphorylation of eIF2α by PERK during UPR is necessary for inhibition of rRNA transcription. Together the requirement for eIF2α phosphorylation and the kinetics of pre-rRNA decrease compared to translation inhibition suggests a novel function of phospho-eIF2α in regulating the transcription of rRNA during UPR.

PERK Is Required for Disruption of the rRNA Preinitiation Complex

To further investigate the mechanism of how UPR downregulates rRNA transcription, we monitored the formation of the preinitiation complex at the rRNA promoter. The major proteins involved in rRNA transcription initiation identified to date are DNA binding proteins upstream binding factor (UBF) and selectivity factor (SL1), and the non-DNA binding protein required for transcription of rDNA by RNA polymerase I (RRN3; Figure 9A). In order to measure promoter occupancy of preinitiation complex components, we employed a chromatin immunoprecipitation (ChIP) assay. In this assay PERK +/+ or -/- MEFs were treated with Tg or ANS for the indicated amount of time,

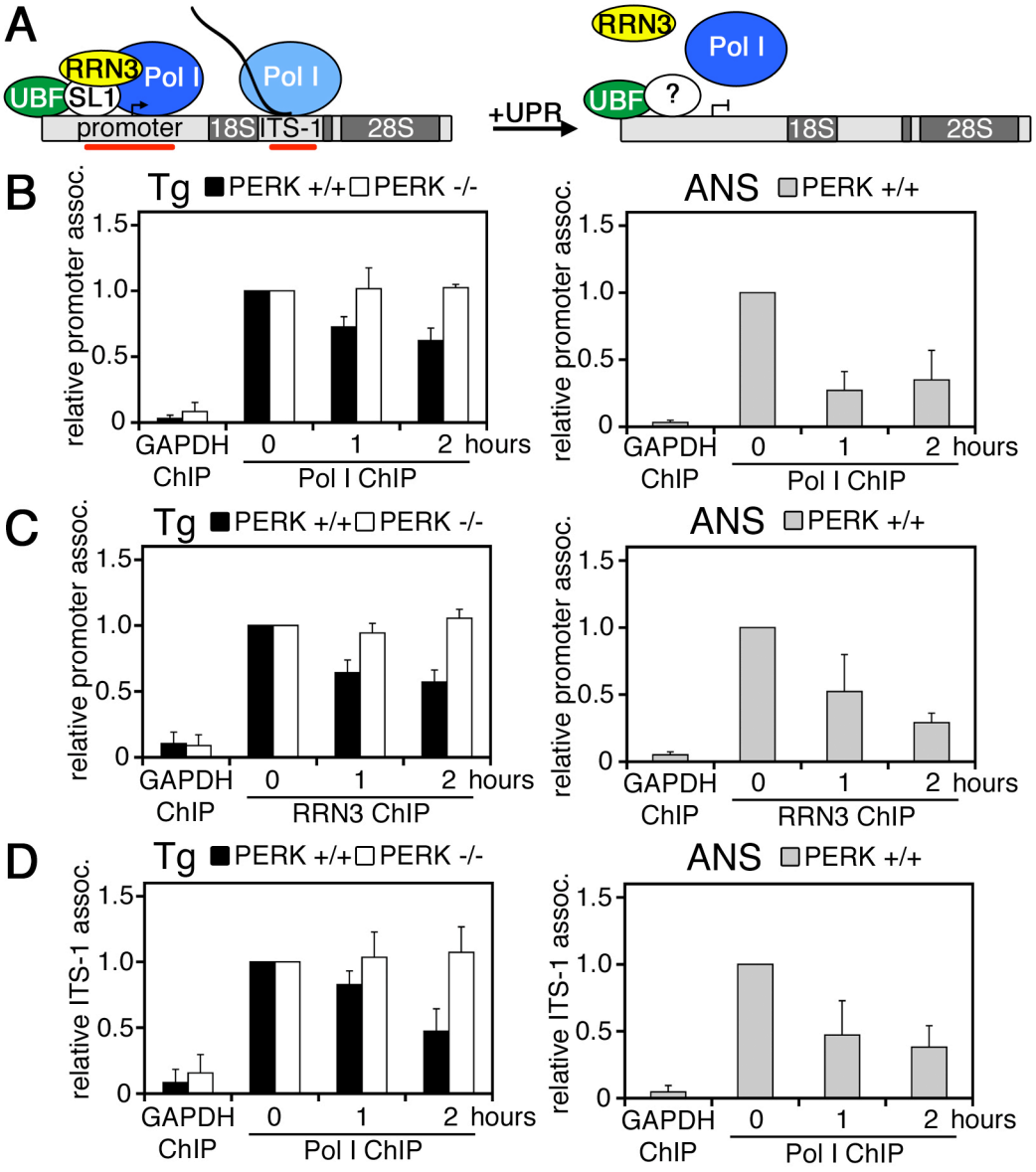

Figure 9. Disruption of rRNA Preinitiation Complex is PERK Dependent.
(A) rRNA gene during normal conditions (right panel, not to scale). Transcription factors UBF, SL1, and RRN3 are shown associated with Pol I in the preinitiation complex on the rRNA promoter, and elongating Pol I is shown associated with the first internal transcribed spacer (ITS-1) DNA. The DNA regions assayed are indicated by red underline. The left panel depicts the dissociation of RRN3 and Pol I from the rRNA promoter and ITS-1 after UPR activation.
(B) Quantitation of rRNA promoter DNA amplified from ChIP samples using antibody against the large subunit of Pol I (RPA194). PERK +/+ MEFs were treated with Tg (200 nM, ■) or ANS (10 μM, ▩). PERK -/- MEFs were treated with Tg (200nM, □). Control ChIP was performed with samples from wild type MEFs using antibodies against GAPDH. Each bar represents the mean and SD of three independent experiments.
(C) Same as in (B) except ChIP was performed with antibodies against RRN3.
(D) Same as in (B) except PCR was performed against ITS-1 DNA.

and cross-linked chromatin was immunoprecipitated with antibodies against the large subunit of Pol I, RRN3, and UBF. Treatment with ANS is known to disrupt the interaction of Pol I and RRN3 with the rRNA promoter resulting in an inhibition of transcription initiation (Mayer et al., 2005). We found that association of promoter DNA with both Pol I and RRN3 was decreased upon treatment with ANS indicating that our assay is functioning as expected (Figure 9B and 9C). Upon Tg treatment in wild type MEFs, we found a decrease in the association of promoter DNA with both Pol I and RRN3 suggesting that the rRNA preinitiation complex is disrupted during UPR activation (Figure 9B and 9C). The dissociation of Pol I during ANS treatment appeared to occur more rapidly and to a greater extent than in Tg cells (Figure 9B), while the extent and kinetics of pre-rRNA downregulation analyzed by RPA appeared very similar (Figure 1C and 1D). The decrease in Pol I and RRN3 promoter occupancy was PERK dependant as there was no change in PERK -/- MEFs (Figure 9B and 9C). We did not detect any change in the promoter occupancy of UBF after Tg treatment in either cell line (Figure 10). We were unable to determine the promoter occupancy of SL1 because antibodies against subunits of SL1 were not suitable for ChIP. Our assay was specific to the targeted proteins as precipitation with control antibody against GAPDH did not pull down significant quantities of rRNA promoter DNA (Figure 9B-9D). To monitor the level of elongating Pol I we performed ChIP against

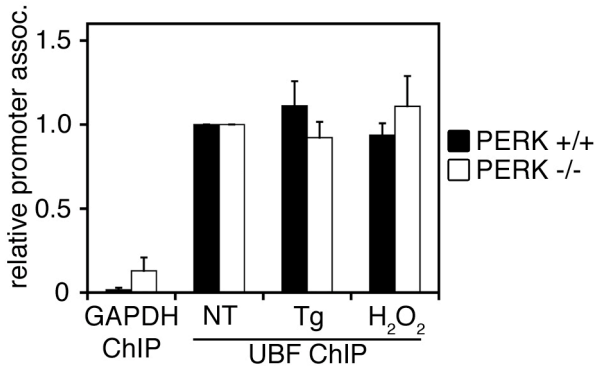

Figure 10. UBF Promoter Occupancy is Not Changed During UPR or H_2O_2 Treatment. Quantitation of rRNA promoter DNA amplified from ChIP samples using antibody against UBF. PERK +/+ (■) and PERK -/- MEFs (□) were either untreated (NT) or treated with Tg (200nM) or hydrogen peroxide (H_2O_2; 30 μM) for 1 hr relative to NT samples. Control ChIP was performed with samples from wild type MEFs using antibodies against GAPDH. Each bar represents the mean and SD of three independent experiments.

the first internal transcribed spacer (ITS-1) of the rRNA gene, and found that there is a PERK-dependent decrease in the association of elongating Pol I with ITS-1 DNA upon Tg treatment (Figure 9D). The same reaction was performed with antibodies against RRN3, which did not significantly pull down ITS-1 DNA as expected as RRN3 is not known to travel with the elongating polymerase (Figure 11). The PERK dependence of pre-rRNA downregulation and disruption of the preinitiation complex was specific to UPR. Treatment of PERK -/- MEFs with ANS reduced pre-rRNA to the same extent as wild type cells (Figure 12A and 12B). Furthermore, ChIP of PERK +/+ and -/- MEFs treated with a known rRNA preinitiation complex disrupter showed similar levels Pol I and RRN3 promoter dissociation (Figure 12C and 12D). Together this suggests that PERK activation decreases the promoter occupancy of both RRN3 and Pol I leading to a decrease in the number of elongating polymerases on the rRNA gene. This correlates with results shown in Figure 1 where the overall level of pre-rRNA and the synthesis of rRNA from isolated nuclei is decreased upon UPR induction.

RRN3 is Inactivated During UPR to Reduce rRNA Transcription

The PERK dependent dissociation of RRN3 and Pol I from the rRNA promoter during UPR suggests that at least one of the components required for transcription initiation are becoming inactivated. Since PERK is responsible for translation repression, we wanted to test the protein levels of

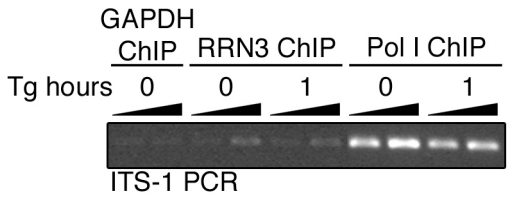

Figure 11. RRN3 is Not Associated With ITS-1 DNA.
Ethidium staining of the first internal transcribed spacer (ITS-1) DNA amplified from ChIP samples using antibodies against GAPDH, RRN3, and Pol I (RPA194) upon treatment with Tg (200 nM). PCR was performed using two dilutions of ChIP template DNA for each sample representing a three-fold dilution of template DNA. Note that GAPDH and RRN3 ChIP do not pull down significant quantities of ITS-1 DNA.

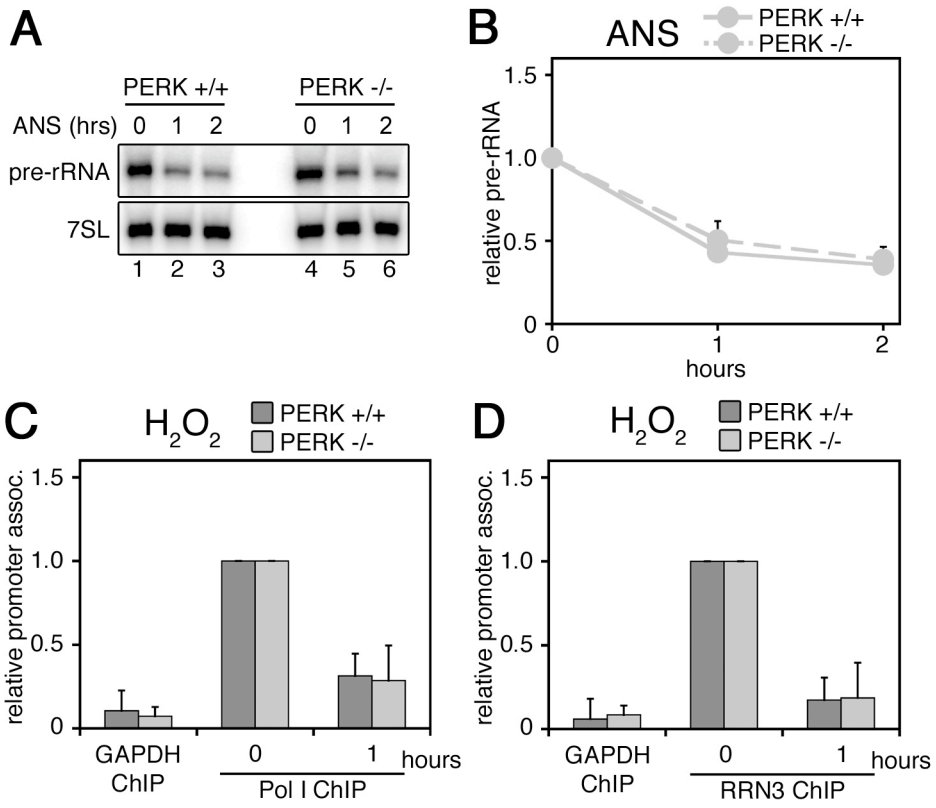

Figure 12. PERK Regulation of rRNA is Specific to UPR.
(A) Time course of PERK +/+ and -/- MEFs treated with ANS (10 μM). Cellular RNA was isolated at the indicated times and analyzed by RPA using probes against pre-rRNA, and 7SL.
(B) Quantitation of pre-rRNA relative to 7SL during ANS treatment in PERK +/+ (—●—) and PERK -/- cells (···●···) as shown in (A). Each point represents the mean ± SD of a minimum of three independent experiments.
(C) and (D) Quantitation of rRNA promoter DNA amplified from ChIP samples using antibody against Pol I (RPA194; C) or RRN3 (D) from PERK +/+ (■) and PERK -/- MEFs (□) treated with H_2O_2 (30 μM) for the indicated times. Control ChIP was performed with samples from wild type MEFs using antibodies against GAPDH. Each bar represents the mean and SD of three independent experiments.

the rRNA transcription factors during UPR. Although antibodies to the TAF_I proteins of the SL1 complex were unsuitable for western blotting, we found the levels of the large Pol I subunit (RPA194), both isoforms of UBF, and RRN3 remain constant during UPR in both PERK +/+ and -/- MEFs suggesting that translation inhibition is not leading to depletion of essential rRNA transcription factors (Figure 13A).

To identify the downstream effectors of PERK rRNA regulation we assayed Pol I transcription activity in nuclear extracts from NT, Tg, and ANS treated MEFs *in vitro*. In this assay, nuclear extracts were allowed to form preinitiation complexes on an rDNA template and transcription was allowed to proceed after addition of radiolabeled nucleotides. The rDNA template contains the rat rRNA promoter from -286 to +630, and when linearized with EcoRI produces a specific 632 nt transcript (Figure 13B). The level of transcript produced *in vitro* correlates with the transcriptional activity of Pol I *in vivo*. In our assay we found that NT extracts robustly transcribe from the rDNA template (Figure 13C and 13D, lanes 1) correlating with the high level of Pol I transcription from isolated nuclei before UPR induction (Figure 1E). In contrast, we found that the Pol I transcriptional activity is reduced by 5-10 folds in nuclear extracts from Tg or ANS treated cells (Figure 13C and 13D, lanes 1). The extent of reduction in Pol I transcription in Tg extracts was comparable to extracts isolated from cells treated with ANS. Treatment with

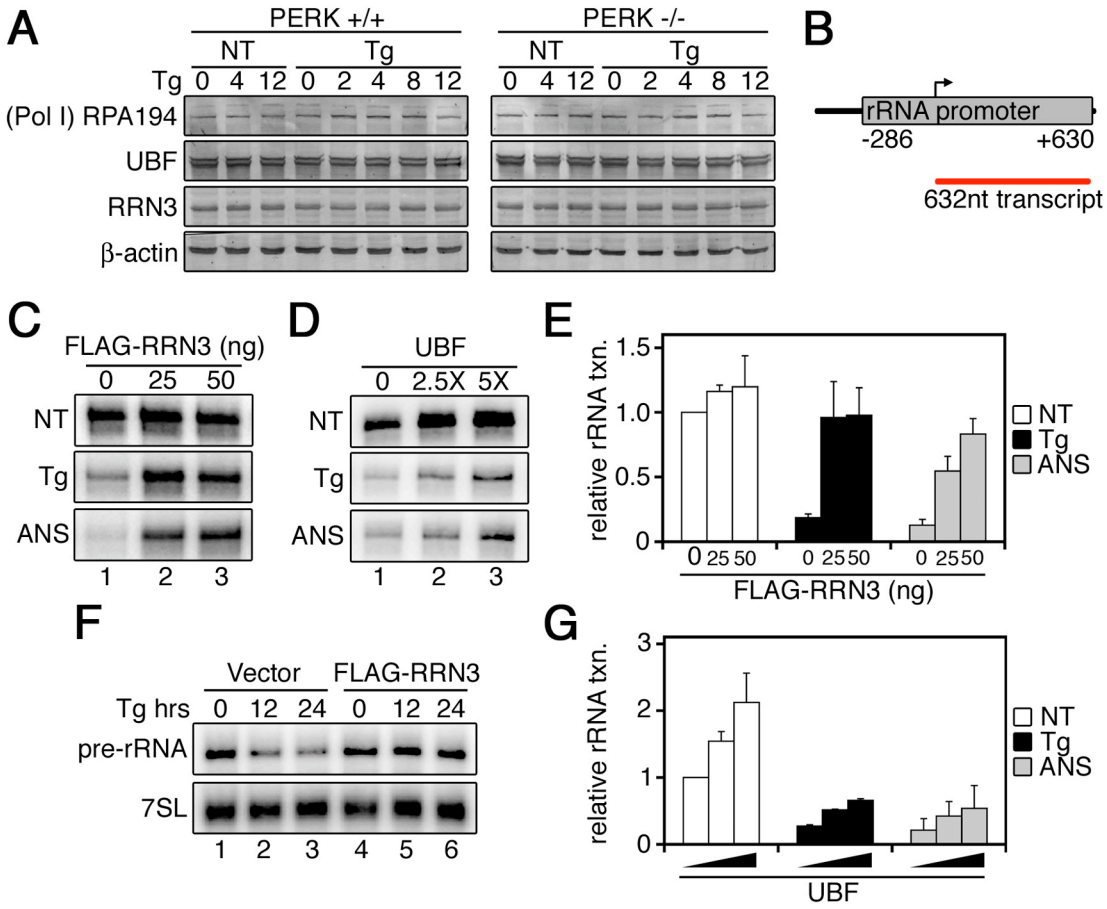

Figure 13. RRN3 is Inactivated During the UPR.

(A) Western blots from PERK +/+ and -/- MEFs treated with Tg (200 nM) or DMSO (NT, 0.1%). Western were blots probed with antibodies against RPA194 (Pol I large subunit), UBF, RRN3, and β-actin. Note UBF antibody recognizes both isoforms of UBF protein.

(B) Depiction of rRNA transcription template and the 632nt transcript that results from correct initiation (red line). The correct site of transcription initiation is indicated by an arrow.

(C) Autoradiograph of 632 nt *in vitro* transcribed product resulting from transcription reactions using 25 μg of nuclear extracts, 10 ng rDNA template, and [α-^{32}P] UTP. Purified FLAG-RRN3 from NT cells was added to reactions at the indicated concentration (lanes 2 and 3). Nuclear extracts were isolated from NT MEFs , or MEFs treated 2hr with Tg (200 nM) or ANS (10 μM).

(D) Same as in (C) except that partially purified UBF protein was added to the reaction in a concentration of 2.5 and 5 fold excess of the endogenous level of UBF (lanes 2 and 3).

(E) Quantitation of transcription products as shown in (C) relative to the level of transcript produced by NT extracts in the absence of exogenous RRN3. Each bar represents the mean and SD of three independent experiments.

(F) HeLa cells were transfected for 24 hrs with empty vector or FLAG-RRN3 before treatment with Tm (0.5 μg/mL). Total cellular RNA was collected and analyzed by RPA against pre-rRNA and 7SL.

(G) Quantitation of transcription products as shown in (D) relative to the level of transcript produced by NT extracts in the absence of exogenous UBF. Each bar represents the mean and SD of three independent experiments.

ANS results in a decrease in Pol I transcription by inactivation of RRN3 (Mayer et al., 2005). Upon addition of FLAG-RRN3 affinity purified from NT cells to Tg extracts, Pol I transcription was restored suggesting RRN3 is inactivated during UPR (Figure 13C, lane 2 and 3). Again this was comparable to the complementation observed by adding FLAG-RRN3 to ANS treated extracts that have been shown to contain inactive RRN3 (Mayer et al., 2005). Our affinity purified FLAG-RRN3 protein was assayed by coomassie stain and western blotting, and no contamination by other proteins or rRNA transcription factors was detected (Figure 14A and 14B). We found that addition of 25-50 ng of FLAG-RRN3 protein is sufficient to fully complement the level of rRNA transcript produced in Tg extracts as compared to NT extracts (Figure 13E). In addition, we observed that over expression of FLAG-RRN3 in HeLa cells prevented the decrease in pre-rRNA upon Tg treatment compared to mock transfected cells (Figure 13F). These results demonstrate that downregulation of rRNA during UPR occurs in both in mouse and humans, and suggests that the mechanism of inactivation of RRN3 is conserved as well.

In order to determine if other rRNA transcription factors are involved in the regulation of UPR induced transcription repression we performed the same *in vitro* transcription complementation assay with UBF protein partially purified from Novikoff hepatoma cells (Figure 13D). The concentration of UBF protein added to the reaction was estimated by western blotting to be 2.5 and 5 folds

over the level of endogenous UBF (Figure 14C). When partially purified UBF was added to NT extracts, the transcriptional activity was increased by 2.5-fold and did not saturate even after a 10-fold excess of UBF protein was added to the reaction (Figure 13D, 13G, and data not shown). When partially purified UBF protein was added to Tg or ANS extracts we observed a proportional increase in transcriptional activity with respect to the NT extracts (Figure 13G). This is in contrast to the effect of adding FLAG-RRN3 to Tg and ANS extracts, where activity increases to the same level as NT extracts (Figure 13C and 13D, compare lanes 3). Together these results suggest that while other transcription factors exert influence on rRNA transcription, RRN3 appears to be the major regulator decreasing rRNA during UPR.

Discussion

In this report we have shown that the PERK signaling branch coordinately regulates rRNA transcription with protein synthesis during the UPR (Figure 15A). The onset of rRNA repression occurs simultaneously with translation inhibition and prior to any major changes in the concentration of ribosomal proteins. In addition to its function in repressing translation initiation, we found that phosphorylation of eIF2α is necessary for downregulation of rRNA upon UPR activation. This suggests there may be a novel function of eIF2α in regulating rRNA transcription, or translation inhibition *per se* is sensed by the rRNA transcriptional machinery.

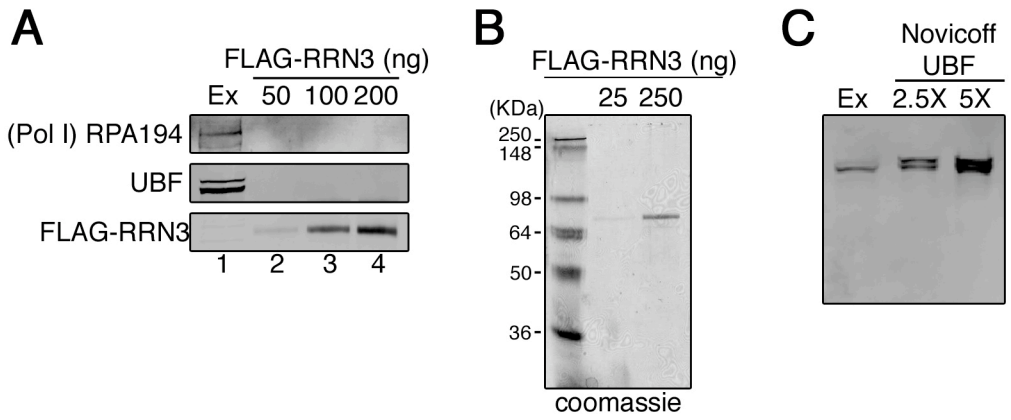

Figure 14. Analysis of Purified RRN3 and UBF.
(A) Western blot of indicated concentrations of purified FLAG-RRN3 protein (lanes 2-4) and 25μg of untreated nuclear extracts used for in vitro transcription (Ex; lane 1). Blots were probed with antibodies against RPA194 (Pol I), UBF, and FLAG. Note the UBF antibody recognizes both isoforms of UBF protein.
(B) Coomassie stained gel of purified FLAG-RRN3 protein. Molecular weights of protein marker is indicated in KDa.
(C) Western blot of indicated concentrations of partially purified UBF protein isolated from Novicoff hepatoma cells and 25μg of untreated nuclear extracts used for in vitro transcription (Ex). Note the UBF antibody recognizes both isoforms of UBF protein.

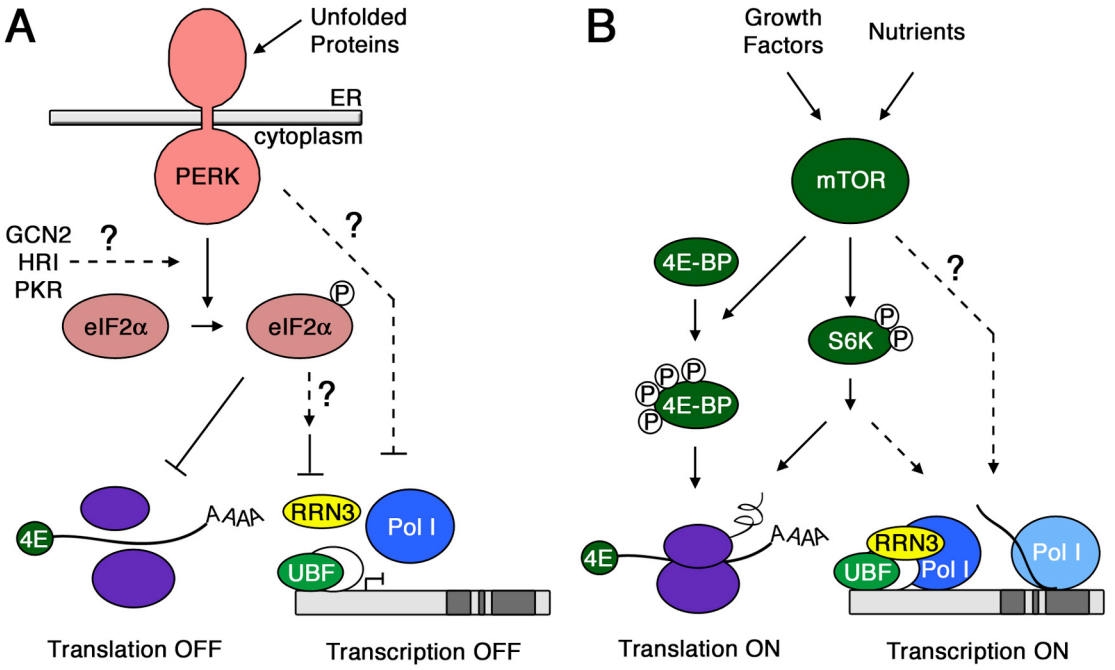

Figure 15. Model of PERK Pathway Controlling rRNA Transcription and Translation in Comparison to mTor Pathway.
(A) PERK Pathway. Unfolded proteins in the ER lumen activates the PERK kinase to phosphorylate eIF2α leading to inhibition of translation initiation and inhibition RRN3 activity resulting in dissociation of RRN3 and Pol I from the PIC. Dashed lines indicate that direct interaction of components have not been demonstrated.
(B) mTOR pathway. During favorable conditions, signaling from growth factors and nutrients activates mTOR leading to phosphorylation of 4E-BP and S6K. Inhibition of 4E-BP and activation of S6K by mTOR phosphorylation cooperate to increase the efficiency of translation initiation. While the entire pathway has yet to be elucidated, mTOR and S6K activity leads to phosphorylation of rRNA transcription factors increasing transcription of rRNA.

In animal cells, there is a strong link between the production of rRNA and protein synthesis. Studies in the 1960s observed that treatment of human and animal cells with translation inhibitors such as puromycin and cycloheximide resulted in a very rapid decline of ribosomal gene transcription (Ennis, 1966; Tamaoki and Mueller, 1963; Warner et al., 1966; Willems et al., 1969). A similar decline of protein and rRNA synthesis was also noted during translation inhibition under more physiological conditions (e.g. nutrient deprivation; Grummt et al., 1976; Hershko et al., 1971; Maden et al., 1969; Pardee, 1974). Prior to cell-free systems allowing biochemical analysis of transcription machinery the favored hypothesis to explain the loss of Pol I activity was that very short-lived proteins were required for rRNA transcription *in vivo* (Benecke et al., 1973; Chesterton et al., 1975; Muramatsu et al., 1970). It wasn't until decades later after the development of in vitro transcription systems and identification Pol I transcription factors that investigators were able to determine that it was not the protein level, but the activity of Pol I transcription factors being regulated in response to nutrient starvation and translational inhibition (Cavanaugh et al., 2002; Claypool et al., 2004; Hannan et al., 2003; Mayer et al., 2005; Mayer et al., 2004; Yuan et al., 2002). It is now well known that the activity of Pol I transcription factors is subject to intense regulation by post-translational modification, and much of the ongoing

research is focused on understanding the pathways and molecular details of this regulation.

To understand the molecular mechanism of PERK-mediated rRNA transcription repression during the UPR we initially focused on the rRNA preinitiation complex. We found that during UPR, Pol I and RRN3 dissociate from the rRNA promoter in a PERK-dependent manner. The observed dissociation of RRN3 and Pol I from the preinitiation complex did not appear to result from reduced RRN3 levels during translation inhibition, but rather inactivation of RRN3 during UPR. Work by others has shown that association of RRN3 is essential for recruitment of Pol I to the promoter and the formation of initiation-competent preinitiation complexes (Hirschler-Laszkiewicz et al., 2003; Miller et al., 2001). In our study, we have shown that addition of active RRN3 can fully rescue the transcriptional activity of inactive UPR-treated nuclear extracts. Under various conditions, it has been shown that the activity of RRN3 can be both positively and negatively regulated by phosphorylation on multiple residues (Cavanaugh et al., 2002; Hirschler-Laszkiewicz et al., 2003; Mayer et al., 2005; Mayer et al., 2004; Zhao et al., 2003). At present we have not identified the molecular mechanism of RRN3 inactivation during UPR, but suspect that phosphorylation is likely involved. Identification of both potential phosphorylation sites and kinases regulating RRN3 activity during UPR is the subject of ongoing work, and will provide the necessary tools for

detailed studies on the functional role of inactivating rRNA transcription during UPR.

One possible role for regulation of rRNA transcription during UPR is to modulate cell cycle progression and activate cell death programs. Recently it has been suggested that UPR activation leads to a PERK-dependent interaction of ribosomal proteins with HDM2, thereby inhibiting its activity resulting in p53 stabilization (Zhang et al., 2006). It is well established that decreasing the transcription of rRNA leads to increased interaction of both HDM2 and MDM2 with ribosomal proteins L5, L11, and L23 leading to p53 stabilization (Dai and Lu, 2004; Dai et al., 2004; Jin et al., 2004; Lohrum et al., 2003; Marechal et al., 1994; Zhang et al., 2003). As such, it is possible that rRNA transcription inhibition reported here is contributing to p53 stabilization during UPR as its PERK dependence is consistent with the observations reported by Zhang *et al*. (2006).

In addition to possible implications in cell fate decisions, rRNA downregulation may serve a more functional role in regaining homeostasis upon ER stress. The rapid nature of rRNA transcription and translation inhibition immediately sets the tone for cells to begin slowing down their anabolic activities in response to ER stress. In addition to reducing the load on the ER, perhaps decreasing anabolic activities during the UPR serves to reserve energy for repair processes as both translation and ribosome

biogenesis consumes a large amount of ATP. Additionally, the resulting metabolic slow-down may allow more time for the cell to initiate an appropriate response in order to counter the stress and restore homeostasis.

The most well characterized pathway coordinately regulating translation and rRNA synthesis is the mTOR pathway (Figure 15B). During favorable conditions, upstream signaling stimulates mTOR to phosphorylate 4E-BP and S6K increasing the efficiency of translation initiation and ribosome biogenesis (Brown et al., 1995; Brunn et al., 1997). While it is unclear whether mTOR directly affects the rRNA preinitiation complex, signaling from active S6K is involved in activating rRNA transcription factors (Hannan et al., 2003; Mayer et al., 2004). In unfavorable conditions such as amino acid deprivation, mTOR activity is reduced leading to hypophosphorylation of 4E-BP and S6K, which has an inhibitory effect on both the initiation of rRNA transcription and translation. Our data suggest that the mTOR pathway is not involved in regulation of rRNA transcription during UPR. It is not difficult to rationalize the importance of coordinately regulating rRNA and protein synthesis in response to nutrient availability as both processes consume vast amounts of cellular resources. However, the rationale behind coordinate regulation of rRNA and protein synthesis in other stress conditions is not as clear-cut.

A literature survey of stresses that activate eIF2α kinases reveals that rRNA transcription is also affected, indicating that coordinate regulation of

translation and rRNA transcription is a common theme among stress responses (Table 1). While the mechanism of activation for each of the eIF2α kinases is distinct, phosphorylation of eIF2α appears to accompany downregulation of rRNA transcription. Our study is the first to link phosphorylation of eIF2α with regulation rRNA transcription. Our results here provide an initial framework for understanding how the UPR coordinately regulates translation and rRNA transcription in order to maintain homeostasis during ER stress. The diversity of conditions regulating both translation and rRNA synthesis including oxidative stress, heat shock, UV exposure, and hypoxia suggests there must be some fundamental advantage for downregulating these major anabolic activities during stress. One of the important questions that remain to be answered is; what is the functional role of inhibiting protein synthesis and rRNA transcription during stress, in general? Further understanding of the regulatory mechanisms and the ability to uncouple eIF2α phosphorylation and rRNA synthesis will be necessary to provide answers to such questions.

Table 1. Comparison of Activation of eIF2α Kinases and rRNA Transcription During Stress.

Stress	eIF2α Kinase	Reference	rRNA TXN	Reference
Oxidative	HRI	Lu et al., 2001	↓	Mayer et al., 2005
Amino Acid	GCN2	Zhang et al., 2002	↓	Grummt et al., 1976
Heat Shock	HRI	Lu et al., 2001	↓	Ghoshal and Jacob, 1996
Hypoxia	PERK	Koumenis et al., 2002	↓	Mekhail et al., 2006
UV	GCN2	Jiang and Wek, 2005	↓	Ayaki et al., 1996
Viral Infection	PKR	Reviewed in Garcia et al., 2007	↑ or ↓	Reviewed in Hiscox, 2002
Rapamycin	GCN2	Kubota et al., 2003	↓	Mayer et al., 2004
Anisomycin	?		↓	Mayer et al., 2005
UPR	PERK	Harding et al., 1999	↓	This study

Experimental Procedures

Cell Culture and Treatment

All cells were cultured in DMEM (Cellgro) supplemented with 10% FBS (Cellgro) and maintained at 5% CO_2 and 37ºC. eIF2a S/S and A/A MEFs were obtained from Dr Randall Kaufman (Scheuner et al., 2001). Cells were incubated 1-2 hr in fresh medium before being treated with the indicated concentrations of stress inducing agents. Tg and Tm was purchased from Calbiochem, while ANS, H_2O_2, and Rap were purchased from Sigma.

Northern Blotting

Total RNA isolated from whole cells or nuclei, was analyzed on a 1% agarose gel containing 1% formaldehyde. Gels were transferred to zeta-probe membranes (BioRad) in 10X SSC by capillary action, and assayed with radiolabeled DNA probes following UV cross-linking.

RNase Protection Assay

RPA probe templates were PCR amplified from mouse cDNA or genomic DNA with the following primers:

XBP1 TTCCGGATTTACAAACGGAAACTGAAAAACAGAGTAGCAG, and TAATACGACTCACTATAGCAGAGGTGCACATAGTCTGAG;

pre rRNA TTCCGGAAAAACAATCTTCAGTCGCTCGTTGTGTTCTC, and TAATACGACTCACTATAGGAGGGCCCGCTGGCAGAACG;

7SL RNA TTCCGGATTTTCAAGCGATCGCTTGAGTCCAGGAG, and TAATACGACTCACTATAGAGCACGGGAGTTTTGACCTGC.

For RPA in HeLa cells, pre-rRNA probe from +309 to +500 was cloned into pCRII (Invitrogen). Probes were transcribed *in vitro* in the presence of [α ^{32}P] UTP (Perkin Elmer) and gel purified. 1-2×10^5 cpm of each probe was hybridized to 2 μg total RNA. Hybridized RNA was digested with RNase A/T1 cocktail (Ambion) followed by Proteinase K digestion (Invitrogen), phenol chloroform extraction, and ethanol precipitation. Isolated RNAs were analyzed on 6% acrylamide gels containing 7 M urea.

Nuclear Run On

Nuclear run on transcription was carried out based on the protocol described in (Banerji et al., 1984). Briefly, nuclei were isolated from 6×10^6 NIH3T3 cells ± 200 nM Tg for the indicated amount of time. Cells were lysed by repeated pipetting in 0.5% NP40, 10 mM Tris (pH 7.4), 10 mM NaCl, 3 mM $MgCl_2$, and nuclei were pelleted by centrifugation. Supernatant was discarded and nuclei were resuspended in 40% glycerol, 50 mM Hepes (pH 8.5), 5 mM $MgCl_2$, 0.1 mM EDTA and snap frozen in liquid N_2. Nuclei were added to an equal volume of reaction mix such that the final concentration was 25 mM Hepes (pH 7.5); 5 mM $MgCl_2$; 2 mM DTT; 75 mM KCl; 25% glycerol; 2.8 mM ATP, GTP, and CTP; 3.2 μM UTP; and 50 μCi [α ^{32}P] UTP (3000 Ci/mmol). Transcription was allowed to proceed 20 min at room temperature (RT) before

stopping with DNase (Promega) followed by incubation for 2 hr at 45ºC with Proteinase K in 10 mM Tris, 2% SDS, 7 M urea, 0.35 M NaCl, 1 mM EDTA. After digestion RNA was isolated, denatured, and hybridized to DNA immobilized on zeta-probe membranes at 42ºC for 36 hr. Washed dot blots were exposed to phosphor screens.

Labeling Nascent Proteins

Cells were treated with stress inducers for the indicated amounts of time. 10 min prior to collection, cells were incubated with 50 μCi/mL [^{35}S] labeled methionine/ cysteine mix (Trans Label, MP Biomedicals) to label nascent proteins. Whole cell extracts from labeled cells were resolved by SDS-PAGE and exposed to phosphor screens.

Chromatin Immunoprecipitation

PERK +/+ or -/- MEFs were treated as indicated and cross-linked in 1% formaldehyde. Isolated nuclei were lysed in 1% SDS, 10 mM EDTA, 50 mM Tris (pH 7.4), and 1 mM PMSF and sonicated to yield DNA fragments averaging 500 bp. Samples were diluted in 1% triton, 2 mM EDTA, 150 mM NaCl, 20 mM Tris (pH 7.4), 1 mM PMSF and immunoprecipitated with antibodies against RRN3, Pol I (RPA194), UBF (all from Santa Cruz Biotechnology), or GAPDH (Research Diagnostics). Washed beads were eluted in 1% SDS and 0.1M $NaHCO_3$ at RT and cross-links were reversed by incubation at 65ºC followed by ethanol precipitation. DNA was digested with

Proteinase K, phenol chloroform extracted, and ethanol precipitated. DNA was PCR amplified with primers against murine rRNA promoter GTCGACCAGTTGTTCCTTTGAG and CCCGGGAAAGCAGGAAGCGTG, or ITS-1 DNA GGCTCTTCCGTGTCTACGAG and GAGGCCAGAAAAGCGTGGCATC. Samples were analyzed on agarose gels stained with ethidium bromide. Relative levels of PCR products from ChIP samples were determined using a standard curve generated from PCR amplified input DNA.

Western Blotting

Whole cell extracts were resolved by SDS PAGE and transferred to nitrocellulose. Membranes were probed with antibodies against RPA194, RRN3, UBF, GAPDH, β-actin (Sigma), phospho S6 and total S6 (both from Cell Signaling). Membranes were developed with ECL Plus Western blotting detection reagent (GE Healthcare).

In Vitro Transcription

Nuclear extracts were prepared from exponentially growing untreated (NT), Tg treated (200 nM, 2h), or ANS treated (10 μM, 2h) MEFs as described in (Dignam et al., 1983). In a standard reaction 25 μg nuclear extract, 10 ng rDNA template pU5.1E/X (Smith et al., 1990), and exogenous transcription factors were preincubated on ice in the absence of nucleotide to allow formation of PICs. Transcription was initiated by addition of 30 mM Hepes (pH

7.9); 0.1 mM EDTA; 10 mM creatine phosphate; 10% glycerol (v/v); 5 mM $MgCl_s$; 97 mM KCl; 200 ng/mL α amanitin; 0.6 mM each of ATP, GTP, and CTP; 0.05 mM UTP; and 10 μCi [α ^{32}P] UTP (3000 Ci/mM); and allowed to proceed at 30ºC for 30 min. RNA was extracted and analyzed on 4% polyacrylamide gels containing 7 M urea.

Purification of Cellular UBF and recombinant RRN3

HeLa cells were transfected with FLAG-tagged RRN3 plasmid (Hirschler-Laszkiewicz et al., 2003) with Effectene (Qiagen) and expressed proteins were purified from cell lysates in 50 mM Tris (pH 7.4), 150 mM NaCl, 1 mM EDTA, 1% Triton X-100, and 1 mM PMSF using anti FLAG agarose beads (Sigma). Beads were washed and eluted with 0.5 mg/mL FLAG peptide (Sigma), and dialyzed with 20 mM Hepes (pH 8.0), 20% glycerol, 100 mM KCl, 5 mM $MgCl_2$, 0.2 mM EDTA, 1 mM PMSF, 0.5 mM DTT. UBF protein was isolated from Novicoff hepatoma cells as previously reported (Smith et al., 1990). Partially purified UBF protein from the DE-500 fraction was used for *in vitro* transcription.

Detection and Quantification

Chemifluorescence of Western blots, ethidium staining of agarose gels, and phosphor screens were visualized using a Typhoon 9400 imager (GE Healthcare). Bands were quantified with ImageQuant 5.2 software (GE Healthcare).

Acknowledgements

PERK +/+ and -/- cells were a gift from Dr Douglas Cavener. eIF2α S/S and A/A cells were provided by Dr Randall Kaufman. We would like to thank Dr Lawrence Rothblum for all of his advice and assistance in developing our *in vitro* system for analyzing ribosomal RNA transcription.

Chapter 2, in part, will be submitted for publication of the material as it may appear. The dissertation author, Jenny Bratlien DuRose was the primary investigator and will be the primary author of this paper.

References

Ayaki, H., Hara, R., and Ikenaga, M. (1996). Recovery from ultraviolet tight-induced depression of ribosomal RNA synthesis in normal human, xeroderma pigmentosum and Cockayne syndrome cells. Journal of radiation research *37*, 107-116.

Banerji, S.S., Theodorakis, N.G., and Morimoto, R.I. (1984). Heat shock-induced translational control of HSP70 and globin synthesis in chicken reticulocytes. Molecular and cellular biology *4*, 2437-2448.

Benecke, B.J., Ferencz, A., and Seifart, K.H. (1973). Resistance of hepatic RNA polymerases to compounds effecting RNA and protein synthesis in vivo. FEBS letters *31*, 53-58.

Beretta, L., Gingras, A.C., Svitkin, Y.V., Hall, M.N., and Sonenberg, N. (1996). Rapamycin blocks the phosphorylation of 4E-BP1 and inhibits cap-dependent initiation of translation. The EMBO journal *15*, 658-664.

Berlanga, J.J., Santoyo, J., and De Haro, C. (1999). Characterization of a mammalian homolog of the GCN2 eukaryotic initiation factor 2alpha kinase. European journal of biochemistry / FEBS *265*, 754-762.

Brown, E.J., Beal, P.A., Keith, C.T., Chen, J., Shin, T.B., and Schreiber, S.L. (1995). Control of p70 s6 kinase by kinase activity of FRAP in vivo. Nature *377*, 441-446.

Brunn, G.J., Hudson, C.C., Sekulic, A., Williams, J.M., Hosoi, H., Houghton, P.J., Lawrence, J.C., Jr., and Abraham, R.T. (1997). Phosphorylation of the translational repressor PHAS-I by the mammalian target of rapamycin. Science (New York, N.Y *277*, 99-101.

Calfon, M., Zeng, H., Urano, F., Till, J.H., Hubbard, S.R., Harding, H.P., Clark, S.G., and Ron, D. (2002). IRE1 couples endoplasmic reticulum load to secretory capacity by processing the XBP-1 mRNA. Nature *415*, 92-96.

Cavanaugh, A.H., Hirschler-Laszkiewicz, I., Hu, Q., Dundr, M., Smink, T., Misteli, T., and Rothblum, L.I. (2002). Rrn3 phosphorylation is a regulatory checkpoint for ribosome biogenesis. The Journal of biological chemistry *277*, 27423-27432.

Chen, J.J., Throop, M.S., Gehrke, L., Kuo, I., Pal, J.K., Brodsky, M., and London, I.M. (1991). Cloning of the cDNA of the heme-regulated eukaryotic initiation factor 2 alpha (eIF-2 alpha) kinase of rabbit reticulocytes: homology to yeast GCN2 protein kinase and human double-stranded-RNA-dependent eIF-2 alpha kinase. Proceedings of the National Academy of Sciences of the United States of America *88*, 7729-7733.

Cherbas, L., and London, I.M. (1976). On the mechanism of delayed inhibition of protein synthesis in heme-defecient rabbit reticulocyte lysates. Proceedings of the National Academy of Sciences of the United States of America *73*, 3506-3510.

Chesterton, C.J., Coupar, B.E., Butterworth, P.H., and Green, M.H. (1975). Studies on the control of ribosomal RNA synthesis in HeLa cells. European journal of biochemistry / FEBS *57*, 79-83.

Chung, J., Kuo, C.J., Crabtree, G.R., and Blenis, J. (1992). Rapamycin-FKBP specifically blocks growth-dependent activation of and signaling by the 70 kd S6 protein kinases. Cell *69*, 1227-1236.

Claypool, J.A., French, S.L., Johzuka, K., Eliason, K., Vu, L., Dodd, J.A., Beyer, A.L., and Nomura, M. (2004). Tor pathway regulates Rrn3p-dependent recruitment of yeast RNA polymerase I to the promoter but does not

participate in alteration of the number of active genes. Molecular biology of the cell *15*, 946-956.

Clemens, M.J., Pain, V.M., Wong, S.T., and Henshaw, E.C. (1982). Phosphorylation inhibits guanine nucleotide exchange on eukaryotic initiation factor 2. Nature *296*, 93-95.

Cox, J.S., Shamu, C.E., and Walter, P. (1993). Transcriptional induction of genes encoding endoplasmic reticulum resident proteins requires a transmembrane protein kinase. Cell *73*, 1197-1206.

Dai, M.S., and Lu, H. (2004). Inhibition of MDM2-mediated p53 ubiquitination and degradation by ribosomal protein L5. The Journal of biological chemistry *279*, 44475-44482.

Dai, M.S., Zeng, S.X., Jin, Y., Sun, X.X., David, L., and Lu, H. (2004). Ribosomal protein L23 activates p53 by inhibiting MDM2 function in response to ribosomal perturbation but not to translation inhibition. Molecular and cellular biology *24*, 7654-7668.

Dignam, J.D., Lebovitz, R.M., and Roeder, R.G. (1983). Accurate transcription initiation by RNA polymerase II in a soluble extract from isolated mammalian nuclei. Nucleic acids research *11*, 1475-1489.

DuRose, J.B., Tam, A.B., and Niwa, M. (2006). Intrinsic capacities of molecular sensors of the unfolded protein response to sense alternate forms of endoplasmic reticulum stress. Molecular biology of the cell *17*, 3095-3107.

Ennis, H.L. (1966). Synthesis of ribonucleic acid in L cells during inhibition of protein synthesis by cycloheximide. Molecular pharmacology *2*, 543-557.

Farrell, P.J., Balkow, K., Hunt, T., Jackson, R.J., and Trachsel, H. (1977). Phosphorylation of initiation factor eIF-2 and the control of reticulocyte protein synthesis. Cell *11*, 187-200.

Grummt, I., Smith, V.A., and Grummt, F. (1976). Amino acid starvation affects the initiation frequency of nucleolar RNA polymerase. Cell *7*, 439-445.

Hannan, K.M., Brandenburger, Y., Jenkins, A., Sharkey, K., Cavanaugh, A., Rothblum, L., Moss, T., Poortinga, G., McArthur, G.A., Pearson, R.B., and Hannan, R.D. (2003). mTOR-dependent regulation of ribosomal gene transcription requires S6K1 and is mediated by phosphorylation of the

carboxy-terminal activation domain of the nucleolar transcription factor UBF. Molecular and cellular biology *23*, 8862-8877.

Harding, H.P., Zhang, Y., Bertolotti, A., Zeng, H., and Ron, D. (2000). Perk is essential for translational regulation and cell survival during the unfolded protein response. Molecular cell *5*, 897-904.

Harding, H.P., Zhang, Y., and Ron, D. (1999). Protein translation and folding are coupled by an endoplasmic-reticulum-resident kinase. Nature *397*, 271-274.

Hershko, A., Mamont, P., Shields, R., and Tomkins, G.M. (1971). "Pleiotypic response". Nature: New biology *232*, 206-211.

Hirschler-Laszkiewicz, I., Cavanaugh, A.H., Mirza, A., Lun, M., Hu, Q., Smink, T., and Rothblum, L.I. (2003). Rrn3 becomes inactivated in the process of ribosomal DNA transcription. The Journal of biological chemistry *278*, 18953-18959.

James, M.J., and Zomerdijk, J.C. (2004). Phosphatidylinositol 3-kinase and mTOR signaling pathways regulate RNA polymerase I transcription in response to IGF-1 and nutrients. The Journal of biological chemistry *279*, 8911-8918.

Jin, A., Itahana, K., O'Keefe, K., and Zhang, Y. (2004). Inhibition of HDM2 and activation of p53 by ribosomal protein L23. Molecular and cellular biology *24*, 7669-7680.

Lohrum, M.A., Ludwig, R.L., Kubbutat, M.H., Hanlon, M., and Vousden, K.H. (2003). Regulation of HDM2 activity by the ribosomal protein L11. Cancer Cell *3*, 577-587.

Maden, B.E., Vaughan, M.H., Warner, J.R., and Darnell, J.E. (1969). Effects of valine deprivation on ribosome formation in HeLa cells. Journal of molecular biology *45*, 265-275.

Marechal, V., Elenbaas, B., Piette, J., Nicolas, J.C., and Levine, A.J. (1994). The ribosomal L5 protein is associated with mdm-2 and mdm-2-p53 complexes. Molecular and cellular biology *14*, 7414-7420.

Mayer, C., Bierhoff, H., and Grummt, I. (2005). The nucleolus as a stress sensor: JNK2 inactivates the transcription factor TIF-IA and down-regulates rRNA synthesis. Genes & development *19*, 933-941.

Mayer, C., Zhao, J., Yuan, X., and Grummt, I. (2004). mTOR-dependent activation of the transcription factor TIF-IA links rRNA synthesis to nutrient availability. Genes & development *18*, 423-434.

Meurs, E., Chong, K., Galabru, J., Thomas, N.S., Kerr, I.M., Williams, B.R., and Hovanessian, A.G. (1990). Molecular cloning and characterization of the human double-stranded RNA-activated protein kinase induced by interferon. Cell *62*, 379-390.

Miller, G., Panov, K.I., Friedrich, J.K., Trinkle-Mulcahy, L., Lamond, A.I., and Zomerdijk, J.C. (2001). hRRN3 is essential in the SL1-mediated recruitment of RNA Polymerase I to rRNA gene promoters. The EMBO journal *20*, 1373-1382.

Miller, K.G., and Sollner-Webb, B. (1981). Transcription of mouse rRNA genes by RNA polymerase I: in vitro and in vivo initiation and processing sites. Cell *27*, 165-174.

Mori, K., Ma, W., Gething, M.J., and Sambrook, J. (1993). A transmembrane protein with a cdc2+/CDC28-related kinase activity is required for signaling from the ER to the nucleus. Cell *74*, 743-756.

Muramatsu, M., Shimada, N., and Higashinakagawa, T. (1970). Effect of cycloheximide on the nucleolar RNA synthesis in rat liver. Journal of molecular biology *53*, 91-106.

Pardee, A.B. (1974). A restriction point for control of normal animal cell proliferation. Proceedings of the National Academy of Sciences of the United States of America *71*, 1286-1290.

Price, D.J., Grove, J.R., Calvo, V., Avruch, J., and Bierer, B.E. (1992). Rapamycin-induced inhibition of the 70-kilodalton S6 protein kinase. Science (New York, N.Y *257*, 973-977.

Scheuner, D., Song, B., McEwen, E., Liu, C., Laybutt, R., Gillespie, P., Saunders, T., Bonner-Weir, S., and Kaufman, R.J. (2001). Translational control is required for the unfolded protein response and in vivo glucose homeostasis. Molecular cell *7*, 1165-1176.

Shi, Y., Vattem, K.M., Sood, R., An, J., Liang, J., Stramm, L., and Wek, R.C. (1998). Identification and characterization of pancreatic eukaryotic initiation factor 2 alpha-subunit kinase, PEK, involved in translational control. Molecular and cellular biology *18*, 7499-7509.

Sidrauski, C., and Walter, P. (1997). The transmembrane kinase Ire1p is a site-specific endonuclease that initiates mRNA splicing in the unfolded protein response. Cell *90*, 1031-1039.

Siekierka, J., Datta, A., Mauser, L., and Ochoa, S. (1982). Initiation of protein synthesis in eukaryotes. Nature of ternary complex dissociation factor. The Journal of biological chemistry *257*, 4162-4165.

Smith, S.D., Oriahi, E., Lowe, D., Yang-Yen, H.F., O'Mahony, D., Rose, K., Chen, K., and Rothblum, L.I. (1990). Characterization of factors that direct transcription of rat ribosomal DNA. Molecular and cellular biology *10*, 3105-3116.

Sonenberg, N., Hershey, J.W.B., and Mathews, M. (2000). Translational control of gene expression, 2nd edn (Cold Spring Harbor, NY: Cold Spring Harbor Laboratory Press).

Sood, R., Porter, A.C., Olsen, D.A., Cavener, D.R., and Wek, R.C. (2000). A mammalian homologue of GCN2 protein kinase important for translational control by phosphorylation of eukaryotic initiation factor-2alpha. Genetics *154*, 787-801.

Tamaoki, T., and Mueller, G.C. (1963). Effect of puromycin on RNA synthesis in HeLa cells. Biochemical and biophysical research communications *11*, 404-410.

Tirasophon, W., Welihinda, A.A., and Kaufman, R.J. (1998). A stress response pathway from the endoplasmic reticulum to the nucleus requires a novel bifunctional protein kinase/endoribonuclease (Ire1p) in mammalian cells. Genes & development *12*, 1812-1824.

Wang, X.Z., Harding, H.P., Zhang, Y., Jolicoeur, E.M., Kuroda, M., and Ron, D. (1998). Cloning of mammalian Ire1 reveals diversity in the ER stress responses. The EMBO journal *17*, 5708-5717.

Warner, J.R., Girard, M., Latham, H., and Darnell, J.E. (1966). Ribosome formation in HeLa cells in the absence of protein synthesis. Journal of molecular biology *19*, 373-382.

Willems, M., Penman, M., and Penman, S. (1969). The regulation of RNA synthesis and processing in the nucleolus during inhibition of protein synthesis. The Journal of cell biology *41*, 177-187.

Yoshida, H., Haze, K., Yanagi, H., Yura, T., and Mori, K. (1998). Identification of the cis-acting endoplasmic reticulum stress response element responsible for transcriptional induction of mammalian glucose-regulated proteins. Involvement of basic leucine zipper transcription factors. The Journal of biological chemistry *273*, 33741-33749.

Yoshida, H., Matsui, T., Yamamoto, A., Okada, T., and Mori, K. (2001). XBP1 mRNA is induced by ATF6 and spliced by IRE1 in response to ER stress to produce a highly active transcription factor. Cell *107*, 881-891.

Yuan, X., Zhao, J., Zentgraf, H., Hoffmann-Rohrer, U., and Grummt, I. (2002). Multiple interactions between RNA polymerase I, TIF-IA and TAF(I) subunits regulate preinitiation complex assembly at the ribosomal gene promoter. EMBO reports *3*, 1082-1087.

Zhang, F., Hamanaka, R.B., Bobrovnikova-Marjon, E., Gordan, J.D., Dai, M.S., Lu, H., Simon, M.C., and Diehl, J.A. (2006). Ribosomal stress couples the unfolded protein response to p53-dependent cell cycle arrest. The Journal of biological chemistry *281*, 30036-30045.

Zhang, Y., Wolf, G.W., Bhat, K., Jin, A., Allio, T., Burkhart, W.A., and Xiong, Y. (2003). Ribosomal protein L11 negatively regulates oncoprotein MDM2 and mediates a p53-dependent ribosomal-stress checkpoint pathway. Molecular and cellular biology *23*, 8902-8912.

Zhao, J., Yuan, X., Frodin, M., and Grummt, I. (2003). ERK-dependent phosphorylation of the transcription initiation factor TIF-IA is required for RNA polymerase I transcription and cell growth. Molecular cell *11*, 405-413.

CHAPTER 3

Conclusions and Future Perspectives

Intrinsic Capacities of ER Stress Sensors

Three proteins spanning the ER membrane initiate the UPR pathway: PERK, IRE1, and ATF6. Each protein has a large lumenal domain that senses the ER protein-folding environment, and transmits the signal across the ER membrane to their cytosolic domains. In Chapter 1, we uncovered that UPR components have an intrinsic capacity to respond to different forms of ER stress. We hypothesize that differential activation of UPR components in response to alternate forms of ER stress may allow the cell to adjust UPR output in order to ensure the response is best fit for the specific stress. For example, each UPR signaling branch activates at least one transcription factor, and based on studies in knockout mice the genes induced by each branch do not entirely overlap. The presence or absence of a particular transcription factor profoundly influences UPR induced gene expression, and thus we propose that this may be utilized by the cell in order to achieve an optimal UPR in physiological settings. Careful analysis of UPR component activation and its affect on gene expression will be necessary to unravel the contribution of each signaling branch towards a best-fit UPR.

Another question that remains to be answered is what is the mechanism controlling differential activation of UPR components in response to alternate forms of ER stress. Prior to publication of our results in DuRose *et al.* (2006) (DuRose et al., 2006) the favored model for UPR component

activation was through the reversible association of BiP with the lumenal domain of each UPR component (Figure 1). BiP is an incredibly abundant ER protein, and during normal conditions the level of BiP is sufficient to bind unfolded proteins and to associate with each UPR component. During ER stress the increasing number of unfolded proteins in the ER competes with binding to the UPR components resulting in BiP dissociation, which correlates with UPR activation. Therefore, it was proposed that BiP association maintained UPR components in an inactive state by preventing dimerization of IRE1 and PERK (Bertolotti et al., 2000; Ma et al., 2002), and by masking the golgi localization signal of ATF6 (Shen et al., 2002). This model was attractive because it could explain how overexpression of BiP could render the UPR components resistant to ER stress, and suggested how increasing BiP expression turned off the pathway. However, more recent results including our observations suggest that UPR component activation occurs through a more complex mechanism.

In our study in Chapter 1, we found that BiP dissociation correlates well with the activation of PERK and IRE1 regardless of the ER stress inducer. However, the BiP dissociation model cannot easily explain the activation kinetics of all three UPR sensors with respect to one another in response to different forms of ER stress. In particular, rapid activation of IRE1 and PERK in response to Tg treatment compared to the relatively slow activation of ATF6

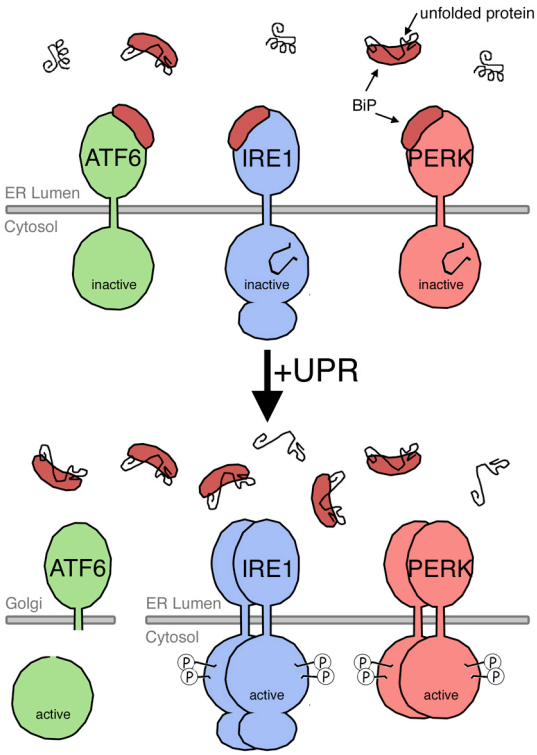

Figure 1. BiP Dissociation Model for UPR Component Activation.
Under normal conditions the ER chaperone BiP is in sufficient supply to bind to and fold nascent proteins in addition to interacting with the UPR components ATF6, IRE1 and PERK maintaining them in an inactive state. Upon UPR induction, the accumulation of unfolded proteins competes with UPR components for BiP binding, leading to dimerization and autophosphorylation of IRE1 and PERK as well as translocation of ATF6 into the golgi where it is cleaved releasing the cytoplasmic transcription factor domain.

suggests the presence of additional regulatory mechanisms. The fact that deletion of the BiP binding site from yeast IRE1 does not lead to constitutive activation, also supports the idea that BiP may play a more modulatory role during UPR rather than directly controlling component activation (Kimata et al., 2004). Possible mechanisms by which this may occur is through direct interaction of lumenal domains with ligands (e.g. unfolded proteins) or direct sensing of the of the ER protein-folding environment by alteration of component modification (e.g. disulfide bonds or glycosylation).

The lumenal domains of PERK and IRE1 share blocks of identity suggesting that they have a similar evolutionary origin. Although there is limited structural information for the PERK lumenal domain, alignment of predicted secondary structures with the IRE1 crystal structure suggest the two proteins may adopt similar conformations (Credle et al., 2005; Zhou et al., 2006). In contrast the lumenal domain of ATF6 does not appear to have any homology with either PERK or IRE1. One interesting feature revealed by the crystal structure of the IRE1 lumenal domain is the formation of a groove formed in the dimerization interface between two IRE1 molecules. This groove appears structurally similar to the peptide-binding groove of the major histocompatibility complex (MHC), suggesting that IRE1 and PERK may actually bind to unfolded peptides, or proteins (Credle et al., 2005; Zhou et al., 2006). However, a physical interaction of IRE1 or PERK with misfolded

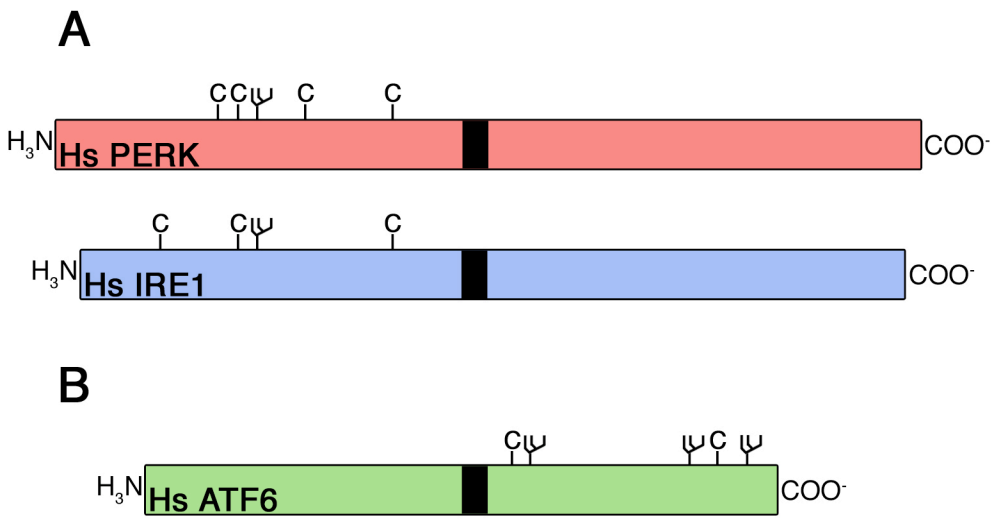

Figure 2. Conserved Cysteines and Glycosylation Sites in Human PERK, IRE1, and ATF6. Conserved cysteine residues (C) and glycosylation sites (Ψ) along the linear sequence of PERK and IRE1 (A) and ATF6 (B).

proteins has yet to be demonstrated. Another possible mechanism for sensing alternate forms of ER stress is through differential modification of the UPR sensors themselves. The lumenal domains of IRE1, PERK and ATF6 contain a number of conserved cysteine residues and glycosylation sites (Figure 2). We hypothesize that modification of the lumenal domains during ER stress such as presence or absence of N-linked glycans or disulfide bonds may modulate the activation kinetics of UPR components in response to different forms of ER stress.

The lumenal domain of human PERK contains four cysteine residues that are highly conserved among vertebrates with more variation existing in nematodes and fruit flies (Table 1). Human IRE1 has three lumenal cysteines that are conserved with other vertebrates and nematodes, however only one appears to be conserved in fruit flies (Table 2). Based on the IRE1 crystal structure, many of the cysteine residues are located in loops adjacent to the primary dimerization interface as well as a predicted secondary dimerization interface (Credle et al., 2005; Zhou et al., 2006). The location of the conserved cysteines in an area where they are likely to interact with unfolded proteins as well as other IRE1 or PERK molecules lead us to question whether they play a role in adjusting UPR signaling in response to different forms of ER stress. When the lumenal cysteine residues are mutated to alanine, both PERK and IRE1 can be activated during ER stress, suggesting that they are

Table 1. Conserved Cysteines and Glycosylation Sites in Metazoan PERK Lumenal Domains.			
H. sapiens	M. musculus[1]	C. elegans	D. melanogaster
C215#	Y	Y	Y
C220#	Y	Y	Y
C335	Y	N	N
C453*	Y	N	N
N257Ψ	Y	Y	Y

* Conserved between PERK and IRE1.
# Location is conserved between predicted structure of PERK and crystal structure of IRE1.
Ψ Universally conserved between PERK and IRE1 in all species to date.
1. Also conserved in X.l., D.r., and G.g.

Table 2. Conserved Cysteines and Glycosylation Sites in Metazoan IRE1α Lumenal Domains.			
H. sapiens	M. musculus[2]	C. elegans	D. melanogaster
C109	Y	Y	Y
C148#	Y	Y	N
C332*	Y	Y	N
N176Ψ	Y	Y	Y

* Conserved between IRE1 and PERK.
# Location is conserved between crystal structure of IRE1 and predicted structure of PERK.
Ψ Universally conserved between IRE1 and PERK in all species to date.
2. Validated IRE1 sequence from X.l., D.r., and G.g. not available.

dispensable for UPR induction (Liu et al., 2003; Ma et al., 2002). However, a careful examination of cysteine mutants in response to different forms of ER stress has not been performed.

Preliminary investigation of PERK and IRE1 on non-reducing gels suggests that some portion of IRE1 exists in a disulfide-bonded high molecular weight complex *in vivo*, while PERK does not (Appendix 1). This is consistent with previous reports indicating that IRE1 forms homodimers *in vivo* through intermolecular disulfide bonding (Liu et al., 2003). While PERK does not contain intermolecular disulfide bonds, it is not known if the cysteine residues within a single PERK molecule can interact, and if that can have an effect on PERK activity. In Chapter 1, we observed that the extent eIF2α phosphorylation was diminished upon treatment of CHO cells with DTT compared to Tg. In a preliminary analysis of PERK kinase activity we found that the level of ^{32}P incorporation into itself was inversely proportional to the level of ^{32}P incorporation into substrate histone H1 (Appendix 2). Interestingly, treatment CHO cells with DTT prior to immunoprecipitation of PERK resulted in the greatest level of self-incorporation and the least amount of activity towards histone H1. This is consistent with the lower level of eIF2α phosphorylation, and low mobility of DTT-treated PERK in CHO cells suggesting that perhaps DTT treatment alters PERK kinase activity *in vivo*. In order to study the role of conserved cysteines in modulating UPR activation we

have constructed a mammalian IRE1 expression plasmids bearing mutations at all three cysteines in different combinations. Generating cell lines expressing IRE1 or PERK cysteine mutants will allow us to carefully analyze the effect of cysteine mutants on component activation and dissect the role of disulfide bonding in modulating the UPR response in the future.

In addition to cysteine residues, there is a single glycosylation site in the PERK and IRE1 lumenal domain that is universally conserved in all species to date (Tables 1 and 2). The glycosylation site is located in the β-sheet that forms the putative peptide-binding pocket, however it does not project into the MHC-like groove (Credle et al., 2005; Zhou et al., 2006). Mutation of a residue adjacent to the glycosylation site impairs IRE1 activation, so it is likely that glycosylation in that region may have an effect of IRE1 activity (Credle et al., 2005). Both PERK and IRE1 have been shown to be glycosylated *in vivo* (Harding et al., 1999; Tirasophon et al., 1998), and mutation of the site in IRE1 indicates that glycosylation is dispensable for IRE1 folding and activation (Liu et al., 2002; Liu et al., 2003; Oikawa et al., 2005). However, like the cysteine mutants careful examination of glycosylation mutants in response to different forms of ER stress has not been performed. We have constructed a mammalian expression plasmid bearing mutation in the conserved glycosylation site, which can be used to generate cells lines for

the future study of the role of glycosylation in regulating UPR component activity.

As stated above, the lumenal domain of ATF6 is not related to IRE1 or PERK however recent studies have shown that glycosylation and disulfide-bonding do play a role in ATF6 activation during ER stress. ATF6 is a type II transmembrane protein with its c-terminus residing in the ER lumen (Haze et al., 1999). Human ATF6 contains two highly conserved cysteine residues and three conserved glycosylation sites (Table 3). ATF6 is glycosylated in vivo, and it has been reported that underglycosylation of ATF6 promotes its activation (Hong et al., 2004). In addition it is has recently been shown that ATF6 exists as disulfide bonded multimers, and that reduction into the monomer form promotes golgi localization and activation (Nadanaka et al., 2007). This is consistent with our results in Chapter 1 where treatment of DTT results in an extremely rapid activation of ATF6, while treatment with Tg and Tm is considerably slower. The studies of ATF6 have demonstrated that at least one UPR component responds to changes in modification of its lumenal domain, suggesting that it is possible that similar regulation occurs with IRE1 and PERK. It is likely that BiP dissociation, binding to unfolded proteins, and modification of lumenal domains all have some affect on UPR component activation. Careful studies will be required to sort out the contribution of each mechanism to the activity of each UPR signaling branch, and to understanding

Table 3. Conserved Cysteines and Glycosylation Sites in Metazoan ATF6 Lumenal Domains.				
H. sapiens	M. musculus	G. gallus	D. rerio	C. elegans
C467	Y	Y	Y	Y
C618	Y	Y	Y	Y
N472	Y	Y	Y	Y
N584	Y	Y	N[$]	Y
N643	Y	Y	Y	N

$ The N residue is conserved, however NXS/T consensus sequence for glycosylation is not.

the downstream consequences of differential activation of UPR components during alternate forms of ER stress.

PERK Regulation of Ribosome Biogenesis

The production of rRNA is the rate-limiting step in ribosome synthesis. While mRNAs can undergo multiple rounds of translation generating many proteins from a single mRNA, each precursor rRNA is consumed in the production of a single ribosome. Thus, in order to keep up with demand for ribosome synthesis, the transcription of rRNA constitutes the majority of all transcription in actively growing cells (Warner, 1999; Zetterberg and Killander, 1965). Translation is one of the major energy consuming processes in all cells and production of ribosomes represents a significant investment of a cells resources. Not only is ribosome biogenesis a costly undertaking in itself with each ribosome requiring the addition of nearly 80 ribosomal proteins and hundreds of processing factors, but the resulting increase in translational capacity by new ribosomes provides an opportunity for faster growth and thus faster depletion of ones resources. As such, the production of ribosomes should only be undertaken by healthy cells with a ready supply of nutrients to ensure viability of the organism. Therefore, it is not surprising that the transcription of rRNA is under an immense amount of regulation.

All eukaryotic cells characterized to date have developed mechanisms to coordinate the rate of rRNA transcription and protein translation with growth

signaling and nutrient availability. This process has been under intense study as it has major implications in numerous pathologies associated with chronic cellular hypertrophy and proliferation, for example in tumor development and in heart disease related to cardiac hypertrophy. The major established function of the nucleolus is to direct rRNA transcription and to coordinate assembly of ribosomes. While the role of the nucleolus has long been associated with increasing growth, it is now becoming apparent that the nucleolus also functions to limit growth particularly during cellular stress and nutrient starvation (Olson, 2004).

In Chapter 2, we have defined a novel stress pathway regulating rRNA synthesis in response to ER stress. We have shown that UPR signaling through the PERK branch coordinately regulates rRNA transcription with protein synthesis. We identified that the nucleolar transcription factor RRN3 is the target of UPR regulation, and that its inactivation leads to dissociation of both RRN3 and Pol I from the rRNA promoter. In addition, we show that phosphorylation of eIF2α by PERK is necessary for rRNA regulation providing the first link between this major mode of translation regulation and rRNA transcription. While we have defined components in the nucleolus that participate in downregulating rRNA during UPR, we have yet to uncover how eIF2α phosphorylation signals to the nucleolus to regulate RRN3 activity. Clearly defining the pathway that connects eIF2α phosphorylation with the

nucleolus is of particular interest as there are currently four eIF2α kinases identified in mammals, and it is not known whether they too can signal to the nucleolus to downregulate rRNA transcription.

Previous reports have shown that PERK signaling is essential for survival during the UPR (Harding et al., 2000), and is responsible for inducing cell cycle arrest in cells experiencing ER stress (Brewer and Diehl, 2000; Brewer et al., 1999; Hamanaka et al., 2005; Zhang et al., 2006). It has been suggested that translation inhibition from phosphorylation of eIF2α mediates these effects. With the newly defined link between eIF2α and rRNA synthesis, a number of exciting question arise with regard to control of cell fate decisions by PERK signaling. For example, is it possible that cell cycle arrest and apoptosis are controlled through impairment of nucleolar function by inhibition of rRNA transcription. Over the last decade the role of nucleolar function on cell cycle progression and apoptosis has become increasingly prominent (Olson, 2004; Visintin and Amon, 2000). For example, the activity of a number of key cell fate regulators such as MDM2, $p19^{ARF}$, and CDC14 have been shown to be controlled by their nucleolar localization. In particular nucleolar function, which requires active rRNA transcription, is critical for maintaining the activity of MDM2, therefore keeping pro-apoptotic proteins such as p53 in an inactive state (Rubbi and Milner, 2003). One of the major questions that remains to be answered is what it the effect of PERK-regulated rRNA

transcription inhibition on cell fate decisions. Further studies will be required to address this question.

References

Bertolotti, A., Zhang, Y., Hendershot, L.M., Harding, H.P., and Ron, D. (2000). Dynamic interaction of BiP and ER stress transducers in the unfolded-protein response. Nature cell biology *2*, 326-332.

Brewer, J.W., and Diehl, J.A. (2000). PERK mediates cell-cycle exit during the mammalian unfolded protein response. Proceedings of the National Academy of Sciences of the United States of America *97*, 12625-12630.

Brewer, J.W., Hendershot, L.M., Sherr, C.J., and Diehl, J.A. (1999). Mammalian unfolded protein response inhibits cyclin D1 translation and cell-cycle progression. Proceedings of the National Academy of Sciences of the United States of America *96*, 8505-8510.

Credle, J.J., Finer-Moore, J.S., Papa, F.R., Stroud, R.M., and Walter, P. (2005). On the mechanism of sensing unfolded protein in the endoplasmic reticulum. Proceedings of the National Academy of Sciences of the United States of America *102*, 18773-18784.

DuRose, J.B., Tam, A.B., and Niwa, M. (2006). Intrinsic capacities of molecular sensors of the unfolded protein response to sense alternate forms of endoplasmic reticulum stress. Molecular biology of the cell *17*, 3095-3107.

Hamanaka, R.B., Bennett, B.S., Cullinan, S.B., and Diehl, J.A. (2005). PERK and GCN2 contribute to eIF2alpha phosphorylation and cell cycle arrest after activation of the unfolded protein response pathway. Molecular biology of the cell *16*, 5493-5501.

Harding, H.P., Zhang, Y., Bertolotti, A., Zeng, H., and Ron, D. (2000). Perk is essential for translational regulation and cell survival during the unfolded protein response. Molecular cell *5*, 897-904.

Harding, H.P., Zhang, Y., and Ron, D. (1999). Protein translation and folding are coupled by an endoplasmic-reticulum-resident kinase. Nature *397*, 271-274.

Haze, K., Yoshida, H., Yanagi, H., Yura, T., and Mori, K. (1999). Mammalian transcription factor ATF6 is synthesized as a transmembrane protein and activated by proteolysis in response to endoplasmic reticulum stress. Molecular biology of the cell *10*, 3787-3799.

Hong, M., Luo, S., Baumeister, P., Huang, J.M., Gogia, R.K., Li, M., and Lee, A.S. (2004). Underglycosylation of ATF6 as a novel sensing mechanism for activation of the unfolded protein response. The Journal of biological chemistry *279*, 11354-11363.

Kimata, Y., Oikawa, D., Shimizu, Y., Ishiwata-Kimata, Y., and Kohno, K. (2004). A role for BiP as an adjustor for the endoplasmic reticulum stress-sensing protein Ire1. The Journal of cell biology *167*, 445-456.

Liu, C.Y., Wong, H.N., Schauerte, J.A., and Kaufman, R.J. (2002). The protein kinase/endoribonuclease IRE1alpha that signals the unfolded protein response has a luminal N-terminal ligand-independent dimerization domain. The Journal of biological chemistry *277*, 18346-18356.

Liu, C.Y., Xu, Z., and Kaufman, R.J. (2003). Structure and intermolecular interactions of the luminal dimerization domain of human IRE1alpha. The Journal of biological chemistry *278*, 17680-17687.

Ma, K., Vattem, K.M., and Wek, R.C. (2002). Dimerization and release of molecular chaperone inhibition facilitate activation of eukaryotic initiation factor-2 kinase in response to endoplasmic reticulum stress. The Journal of biological chemistry *277*, 18728-18735.

Nadanaka, S., Okada, T., Yoshida, H., and Mori, K. (2007). Role of disulfide bridges formed in the luminal domain of ATF6 in sensing endoplasmic reticulum stress. Molecular and cellular biology *27*, 1027-1043.

Oikawa, D., Kimata, Y., Takeuchi, M., and Kohno, K. (2005). An essential dimer-forming subregion of the endoplasmic reticulum stress sensor Ire1. The Biochemical journal *391*, 135-142.

Olson, M.O. (2004). Sensing cellular stress: another new function for the nucleolus? Sci STKE *2004*, pe10.

Rubbi, C.P., and Milner, J. (2003). Disruption of the nucleolus mediates stabilization of p53 in response to DNA damage and other stresses. The EMBO journal *22*, 6068-6077.

Shen, J., Chen, X., Hendershot, L., and Prywes, R. (2002). ER stress regulation of ATF6 localization by dissociation of BiP/GRP78 binding and unmasking of Golgi localization signals. Developmental cell *3*, 99-111.

Tirasophon, W., Welihinda, A.A., and Kaufman, R.J. (1998). A stress response pathway from the endoplasmic reticulum to the nucleus requires a novel bifunctional protein kinase/endoribonuclease (Ire1p) in mammalian cells. Genes & development *12*, 1812-1824.

Visintin, R., and Amon, A. (2000). The nucleolus: the magician's hat for cell cycle tricks. Current opinion in cell biology *12*, 752.

Warner, J.R. (1999). The economics of ribosome biosynthesis in yeast. Trends Biochem Sci *24*, 437-440.

Zetterberg, A., and Killander, D. (1965). Quantitative cytophotometric and autoradiographic studies on the rate of protein synthesis during interphase in mouse fibroblasts in vitro. Experimental cell research *40*, 1-11.

Zhang, F., Hamanaka, R.B., Bobrovnikova-Marjon, E., Gordan, J.D., Dai, M.S., Lu, H., Simon, M.C., and Diehl, J.A. (2006). Ribosomal stress couples the unfolded protein response to p53-dependent cell cycle arrest. The Journal of biological chemistry *281*, 30036-30045.

Zhou, J., Liu, C.Y., Back, S.H., Clark, R.L., Peisach, D., Xu, Z., and Kaufman, R.J. (2006). The crystal structure of human IRE1 luminal domain reveals a conserved dimerization interface required for activation of the unfolded protein response. Proceedings of the National Academy of Sciences of the United States of America *103*, 14343-14348.

APPENDIX 1

Disulfide Bonding of PERK and IRE1

Results and Discussion

The Lumenal domains of IRE1 and PERK contain multiple conserved cysteine residues, and their location within the crystal structure of IRE1 suggests they may be involved in intermolecular disulfide bonding. In order to determine if PERK or IRE1 contained intermolecular disulfide bonds *in vivo*, we analyzed CHO whole cell extracts by non-reducing SDS polyacrylamide gel electrophoresis (SDS-PAGE; Figure 1). CHO cells were treated with dithiothreitol (DTT) or thapsigargin (Tg) over a 1 hr time course. Whole cell extracts were collected with or without the addition of N-ethylmaleimide (NEM) in the wash and lysis buffers. NEM, a sulfhydryl alkylating agent, was used in order to alkylate reduced cysteines thereby preventing the formation of post-lysis disulfide bonds. In the presence of NEM, PERK has an apparent molecular weight of a monomer when analyzed by non-reducing SDS-PAGE indicating that PERK does not contain intermolecular disulfide bonds *in vivo* (Figure 1A. +NEM). In the absence of NEM, PERK has the apparent molecular weight of a dimer, suggesting that PERK has at least one free –SH containing cysteine available for forming disulfide bonds after lysis. PERK activation upon DTT and Tg treatment is indicated by the shift in mobility upon autophosphorylation of PERK (pPERK) during UPR induction (Figure 1A). Unfortunately the mobility shift upon UPR activation requires more sophisticated methods in order to monitor intramolecular disulfide bonds.

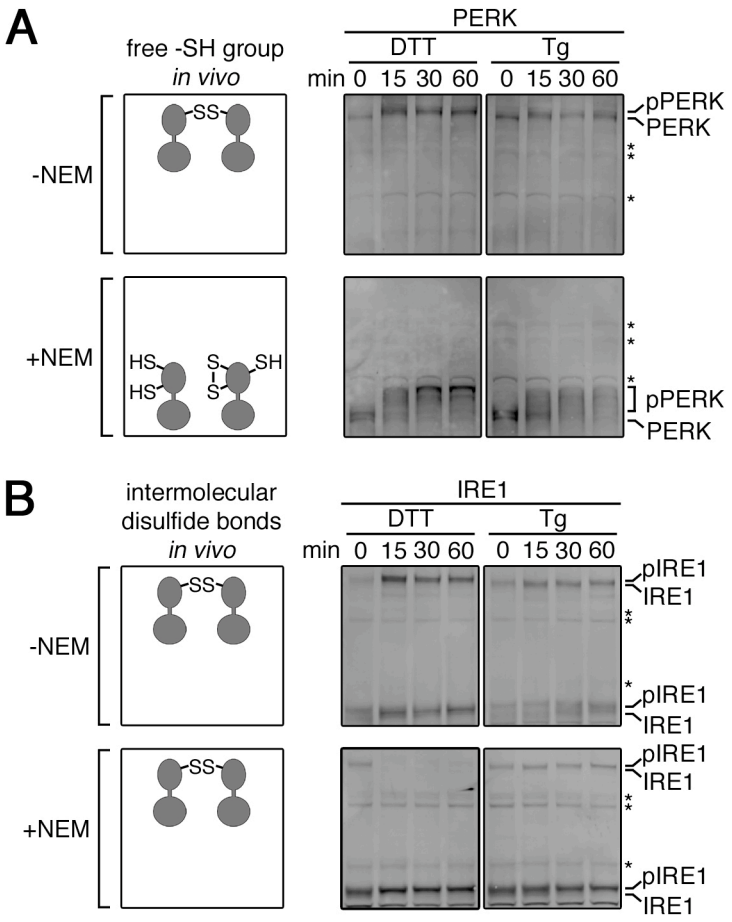

Figure 1. Analysis of PERK and IRE1 by Non-Reducing Gel Electrophoresis.
(A) Western blots of CHO whole cell extracts probing for PERK in the presence or absence of NEM upon treatment with DTT (2 mM) or Tg (200nM; left panels). Right panels depict cartoons of UPR components on non-reducing gels indication the status of their disulfide bonds.
(B) Same as in (A) except western blots were probed for IRE1.

In contrast, IRE1 has the apparent molecular weight of both a dimer and monomer in the presence of NEM, indicating that it does form intermolecular disulfide bonds *in vivo* in untreated cells (Figure 1B). This is consistent with a previous report that IRE1 forms intermolecular disulfide bonded homodimers under normal conditions (Liu et al., 2003). Cells treated with reducing agent DTT prior to treatment with NEM lose the "dimer" form while cells treated with Tg (an ER calcium disruptor) do not further supporting that the intermolecular disulfide bond form *in vivo* (Figure 1B, compare ± NEM). While the function of the intermolecular disulfide bonding of IRE1 has yet to be determined, it is possible that the difference in disulfide bonding between PERK and IRE1 may influence how each component responds to alternate forms of ER stress, particularly stresses that modify the oxidative environment of the ER.

Experimental Procedures

CHO cells were maintained in DMEM-F12 media (Cellgro) supplemented with 5% fetal bovine serum (Gibco). To induce UPR cells were incubated 1 hr in fresh media prior to treatment with DTT (2 mM; Invitrogen) or Tg (200 nM, Calbiochem). At the indicated time points, media was removed and cells were washed 2X in PBS ± 20 mM NEM (Pierce) and lysed 1% triton buffer (see Chapter 1) ± 20 mM NEM. 10 μg of whole cell extracts were

analyzed by non denaturing SDS-PAGE after boiling 10 min in Laemmli buffer. Gels were transferred to nitrocellulose and probed with rabbit polyclonal antibodies to the c-terminal domains of PERK and IRE1 (DuRose et al., 2006).

References

DuRose, J.B., Tam, A.B., and Niwa, M. (2006). Intrinsic capacities of molecular sensors of the unfolded protein response to sense alternate forms of endoplasmic reticulum stress. Molecular biology of the cell *17*, 3095-3107.

Liu, C.Y., Xu, Z., and Kaufman, R.J. (2003). Structure and intermolecular interactions of the luminal dimerization domain of human IRE1alpha. The Journal of biological chemistry *278*, 17680-17687.

APPENDIX 2

Analysis of PERK Kinase Activity Upon UPR Induction

Results and Discussion

During the UPR, PERK activation leads to a repression of translation initiation by phosphorylation of eIF2α. In Chapter 1, we observed that treatment of CHO cells with DTT lead to a minimal increase in eIF2α phosphorylation compared to Tg treatment, while PERK activation indicated by mobility shift seemed to occur to the same extent if not more during DTT treatment. These results suggest that PERK kinase activity towards itself is normal, and its kinase activity towards its substrate eIF2α is altered during DTT treatment.

In order to further investigate the affect of UPR inducers on PERK kinase activity, we immunoprecipitated (IP) PERK from CHO cells treated with dithiothreitol (DTT), thapsigargin (Tg), and tunicamycin (Tm) over a 1 hr time course. PERK IPs were then incubated with [γ-^{32}P]-ATP with or without histone H1 in order to monitor substrate and self kinase activity respectively (Figure 1). Upon treatment with UPR inducers DTT, Tg, and Tm we found that PERK was activated within 1 hr of treatment indicated by the mobility shift of PERK western blots (Figure 1A, top panels). In the absence of substrate, PERK incorporated ^{32}P label indicating that PERK was self phosphorylating, and the level of self phosphorylation increased upon UPR activation (Figure 1A, middle panels; and 1B). Curiously, the level of ^{32}P incorporation was significantly higher upon treatment of CHO cells with DTT compared to

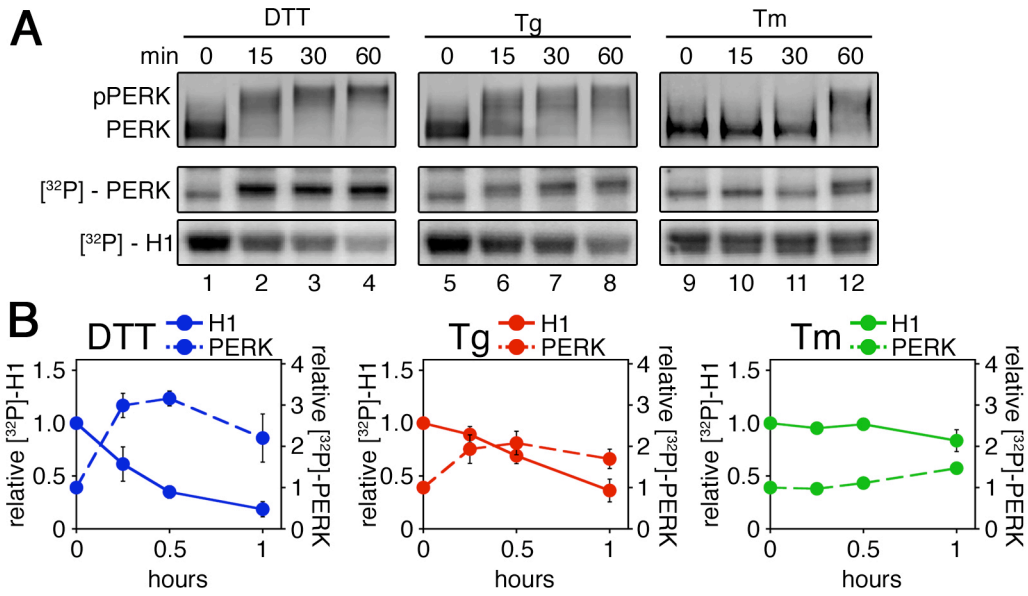

Figure 1. PERK Kinase Activity Upon UPR Activation.
(A) Top panel is a western blot of a PERK IPs upon treatment of CHO cells with DTT (2 mM), Tg (200 nM), and Tm (10 μg/mL). Bottom panels are autoradiographs of kinase assays using PERK IPs from CHO cells in the absence or presence of histone H1 substrate.
(B) Graphical representation of ^{32}P incorporation into PERK and histone H1 as shown in (A). Each point represents the mean ± standard deviation a minimum of three independent experiments.

treatment with Tg or Tm, suggesting that treatment of PERK with ER stressing agents *in vivo*, could affect its activity *in vitro*. In addition, ^{32}P incorporation into histone H1 decreased upon UPR activation, inversely correlating with self phosphorylation (Figure 1A, bottom panels; 1B). These results are consistent with the low mobility PERK and low level of eIF2α phosphorylation observed upon DTT treatment in CHO cells (Chapter 1).

While it is unclear whether the activity of the PERK kinase is affected by modifications in the lumenal domain, these results suggest that treatment of cells with agents disrupting ER protein-folding by different mechanisms can alter the activity of the PERK kinase towards itself and towards substrates. Interestingly the interaction of PERK with eIF2α is regulated by phosphorylation of the kinase insert loop of the PERK kinase domain. Phosphorylation of the kinase insert loop by PERK is thought to cause a conformational change enhancing PERKs affinity for the nonphosphorylated eIF2 complex (Marciniak et al., 2006). Perhaps the inverse correlation of PERK self and substrate kinase activity seen here represents negative feedback regulation whereby phosphorylation of the kinase insert loop past a certain level leads to a decrease in affinity towards substrate. This may serve to dampen PERK signaling upon overactivation or perhaps alter PERKs substrate specificity depending of the level of ER stress. Further studies will be required to investigate these possibilities.

Experimental Procedures

CHO cells were maintained in DMEM-F12 media (Cellgro) supplemented with 5% fetal bovine serum (Gibco). To induce UPR cells were incubated 1 hr in fresh media prior to treatment with DTT (2 mM; Invitrogen) or Tg (200 nM, Calbiochem). At the indicated time points, cells were lysed 1% triton buffer and immunoprecipitated with anti PERK antibody (Santa Cruz Biotech; see Chapter 1). Immunoprecipitates were then incubated with 10 μCi [γ-^{32}P]-ATP in kinase buffer with or without 10 μg of histone H1 (Upstate). PERK IPs or kinase assays were analyzed by SDS-PAGE after boiling 10 min in Laemmli buffer containing 100 mM DTT. Gels were transferred to nitrocellulose and probed with rabbit polyclonal antibodies to the c-terminal domains of PERK (DuRose et al., 2006).

References

DuRose, J.B., Tam, A.B., and Niwa, M. (2006). Intrinsic capacities of molecular sensors of the unfolded protein response to sense alternate forms of endoplasmic reticulum stress. Molecular biology of the cell *17*, 3095-3107.

Marciniak, S.J., Garcia-Bonilla, L., Hu, J., Harding, H.P., and Ron, D. (2006). Activation-dependent substrate recruitment by the eukaryotic translation initiation factor 2 kinase PERK. The Journal of cell biology *172*, 201-209.